

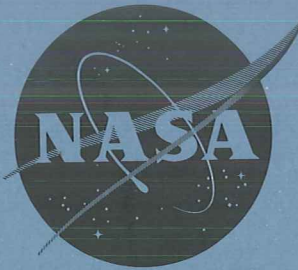
Copy

44

CONFIDENTIAL

NASA TM X-656

GROUP 4
Downgraded at 3 year
intervals; declassified
after 12 years



X63-10891

Code 2

TECHNICAL MEMORANDUM

X-656

Declassified by authority of NASA
Classification Change Notices No. 207
Dated **11-30-70

AERODYNAMIC CHARACTERISTICS FOR A BOOSTER-LAUNCHED
FOLDING-WING ENTRY VEHICLE SUITABLE FOR SUSTAINED
OPERATION AS A SUPERSONIC AIRCRAFT

By Horace F. Emerson, John B. McDevitt,
and John A. Wyss

Ames Research Center
Moffett Field, Calif.

CLASSIFICATION CHANGED
UNCLASSIFIED

TO

By Authority of TH-70-513 Date 9-15-78

CLASSIFIED DOCUMENT - TITLE AND CLASSIFIED

This material contains neither recommendations nor conclusions of the National Aeronautics and Space Administration. It is the property of the Government, is not to be distributed outside your organization, and does not necessarily reflect current NASA positions or policies.

Facility Form 602

NATIONAL AERONAUTICS AND SPACE ADMINISTRATION

WASHINGTON

January 1963

NATIONAL AERONAUTICS AND SPACE ADMINISTRATION

TECHNICAL MEMORANDUM X-656

AERODYNAMIC CHARACTERISTICS FOR A BOOSTER-LAUNCHED
FOLDING-WING ENTRY VEHICLE SUITABLE FOR SUSTAINED
OPERATION AS A SUPERSONIC AIRCRAFT*

By Horace F. Emerson, John B. McDevitt,
and John A. Wyss

SUMMARY

The results of wind-tunnel tests at Mach numbers from 0.2 to 5 of a folding-wing entry vehicle are presented. The vehicle is of essentially blunt, conical shape in the launch and entry configuration. With wings unfolded and nose heat-shield jettisoned, it is a relatively conventional air-breathing cruise vehicle. The considerations leading to the selection of the particular configuration tested are also presented in some detail.

The test results indicate that the aerodynamics of the vehicle pose no problems that would preclude satisfactory operation in any of three phases of operation; namely, entry, wing unfolding, and cruise. In the entry configuration the vehicle was trimmed at an angle of attack of about 40° at a lift-drag ratio of 0.8. The cruise configuration has a maximum lift-drag ratio of about 5 at a Mach number of 2.

INTRODUCTION

It may be considered desirable from several viewpoints to develop a rocket-boosted vehicle suitable for atmosphere entry from near-satellite speeds and also suitable for sustained cruise flight following entry. Such a vehicle would be capable, for military purposes, of rapid deployment for immediate operations to any point on the earth, or would provide for relatively sophisticated satellite or space-ferry capabilities.

The prime aerodynamic requirements for such a vehicle are (1) that it have a compact launch configuration compatible with booster rockets, (2) that it have a relatively blunt, low lift-drag ratio entry configuration, and (3) that it be an efficient powered cruise vehicle. The third requirement, being directly contradictory with the first two, leads to the desirability of changing the vehicle geometry for efficient performance in the various phases of flight. It is

* [REDACTED] Unclassified

not immediately obvious, however, that a single vehicle incorporating relatively simple configuration variations can be designed to perform efficiently in all of the three flight regimes.

One proposal for a variable-geometry vehicle designed to meet the requirements outlined above was presented in reference 1. This vehicle employs foldable wings and jettisonable nose fairings over an air-breathing-engine inlet. In the launch and entry conditions it is essentially of blunt, conical shape contoured to trim at an attitude compatible with entry requirements. For the cruise condition the wings and associated stabilizing fins are unfolded from the top of the vehicle, the heat-shield fairings are jettisoned, and the vehicle becomes a relatively conventional aircraft with air-breathing jet engines.

It is the purpose of this report to present the results of aerodynamic force and moment tests of the vehicle from subsonic to moderate supersonic speeds. It was desired to determine if the configuration is stable and capable of being trimmed to the required attitude for the entry phase, the aerodynamic properties during the wing unfolding phase, and to evaluate the performance and stability characteristics of the cruise configuration.

NOTATION

b	width of model at base (span)
c	local chord
\bar{c}	mean aerodynamic chord, $\frac{\int c^2 dy}{\int c dy}$
C_D	drag coefficient, $\frac{\text{drag}}{q_\infty S}$
C_l	rolling-moment coefficient, $\frac{\text{rolling moment}}{q_\infty Sb}$
C_L	lift coefficient, $\frac{\text{lift}}{q_\infty S}$
C_m	pitching-moment coefficient, $\frac{\text{pitching moment}}{q_\infty S\bar{c}}$
C_n	yawing-moment coefficient, $\frac{\text{yawing moment}}{q_\infty Sb}$
C_Y	side-force coefficient, $\frac{\text{side force}}{q_\infty S}$
l	body length

$\frac{L}{D}$	lift-drag ratio, $\frac{C_L}{C_D}$
M_∞	free-stream Mach number
q_∞	free-stream dynamic pressure
S	wing plan-form area, $\theta_t = \theta_w = 0^\circ$
\bar{V}	fraction of satellite velocity
$\bar{x}, \bar{y}, \bar{z}$	Cartesian coordinate system normalized with body length, l
\bar{w}	vehicle weight
α	angle of attack, deg
β	angle of sideslip, deg
θ_t	wing-tip deflection angle, deg, positive downward
θ_w	wing deflection angle
$C_{L\alpha}, C_{m\alpha}$	derivatives with respect to angle of attack α , evaluated at $\alpha = 0$, per deg
$C_{l\beta}, C_{n\beta}, C_{Y\beta}$	derivatives with respect to sideslip angle β , evaluated at $\beta = 0$, per deg

EXPERIMENT

The variable-geometry vehicle and the factors considered in its development are described in detail in the appendix. Figures 1, 2, and 3 show, respectively, the entry configuration, the wings being unfolded, and the cruise configuration. Figure 4 shows how the vehicle might appear on a booster. Some of the models of the vehicle that were tested differed in detail from the desired configuration because of the necessity for balance installation and attachments as required by the particular test facilities.

Wind Tunnels and Models

Subsonic tests.- Tests were conducted in the Ames 7- by 10-Foot Wind Tunnel at a Mach number of 0.2 and a dynamic pressure of 50 psf for the model shown in figure 3. The model was supported from the scale balance assembly by means of two steel rods driven into the two outboard simulated jet-exhaust openings in the model.

Transonic tests. - Transonic aerodynamic characteristics were determined in the Ames 2- by 2-Foot Transonic Wind Tunnel (ref. 2) at Mach numbers from 0.6 to 1.3. A six-component strain-gage balance mounted on a sting support was used to measure the aerodynamic forces and moments. A pressure cell was used to measure the base pressure. A sketch of the model is shown in figure 5. This sketch, when compared to figures 1 and 3, indicates the modifications necessary to accommodate the balance. Different wings were constructed for investigating the effects of deflecting the wing-tip panel 45° and 90° . Three nose shapes were used: a 90° semicone, a 39.5° semicone, and a semi-hemisphere. A view of the model with the 39.5° semicone nose, and the wing-tip panels deflected 90° is shown mounted in the tunnel in figure 6.

Supersonic tests. - The same models shown in figures 5 and 6 were tested at low angles of attack in the Ames 10- by 14-Inch Supersonic Wind Tunnel (ref. 3) at Mach numbers from 3 to 5.

In order to investigate the wing folding process at high angles of attack, additional smaller models were constructed with an offset sting support angle of 40° . A three-view drawing of a model representing the entry configuration is shown in figure 7. A series of wings representing various stages of the wing-folding process was tested on the body shown in figure 8. Wings having fold angles of 120° , 90° , 60° , 30° , and 0° were tested. The fully folded condition represents a wing-fold angle of 135° . A view with the wings folded 60° is shown in figure 9.

A drawing of the model representing the entry configuration with a sting support angle of 0° is shown in figure 10. This wind-tunnel model was previously shown in figure 1.

Range of Test Variables

Subsonic tests were conducted at a dynamic pressure of 50 pounds per square foot corresponding to a Mach number of 0.2 over an angle-of-attack range from -4° to $+14^\circ$. Transonic results were obtained at free-stream Mach numbers from 0.60 to 1.3 at angles of attack from -4° to $+10^\circ$. Supersonic tests were conducted at free-stream Mach numbers from 3.0 to 5.0 at angles of attack from -4° to $+50^\circ$. Lateral stability and directional data were obtained at several angles of attack for Mach numbers of 3.0, 4.0, and 5.0 through a range of sideslip angles from -4° to $+4^\circ$. Reynolds numbers for the wind-tunnel test conditions are tabulated below:

Mach number, M_∞	Total pressure, psia	Total temperature, °F	Reynolds number, ft^{-1}
0.2	14.7	68	1.5×10^6
.6	11.8	70	2.8×10^6
.9	8.9	70	2.7×10^6
1.0	8.0	70	2.5×10^6
1.1	7.0	70	2.2×10^6
1.3	5.4	70	1.7×10^6
3.0	30	50	5.1×10^6
4.0	85	50	8.7×10^6
5.0	85	200	3.7×10^6

Reduction of Data

The force and moment data were reduced to standard coefficient form using the plan-form area with wing tips undeflected as the reference area. The lift and drag coefficients are referred to the wind axes, while the remaining coefficients are referred to the body axes. The moment reference center was chosen to correspond to an estimated longitudinal center-of-gravity location at 53.5 percent of the aircraft configuration reference length, l , as shown in figure 5. This location corresponds to $0.35\bar{c}$. The vertical center-of-gravity location was taken to coincide with the center of the strain-gage balance for the model shown in figure 5. Base pressure was corrected to free-stream static pressure for the reduction of the force measurements. No correction has been applied for interference effects since these effects are considered to be small.

RESULTS AND DISCUSSION

The experimental results are presented in tables I through VI. The longitudinal and lateral aerodynamic characteristics for the aircraft configuration are given in tables I and II, respectively. Tables III and IV contain data for the entry configuration, while tables V and VI contain data for the unfolding process. Various portions of these data will be presented in graphical form to illustrate the experimental aerodynamic characteristics of the airplane configuration, the entry shape, and the wing-unfolding process.

Entry Configuration

The longitudinal and lateral aerodynamic characteristics for the entry configuration, as a function of angle of attack, are shown in figures 11 and 12, respectively. In figure 11, the experimental results for a Mach number of 5 are compared with estimated values obtained by application of Newtonian impact theory together with an estimated skin-friction drag coefficient of 0.001 (see ref. 4, appendix A). The estimated and experimental values appear to be in reasonable agreement. It may be noted that a trim angle of about 40° angle of attack and a maximum lift-drag ratio less than 1.5 were realized. The lateral stability derivatives in figure 12 indicated essentially neutral lateral stability through a wide range of angles of attack.

Wing-Unfolding Configuration

Experimental results as a function of wing-fold angle are presented in figures 13 and 14 for a Mach number of 3, and for angles of attack of 40° and 25° , respectively. From figure 13(a), it may be noted that an abrupt change occurs in pitching moment with a nose-down moment as the wings reach their fully opened position. This effect is not so pronounced at an angle of attack of 25° , illustrated in figure 13(b). These results indicate that it would be necessary

to deflect the wing tips to maintain control of the aerodynamic center as the wing-unfolding process neared completion. Insofar as the wing tips would normally be deflected at supersonic speeds, no particular problem with pitching-moment variation should be encountered. However, from figure 14(a), it appears that an unstable yawing moment occurs early in the wing opening procedure at a wing-fold angle of 90° and at an angle of attack of 40° . Although this does not occur at an angle of attack of 25° , it appears that the reaction control system may be required to provide artificial stabilization in the yaw direction. As an alternative the vehicle could be pitched to 25° just prior to initiating the unfolding procedure. In any event, the unfolding process is not a lengthy one and a momentary instability should not preclude satisfactory operation.

Aircraft Configuration

Typical aerodynamic characteristics as a function of angle of attack for subsonic, transonic, and supersonic Mach numbers are illustrated in figures 15, 16, and 17. Figure 15 contains results for the aircraft configuration, previously shown in figure 3. Figures 16 and 17 contain data for the basic model shown in figure 5 with the 90° cone nose, and with the wing tips undeflected. For angles of attack up to 8° , which is well beyond that for maximum lift-drag ratio, the lift and moment coefficients are essentially linear. However, the moment curves appear to break in the unstable direction above an angle of attack of 7° at subsonic and transonic speeds. It may be noted from figure 15 that the aircraft configuration achieves a lift-drag ratio of about 10 at low subsonic speed at an angle of attack of about 1° .

The effects of Mach number on lift- and moment-curve slope, minimum drag, and maximum lift-drag ratio are shown in figure 18. Data are included for all three nose shapes, again with the wing tips undeflected.

The hemispherical nose shape was used to represent the full-scale configuration with the fairing retained over the engine nose inlet. This fairing could be retained after atmosphere entry until the vehicle speed was reduced to a Mach number less than 2 in order to prevent a "buzz" phenomenon from occurring in the inlet at higher speeds. The 39.5° nose cone is assumed to represent the configuration with blocked flow at the inlet with complete spillage, and is assumed to represent the full-scale configuration until the engines were started. It was impractical to simulate the nose inlet on the small models. The 90° nose cone is considered to be more nearly representative of the full-scale vehicle because it was estimated to have the same drag (within 5 percent) as the exposed portion of the full-scale inlet. Full flow was assumed through the inlet for this calculation.

Lift-curve slope, measured at $\alpha = 0$, is presented in figure 18(a). Theoretical values for wings of moderate aspect ratio at near-sonic speeds (ref. 5) and for a flat plate at supersonic speeds (ref. 6) are included for comparison.

The effects of nose shape on minimum drag (fig. 18(c)) are about as expected, with the 39.5° nose cone causing a large drag increase. The measured drag increment between the 9° and 39.5° nose cones at a Mach number of 3 was within 5 percent of a drag increment calculated independently from theoretical cone pressures and estimated skin-friction coefficients.

The variation in drag due to nose shape is reflected in maximum lift-drag ratios. At the design Mach number of 2, it appears possible to realize maximum lift-drag ratios of about 5.

Longitudinal stability.- Deflection of the wing tips about streamwise hinge lines at supersonic speeds reduces the rearward movement of the aerodynamic center and, at the same time, introduces additional vertical stabilizing area. In this manner drag penalties associated with excessively large control surfaces and vertical stabilizing area can be minimized (see ref. 7). However, the deflection of the wing tips can be expected to have an effect on other aerodynamic characteristics as well as pitching moment. These effects are shown in figure 19 for tip deflections of 0° , 45° , and 90° . It may be noted from figure 19 that a tip deflection of 45° has very little effect on lift-curve slope and maximum lift-drag ratio, whereas a tip deflection of 90° reduces the lift-curve slope and causes a corresponding reduction in maximum lift-drag ratio. The reduction in static stability at supersonic speeds due to wing-tip deflection is indicated in the variation of moment-curve slope. In order to show these effects on the aerodynamic center more directly, this parameter is shown for each tip condition as a function of Mach number in figure 20. This figure illustrates the important result that by programming wing tip deflection from subsonic to supersonic speeds, the rearward travel of the aerodynamic center can be limited to only about 2 percent of the mean aerodynamic chord up to a Mach number of 2, and about 4 percent at a Mach number of 3. These results are in essential agreement with reference 7. Data in figures 19 and 20 showing a slight subsonic unstable moment were obtained with one of the models modified to accommodate the strain-gage balance. Data obtained with the model shown in figure 3 without modification to accept a balance do not indicate a longitudinal instability at a Mach number of 0.2.

Lateral stability.- The supersonic lateral stability derivatives evaluated at $\alpha = 0^\circ$ are presented in figure 21. Data for the body alone, and for the body and wing combination without the vertical stabilizers are also included. The addition of the vertical stabilizers provides a stabilizing yawing moment. Deflecting the tips 90° essentially doubles the stability coefficient in the yaw direction.

CONCLUDING REMARKS

The results of the study indicate that the aerodynamics of the vehicle pose no problems that would preclude the satisfactory operation of the vehicle. Folding the wings provided a suitably compact and blunt configuration for atmosphere entry, with a maximum lift-drag ratio less than 1.5, and an angle of trim of about 40° . The favorable interference effect would permit the aircraft configuration to achieve a lift-drag ratio of about 5 at a Mach number of 2, and a maximum lift-drag ratio of about 10 at a Mach number of 0.2.

[REDACTED]

The use of wing-tip droop provided satisfactory control of the static margin from subsonic to supersonic speeds.

Ames Research Center
National Aeronautics and Space Administration
Moffett Field, Calif., June 27, 1962

APPENDIX

SELECTION OF STUDY CONFIGURATION

Prior to the present wind-tunnel investigation, a study was made to define a vehicle complying with the requirements outlined in the Introduction of this report (see also ref. 1). It should be noted at the outset, however, that the configuration selected in the present study represents only one example of this type of vehicle. A résumé of the considerations that went into the selection of this particular configuration, which is shown in figures 1 to 4, is included in this appendix for the interested reader. Both the selection of geometry and a simple weight and performance analysis are discussed.

SELECTION OF GEOMETRY

The geometry of the present configuration was determined by the three requirements noted earlier; namely, it had to be (1) a compact launch configuration compatible with booster rockets, (2) a relatively blunt low lift-drag ratio entry configuration, and (3) an efficient powered-cruise vehicle. A configuration satisfying the second of these requirements will almost automatically satisfy the first. For this reason, no further attention will be given to the launch phase of flight other than to note that the present configuration with its wings folded is indeed a compact launch configuration as is illustrated in figure 4. The second two requirements are those which, in the main, dictate the configuration geometry.

Entry Requirements

The entry configuration was designed to have a lift-drag ratio between 0.5 and 1.5. The lower limit was selected so that the vehicle would have suitable entry decelerations and range control. The upper limit was selected to limit the entry heat loads to levels compatible with the use of an ablation heat shield (refs. 8 and 9). To satisfy this condition in part, the entry vehicle was designed to trim at about 40° angle of attack. This relatively large trim angle increases the bluntness of the vehicle for better heat dissipation (ref. 10). The desired trim angle and adequate longitudinal stability were obtained by the use of a fuselage with a blunted conical forebody and with an afterbody boattailed into an elliptic section (refs. 4 and 11). The lift-drag ratio and the center-of-pressure locations as functions of angle of attack for hypersonic Mach numbers are shown in figures 22 and 23. The inherent longitudinal stability indicated by the rearward travel of the center of pressure as angle of attack increases is a direct result of the rather severe boattailing of the configuration. For the assumed center-of-gravity location, trim is obtained at the desired angle of attack. With entry at this attitude the folded wings are stowed in the shadowed region above the body, and the wings are thus in a region of relatively low

[REDACTED]

heating. Recognition was given to the advantages of closing the wings so that the leading edges joined along a line from the apex of the body. This arrangement minimized the size of the entry fairings and also provided structural rigidity. After the period of high heating, the wings are rotated 135° about a skewed hinge line. The unfolding should occur at a point where the dynamic pressure is low. If the altitude is high, a reasonable increment in range is obtained as the vehicle glides to its operational altitude. In figure 24, equilibrium glide trajectories are presented for a range of values of the parameter W/C_{LS} representative of the entry configuration. The curve for W/C_{LS} of 200 pounds per square foot intersects an altitude of 120,000 feet at a Mach number of 5 which is a suitable condition to initiate the unfolding process. Presently available engines will not start at this condition, of course, and the vehicle may be required to glide to an altitude between 20,000 and 30,000 feet and to be at a subsonic Mach number before the cruise engines can be started. With the addition of auxiliary starting equipment, however, windmilling starts could be accomplished at an altitude of 60,000 feet and at Mach numbers between 1 and 2.

Cruise Requirements

With the wings unfolded, and with the nose fairing over the inlet jettisoned, the cruise configuration is obtained. For cruise flight, aerodynamic efficiency is a prime consideration and a maximum lift-to-drag ratio of at least 5 was taken as a requirement for the present configuration. The achievement of a lift-drag ratio of 5 required that a reasonably high fineness ratio fuselage be used and that maximum advantage be taken of favorable lift interference effects. The 90° semicone fuselage represents a reasonable compromise between the minimum lift-drag ratio acceptable for the cruise configuration and the maximum lift-drag ratio acceptable for the entry configuration. Favorable lift interference (see refs. 12, 13, 14, and 15) results from the interaction of the pressure fields on the semicone body and the lower surface of the wing. At each supersonic Mach number there is a point on the body beyond which the pressure field generated by the body does not interact with the pressure field of the wing, and hence, has no further effect on the lift characteristics. At this point on the body for the design Mach number, the boattailing of the lower surface was begun. The boattailing, as noted previously, is useful in the attainment of the desired entry trim angle, and also provides the cruise configuration with an incremental pitching moment that reduces the trim-drag penalty. The upper surface of the fuselage was severely contoured to minimize base area, thus reducing base drag. Care was taken in locating the canopy in order that its pressure influence on the wing would not adversely affect drag (ref. 16).

A desire to limit the over-all length of the fuselage to about 30 feet led to the use of four small engines rather than a single large one. The engines selected are about 9 feet long and weigh about 500 pounds each. The sea-level thrust rating of the four engines is about 14,000 pounds; thus a high thrust-to-weight ratio suitable for short field takeoffs and, with thrust reversal, landings is provided. The maximum Mach number of the engines is 2 and this dictated the inlet geometry.

The basically triangular wing plan form was faired smoothly to the nose inlet (ref. 17). The wing trailing edge was swept slightly to encourage a more rearward location of the center of pressure without unduly lengthening the overall configuration. An added advantage results from a slightly more rearward location of the directional control and stabilizing surfaces. Additional directional stability at supersonic speeds was obtained from wing-tip droop which was also used to minimize the travel of the aerodynamic center from subsonic to supersonic speeds (refs. 7 and 18).

WEIGHT AND PERFORMANCE ANALYSIS

With the geometry of the configuration selected, a simple estimate of the weight was made. In addition, various internal arrangements of the fuselage were considered in order to determine that the center of gravity could be located to provide a small static margin throughout the operating Mach number range. Two of the arrangements are shown in figures 25 and 26. The vehicle arrangement shown in figure 25 is a high-performance configuration with four engines and 6000 pounds of fuel. This vehicle is equipped to perform some type of military mission with the result that there is no space or weight allowance for material that does not pertain to the execution of the military mission. Figure 26 presents an alternate arrangement with a single engine, 1000 pounds of fuel, and cargo or passenger space. This latter configuration would have a payload capability of 7200 pounds. The weight breakdown for these two configurations is shown in figures 25 and 26. The following table itemizes some of the pertinent weights.

Item	Military version, lb	Cargo version, lb
Launch weight	20,000	20,000
Entry weight	19,500	19,500
Cruise weight full	16,500	16,500
Cruise weight empty	10,500	8,300

For these estimates, the structural weight was taken as 27 percent of the gross weight. This ratio is considered suitable for a supersonic aircraft with a largely steel structure. It should be noted that supersonic transport and military aircraft currently under consideration will be constructed extensively of steel to maintain a safe stress limit at elevated temperatures. The weight needed for thermal protection during entry was estimated to be 2000 pounds or 10 percent of the launch weight. The calculations which led to this weight were based on the use of Teflon as an ablative material and included the material needed to insulate the vehicle from the convective heat transfer not blocked by the ablation process. No attempt was made to optimize the means by which adequate thermal protection could be provided; however, some other method such as film cooling utilizing the fuel supply could possibly also provide thermal protection. As noted earlier, each of the four engines was taken to weigh 500 pounds. An allowance of 6000 pounds was made for fuel. An additional allowance of 1500 pounds was made for retrorockets, reaction controls, and fairings. This latter weight as well as all the thermal protection was assumed to be jettisoned for cruise operation.

The flight operation envelope for the military version of the vehicle is shown in figure 27. The performance is based on current engine thrust characteristics, including the standard aircraft industry association inlet losses and on calculated values of lift-drag ratio. From these estimates, and with 6000 pounds of fuel when reaching the operational altitude, the vehicle would have a radius of action of 400 miles at a Mach number of 2 with 12 minutes of flight time. Similarly at a Mach number of 0.8, a radius of action of 800 miles providing 1 hour and 28 minutes of flight time would be obtainable.

[REDACTED]

REFERENCES

1. Eggers, Alfred J., Jr., and Wong, Thomas J.: Motion and Heating of Lifting Vehicles During Atmosphere Entry. ARS Journal, vol. 31, no. 10, Oct. 1961, pp. 1364-1375.
 2. Spiegel, Joseph M., and Lawrence, Leslie F.: A Description of the Ames 2- by 2-Foot Transonic Wind Tunnel and Preliminary Evaluation of Wall Interference. NACA RM A55I21, 1956.
 3. Eggers, A. J., Jr., and Nothwang, George J.: The Ames 10- by 14-Inch Supersonic Wind Tunnel. NACA TN 3095, 1954.
 4. McDevitt, John B., and Rakich, John V.: The Aerodynamic Characteristics of Several Thick Delta Wings at Mach Numbers to 6 and Angles of Attack to 50°. NASA TM X-162, 1960.
 5. Jones, Robert T.: Properties of Low-Aspect-Ratio Pointed Wings at Speeds Below and Above the Speed of Sound. NACA Rep. 835, 1946. (Formerly NACA TN 1032)
 6. Staff of the Ames 1- by 3-Foot Supersonic Wind-Tunnel Section: Notes and Tables for Use in the Analysis of Supersonic Flow. NACA TN 1428, 1947.
 7. Peterson, Victor L.: The Effects of Streamwise-Deflected Wing Tips on the Aerodynamic Characteristics of an Aspect-Ratio-2 Triangular Wing, Body, and Tail Combination. NASA MEMO 5-18-59A, 1959.
 8. Eggers, Alfred J., Jr., and Wong, Thomas J.: Reentry and Recovery of Near-Earth Satellites, With Particular Attention to a Manned Vehicle. NASA MEMO 10-2-58A, 1958.
 9. Allen, H. Julian, and Eggers, A. J., Jr.: A Study of the Motion and Aerodynamic Heating of Missiles Entering the Earth's Atmosphere at High Supersonic Speeds. NACA TN 4047, 1957.
 10. Reller, John O., Jr.: Heat Transfer to Blunt Axially Symmetric Bodies. NASA TM X-391, 1960.
 11. Rakich, John V.: Supersonic Aerodynamic Performance and Static-Stability Characteristics of Two Blunt-Nosed, Modified 13° Half-Cone Configurations. NASA TM X-375, 1960.
 12. Eggers, A. J., Jr., and Syvertson, Clarence A.: Aircraft Configurations Developing High Lift-Drag Ratios at High Supersonic Speeds. NACA RM A55L05, 1956.
 13. Syvertson, Clarence A., Wong, Thomas J., and Gloria, Hermilo R.: Additional Experiments With Flat-Top Wing-Body Combinations at High Supersonic Speeds. NACA RM A56I11, 1957.
- [REDACTED]

- [REDACTED]
14. Eggers, A. J., Jr.: Some Considerations of Aircraft Configurations Suitable for Long-Range Hypersonic Flight. Colston Papers, Proceedings of the Eleventh Symposium of the Colston Research Society held in the University of Bristol, April 6-8, 1959.
 15. Migotsky, Eugene, and Adams, Gaynor J.: Some Properties of Wing and Half-Body Arrangements at Supersonic Speeds. NACA RM A57E15, 1957.
 16. Dennis, David H., and Petersen, Richard H.: Aerodynamic Performance and Static Stability at Mach Numbers Up to 5 of Two Airplane Configurations With Favorable Lift Interference. NASA MEMO 1-8-59A, 1959.
 17. Seiff, Alvin, and Allen, H. Julian: Some Aspects of the Design of Hypersonic Boost-Glide Aircraft. NACA RM A55E26, 1955.
 18. Petersen, Richard H.: The Effects of Wing-Tip Droop on the Aerodynamic Characteristics of a Delta-Wing Aircraft at Supersonic Speeds. NASA TM X-363, 1960.

TABLE I.-LONGITUDINAL AERODYNAMIC CHARACTERISTICS FOR THE AIRCRAFT CONFIGURATION; $\theta_w = 0^\circ$
 (a) Body Alone, 9° Nose

$M_\infty = 3.0$					$M_\infty = 4.0$					$M_\infty = 5.0$				
α deg	C_L	C_D	C_m	L/D	α deg	C_L	C_D	C_m	L/D	α deg	C_L	C_D	C_m	L/D
-4.1	-0.020	0.011	0.0048	-1.86	-4.1	-0.014	0.009	0.0027	-1.64	-4.0	-0.012	0.008	0.0003	-1.52
-3.0	.014	.010	.0051	-1.43	-3.0	-.009	.008	.0033	-1.19	-3.0	-.007	.007	.0010	-.92
-2.0	-.009	.009	.0057	-.94	-2.0	-.005	.008	.0040	-.63	-2.0	-.002	.007	.0025	-.34
-1.0	-.003	.009	.0064	-.35	-1.0	.001	.007	.0045	.09	-1.0	.004	.007	.0024	.51
.1	.004	.009	.0071	.39	.1	.006	.007	.0050	.79	0	.008	.007	.0034	1.16
1.1	.010	.010	.0076	1.06	1.1	.011	.008	.0055	1.46	1.0	.014	.008	.0036	1.82
2.1	.017	.010	.0080	1.65	2.1	.017	.009	.0059	2.00	2.1	.018	.008	.0051	2.19
3.1	.024	.011	.0086	2.14	3.1	.023	.009	.0063	2.43	3.1	.023	.009	.0059	2.51
4.2	.030	.012	.0095	2.48	4.2	.028	.010	.0072	2.72	4.1	.029	.011	.0064	2.72
5.2	.038	.014	.0098	2.73	5.2	.035	.012	.0076	2.91	5.1	.034	.012	.0062	2.90
6.2	.046	.016	.0105	2.88	6.2	.041	.014	.0084	2.98	6.1	.039	.014	.0073	2.89
7.3	.053	.018	.0111	2.95	7.3	.047	.016	.0091	2.99	7.1	.044	.015	.0082	2.88
8.3	.061	.021	.0120	2.96	8.3	.053	.018	.0099	2.96	8.1	.049	.018	.0090	2.79
9.3	.068	.023	.0128	2.92	9.3	.058	.020	.0108	2.89	9.1	.054	.020	.0099	2.71
10.4	.076	.026	.0135	2.86	10.4	.064	.023	.0116	2.80	10.2	.059	.023	.0103	2.62
11.4	.082	.030	.0147	2.76						11.2	.064	.025	.0113	2.52
$M_\infty = 0.60$					$M_\infty = 0.80$					$M_\infty = 0.90$				
-4.1	-.050	.0112	.0125	-4.42	-4.1	-.052	.0104	.0128	-5.00	-4.1	-.056	.0118	.0145	-4.73
-2.0	-.035	.0093	.0134	-3.76	-2.1	-.037	.0085	.0139	-4.41	-2.1	-.041	.0095	.0157	-4.32
0	-.020	.0080	.0143	-2.51	0	-.022	.0072	.0147	-2.98	0	-.024	.0082	.0164	-2.93
2.0	-.003	.0077	.0158	-.45	2.1	-.005	.0070	.0165	-.65	2.1	-.006	.0077	.0174	-.78
4.1	.013	.0086	.0175	1.49	4.1	.014	.0078	.0174	1.83	4.1	.014	.0086	.0183	1.61
6.1	.032	.0105	.0185	3.07	6.2	.034	.0097	.0191	3.45	6.2	.033	.0104	.0197	3.19
8.2	.050	.0137	.0209	3.67	8.3	.053	.0131	.0210	4.04	8.3	.054	.0141	.0216	3.82
$M_\infty = 1.00$					$M_\infty = 1.10$					$M_\infty = 1.30$				
-4.2	-.072	.0186	.0245	-3.88	-4.2	-.068	.0203	.0246	-3.37	-4.1	-.057	.0192	.0217	-2.98
-2.1	-.055	.0158	.0242	-3.46	-2.1	-.051	.0175	.0241	-2.92	-2.1	-.041	.0168	.0212	-2.42
0	-.036	.0137	.0237	-2.62	0	-.033	.0157	.0237	-2.10	0	-.023	.0155	.0211	-1.50
2.1	-.014	.0128	.0232	-1.10	2.1	-.013	.0152	.0232	-.84	2.1	-.004	.0153	.0210	-.29
4.1	.007	.0130	.0226	.54	4.2	.009	.0157	.0227	.55	4.2	.016	.0163	.0206	.98
6.2	.030	.0151	.0221	1.99	6.3	.030	.0181	.0226	1.66	6.3	.037	.0187	.0210	1.96
8.3	.054	.0187	.0223	2.89	8.4	.052	.0218	.0230	2.40	8.4	.058	.0226	.0217	2.55

6

TABLE I.-LONGITUDINAL AERODYNAMIC CHARACTERISTICS FOR THE AIRCRAFT CONFIGURATION - Continued
 (b) Complete Model, 39.5° Nose, $\theta_T = 0^\circ$

TABLE I.-LONGITUDINAL AERODYNAMIC CHARACTERISTICS FOR THE AIRCRAFT CONFIGURATION - Continued
 (c) Complete Model, 9° Nose, $\theta_t = 0^{\circ}$

$M_{\infty} = 3.0$					$M_{\infty} = 4.0$					$M_{\infty} = 5.0$				
α deg	C_L	C_D	C_m	I/D	α deg	C_L	C_D	C_m	I/D	α deg	C_L	C_D	C_m	I/D
-4.2	-0.065	0.020	0.0099	-3.24	-4.2	-0.048	0.015		-3.22	-4.1	-0.051	0.016	0.0073	-3.18
-3.2	-.056	.018	0.0099	-3.07	-3.1	-.041	.015		-2.76	-3.1	-.037	.014	.0071	-2.62
-2.1	-.031	.017		-1.88	-2.1	-.025	.013	0.0077	-1.91	-2.0	-.021	.013	.0059	-1.60
-1.0	-.002	.015	.0051	.14	-1.0	-.006	.012	.0056	-.45	-1.0	-.004	.012	.0043	-.30
.1	.027	.016	.0026	1.72	.1	.017	.012	.0025	1.38	0	.016	.013	.0016	1.26
1.2	.054	.017	.0003	3.19	1.2	.037	.013	.0003	2.77	1.1	.031	.013	.0014	2.32
2.3	.082	.019	-.0024	4.27	2.3	.057	.015	-.0018	3.84	2.1	.048	.015	-.0003	3.24
3.4	.109	.023	-.0045	4.76	3.3	.077	.017	-.0037	4.44	3.1	.065	.017	-.0019	3.80
4.5	.136	.027	-.0072	4.97	4.4	.097	.021	-.0054	4.71	4.2	.082	.020	-.0038	4.09
5.6	.166	.034	-.0105	4.96	5.5	.120	.025	-.0076	4.75	5.2	.102	.024	-.0058	4.23
6.7	.192	.040	-.0125	4.78	6.6	.140	.030	-.0092	4.60	6.2	.120	.029	-.0075	4.17
7.8	.212	.047	-.0134	4.54	7.7	.161	.037	-.0107	4.40	7.3	.137	.034	-.0086	4.08
8.9	.236	.055	-.0154	4.28	8.8	.180	.043	-.0117	4.16	8.3	.156	.040	-.0106	3.92
9.9	.260	.065	-.0159	4.02	9.9	.199	.051	-.0109	3.91					
11.0	.276	.073	-.0173	3.79										
12.1	.300	.084	-.0192	3.55										
$M_{\infty} = 0.60$					$M_{\infty} = 0.80$					$M_{\infty} = 0.90$				
-4.4	-.195	.0254	.0240	-7.66	-4.6	-.223	.0287	.0332	-7.79	-4.7	-.256	.0347	.0508	-7.37
-2.1	-.094	.0156	.0246	-6.04	-2.2	-.112	.0163	.0308	-6.84	-2.3	-.135	.0197	.0442	-6.85
0	-.008	.0128	.0241	-.59	.1	-.011	.0127	.0275	-.87	.1	-.025	.0140	.0358	-1.80
2.2	.078	.0152	.0260	5.14	2.4	.083	.0155	.0278	5.35	2.5	.085	.0168	.0328	5.04
4.4	.174	.0244	.0283	7.12	4.7	.188	.0261	.0283	7.21	4.8	.194	.0278	.0311	6.97
6.7	.266	.0403	.0329	6.61	7.1	.296	.0452	.0308	6.53	7.3	.309	.0492	.0332	6.28
8.9	.366	.0647	.0385	5.66	9.4	.398	.0731	.0376	5.44	9.7	.381	.0551		5.62
$M_{\infty} = 1.00$					$M_{\infty} = 1.10$					$M_{\infty} = 1.30$				
-4.7	-.259	.0465	.0718	-5.56	-4.6	-.238	.0461	.0700	-5.16	-4.5	-.170	.0385	.0413	-4.40
-2.2	-.145	.0315	.0667	-4.58	-2.2	-.117	.0321	.0601	-3.64	-2.1	-.061	.0279	.0313	-2.17
.1	-.040	.0255	.0590	-1.58	.3	-.002	.0276	.0481	-.07	.3	.043	.0257	.0223	1.69
2.6	.077	.0273	.0522	2.83	2.7	.107	.0315	.0372	3.38	2.7	.141	.0316	.0132	4.44
5.0	.208	.0401	.0405	5.17	5.1	.230	.0455	.0258	5.04	5.2	.245	.0461	.0043	5.31
7.5	.336	.0642	.0294	5.24	7.6	.325	.0634	.0335	5.13	7.6	.305		.0248	
9.7	.372		.0436	5.03	9.7			.0392		9.7			.0348	

TABLE I.-LONGITUDINAL AERODYNAMIC CHARACTERISTICS FOR THE AIRCRAFT CONFIGURATION - Continued
 (d) Complete Model, Semi-hemisphere Nose, $\theta_+ = 0^\circ$

TABLE I.-LONGITUDINAL AERODYNAMIC CHARACTERISTICS FOR THE AIRCRAFT CONFIGURATION - Continued
 (d) Complete Model, Semi-hemisphere Nose, $\theta_t = 0^\circ$ - Concluded

$M_\infty = 0.60$					$M_\infty = 0.80$					$M_\infty = 0.90$				
α deg	C_L	C_D	C_m	L/D	α deg	C_L	C_D	C_m	L/D	α deg	C_L	C_D	C_m	L/D
-4.3	-0.193	0.0260	0.0242	-7.43	-4.6	-0.221	0.0288	0.0342	-7.66	-4.7	-0.258	0.0359	0.0526	-7.19
-2.1	-.095	.0164	.0250	-5.81	-2.2	-.114	.0173	.0318	-6.58	-2.3	-.133	.0203	.0432	-6.53
0	-.009	.0134	.0247	-.67	.1	-.010	.0133	.0292	-.73	.1	-.025	.0148	.0358	-1.66
2.2	.074	.0156	.0272	4.70	2.4	.080	.0157	.0302	5.08	2.5	.082	.0172	.0335	4.74
4.4	.171	.0244	.0288	7.00	4.7	.185	.0261	.0313	7.07	4.8	.192	.0281	.0324	6.83
6.7	.262	.0401	.0341	6.53	7.1	.290	.0452	.0337	6.42	7.3	.305	.0492	.0353	6.20
8.9	.355	.0630	.0389	5.64	9.4	.385	.0718	.0395	5.36	9.6	.385	.0751	.0482	5.12
$M_\infty = 1.00$					$M_\infty = 1.10$					$M_\infty = 1.30$				
-4.7	-.256	.0469	.0713	-5.45	-4.6	-.233	.0472	.0663	-4.93	-4.6	-.172	.0422	.0414	-4.07
-2.3	-.147	.0327	.0670	-4.48	-2.2	-.116	.0337	.0588	-3.45	-2.1	-.063	.0315	.0318	-2.00
.1	-.041	.0262	.0590	-1.56	.2	-.005	.0290	.0482	-.16	.3	.041	.0292	.0231	1.39
2.6	.078	.0279	.0507	2.79	2.7	.105	.0326	.0378	3.22	2.7	.137	.0346	.0140	3.95
5.0	.204	.0400	.0419	5.09	5.1	.228	.0464	.0269	4.92	5.2	.241	.0487	.0059	4.95
7.5	.335	.0645	.0297	5.19	7.6	.330	.0671	.0306	4.91	7.6	.309	.0646	.0225	4.79
9.7	.377	.0449	6.09	9.8	.359		.0398	5.91	9.8	.337	.0518	.0352		6.49

TABLE I.-LONGITUDINAL AERODYNAMIC CHARACTERISTICS FOR THE AIRCRAFT CONFIGURATION - Continued
(e) Complete Model, 9° Nose, $\theta_t = 45^\circ$

$M_\infty = 3.0$					$M_\infty = 4.0$					$M_\infty = 5.0$				
α deg	C_L	C_D	C_m	L/D	α deg	C_L	C_D	C_m	L/D	α deg	C_L	C_D	C_m	L/D
-4.2	-0.074	0.021	0.0107	-3.52	-3.1	-0.033	0.014	0.0042	-2.32	-2.5	-0.021	0.013	0.0023	-1.56
-3.1	-.049	.018	.0087	-2.70	-2.1	-.015	.013	.0035	-1.17	-2.0	-.014	.013	.0025	-1.09
-2.1	-.023	.016	.0061	-1.41	-1.0	.001	.012	.0027	.09	-1.5	-.003	.013	-.0006	-.20
-1.0	.007	.015	-.0003	.46	.1	.019	.012	.0018	1.55	-1.0	0	.013	.0022	.03
.1	.037	.016	-.0030	2.36	1.2	.036	.013	.0013	2.68	0	.017	.013	.0012	1.32
1.2	.063	.017	-.0053	3.68	2.3	.054	.015	.0004	3.54	1.1	.031	.014	.0010	2.25
2.3	.090	.019	-.0076	4.64	3.3	.072	.018	-.0003	4.11	2.1	.046	.015	.0005	3.13
3.4	.116	.023	-.0068	5.03	3.6	.089	.019	-.0056	4.69	2.9	.058	.017	.0001	3.36
4.5	.143	.028	-.0092	5.11	4.4	.104	.022	-.0074	4.79					
5.6	.169	.034	-.0113	5.01	5.5	.124	.026	-.0093	4.73					
6.7	.194	.040	-.0136	4.80	6.6	.139	.031	-.0080	4.49					
7.8	.221	.048	-.0174	4.55	7.7	.167	.038	-.0131	4.37					
8.8	.245	.057	-.0184	4.28	8.8	.188	.045	-.0136	4.13					
9.9	.268	.067	-.0189	4.01	9.9	.207	.053	-.0139	3.88					
11.0	.294	.078	-.0222	3.77	10.4	.218	.058	-.0148	3.77					
12.1	.316	.089	-.0238	3.54										
$M_\infty = 0.60$					$M_\infty = 0.80$					$M_\infty = 0.90$				
-4.3	-.182	.0236	.0179	-7.71	-4.6	-.208	.0262	.0278	-7.92	-4.7	-.242	.0328	.0463	-7.38
-2.1	-.091	.0146	.0230	-6.21	-2.2	-.109	.0157	.0301	-6.91	-2.3	-.135	.0191	.0439	-7.04
0	-.008	.0119	.0246	-.67	-2.2	-.109	.0156	.0300	-6.99	.1	-.031	.0137	.0397	-2.24
2.2	.071	.0143	.0302	4.97	.1	-.018	.0121	.0300	-1.50	2.4	.075	.0159	.0381	4.68
4.4	.168	.0232	.0311	7.24	2.4	.077	.0147	.0328	5.21	4.8	.184	.0265	.0390	6.96
6.6	.252	.0378	.0407	6.65	4.7	.174	.0240	.0363	7.22	7.3	.295	.0465	.0437	6.34
8.9	.347	.0611	.0499	5.67	7.1	.282	.0429	.0418	6.57	9.6	.374	.0706	.0595	5.29
$M_\infty = 1.00$					$M_\infty = 1.10$					$M_\infty = 1.30$				
-4.6	-.238	.0442	.0628	-5.37	-4.6	-.216	.0434	.0586	-4.96	-4.5	-.156	.0369	.0337	-4.23
-2.2	-.137	.0311	.0640	-4.38	-2.2	-.107	.0318	.0557	-3.35	-2.1	-.055	.0274	.0287	-2.01
.1	-.039	.0250	.0595	-1.55	.2	-.006	.0276	.0499	-.20	.3	.044	.0256	.0223	1.72
2.6	.077	.0271	.0538	2.85	2.7	.105	.0312	.0404	3.36	2.7	.138	.0313	.0153	4.38
5.0	.205	.0388	.0443	5.27	5.1	.224	.0446	.0307	5.02	5.2	.240	.0452	.0073	5.30
7.5	.335	.0627	.0347	5.34	7.6	.320	.0625	.0371	5.12	7.6	.303	.0585	.0276	5.17
9.7	.370				9.7	.350	.0422		5.48	9.7	.331		.0372	7.39

TABLE I.-LONGITUDINAL AERODYNAMIC CHARACTERISTICS FOR THE AIRCRAFT CONFIGURATION - Continued
 (f) Complete Model, 9° Nose, $\theta_t = 90^{\circ}$

$M_{\infty} = 3.0$					$M_{\infty} = 4.0$					$M_{\infty} = 5.0$				
α deg	C_L	C_D	C_m	L/D	α deg	C_L	C_D	C_m	L/D	α deg	C_L	C_D	C_m	L/D
-4.2	-0.066	0.020	0.0058	-3.28	-3.1	-0.030	0.013	0.0040	-2.28	-2.0	-0.010	0.013	0.0011	-0.74
-3.1	-.041	.018	.0044	-2.34	-2.0	-.014	.012	.0029	-1.13	-1.5	-.003	.013	.0011	-.21
-2.0	.017	.016	.0033	-1.08	-1.0	.003	.012	.0020	.24	-1.0	-.006	.013	.0004	.43
-1.0	.007	.015	.0022	.48	.1	.022	.012	.0008	1.83	0	.020	.013	0	1.53
.1	.033	.016	.0011	2.09	1.2	.040	.013	-.0003	3.04	1.1	.035	.014	-.0005	2.47
1.2	.058	.017	.0003	3.37	2.3	.058	.015	-.0013	3.84	1.6	.044	.015	-.0010	2.90
2.3	.081	.020	-.0003	4.15	3.3	.075	.017	-.0020	4.27	2.1	.051	.016	-.0015	3.17
3.4	.104	.023	-.0004	4.53	4.4	.094	.021	-.0025	4.37	4.2	.101	.023	-.0120	4.46
4.5	.126	.027	-.0025	4.72	5.5	.112	.026	-.0031	4.38	5.2	.120	.027	-.0148	4.47
5.5	.148	.032	-.0032	4.66	6.6	.131	.030	-.0036	4.28	6.2	.140	.032	-.0176	4.35
6.6	.171	.038	-.0041	4.51	7.7	.147	.036	-.0035	4.11	7.3	.159	.038	-.0202	4.22
7.7	.189	.044	-.0040	4.31	8.8	.166	.042	-.0027	3.91	8.3	.142	.039	-.0031	3.60
8.8	.207	.050	-.0036	4.10	9.9	.181	.049	-.0017	3.70	8.6	.147	.041	-.0033	3.57
9.8	.224	.058	-.0041	3.88	10.4	.192	.053	-.0041	3.61	8.8	.151	.043	-.0038	3.53
10.9	.247	.068	-.0048	3.65										
12.0	.268	.078	-.0061	3.45										
$M_{\infty} = 0.60$					$M_{\infty} = 0.80$					$M_{\infty} = 0.90$				
-4.3	-.153	.0207	.0101	-7.39	-4.5	-.172	.0227	.0161	-7.60	-4.6	-.196	.0270	.0280	-7.26
-2.1	-.079	.0141	.0201	-5.60	-2.2	-.092	.0150	.0263	-6.15	-2.2	-.111	.0176	.0352	-6.27
0	-.012	.0123	.0267	-.97	.1	-.017	.0124	.0314	-1.34	.1	-.029	.0141	.0389	-2.07
2.2	.064	.0145	.0353	4.38	2.4	.066	.0148	.0387	4.49	2.4	.064	.0163	.0435	3.92
4.4	.135	.0217	.0453	6.24	4.7	.147	.0230	.0483	6.39	4.8	.151	.0248	.0520	6.10
6.6	.212	.0346	.0585	6.11	7.0	.234	.0385	.0595	6.08	7.2	.242	.0412	.0644	5.86
8.8	.290	.0541	.0726	5.35	9.3	.310	.0599	.0759	5.17	7.2	.243	.0413	.0640	5.88
$M_{\infty} = 1.00$					$M_{\infty} = 1.10$					$M_{\infty} = 1.30$				
-4.6	-.202	.0392	.0472	-5.16	-4.5	-.181	.0391	.0429	-4.62	-4.5	-.133	.0341	.0246	-3.90
-2.2	-.118	.0287	.0548	-4.12	-2.1	-.092	.0301	.0480	-3.04	-2.1	-.047	.0266	.0254	-1.75
.1	-.035	.0250	.0571	-1.40	.3	0	.0275	.0471	.01	.3	.039	.0262	.0245	1.49
2.6	.065	.0270	.0594	2.41	2.7	.093	.0309	.0468	3.02	2.7	.122	.0314	.0230	3.89
5.0	.171	.0366	.0595	4.66	5.1	.193	.0424	.0467	4.53	5.1	.211	.0438	.0225	4.82
7.4	.287	.0575	.0557	5.00	7.5	.297	.0639	.0447	4.64	7.5	.294	.0641	.0271	4.58
9.7	.358	.0768	.0499	4.66	9.7	.337	.0793	.0461	4.24	9.7	.318	.0754	.0395	4.21

TABLE I.--LONGITUDINAL AERODYNAMIC CHARACTERISTICS FOR THE AIRCRAFT CONFIGURATION - Concluded
 (g) Complete Model, Except No Vertical Stabilizers, 9° Nose, $\theta_t = 0^\circ$

$M_\infty = 3.0$					$M_\infty = 4.0$					$M_\infty = 5.0$				
α deg	C_L	C_D	C_m	I/D	α deg	C_L	C_D	C_m	I/D	α deg	C_L	C_D	C_m	I/D
-4.2	-0.076	0.020	0.0101	-3.79	-4.2	-0.057	0.016	0.0087	-3.59	-4.1	-0.050	0.014	0.0064	-3.47
-3.1	-.055	.017	.0107	-3.13	-3.1	-.030	.013	-.0022	-2.32	-3.1	-.034	.013	.0053	-2.71
-2.1	-.029	.015	.0081	-1.91	-2.1	-.022	.012	.0068	-1.79	-2.0	-.018	.012	.0046	-1.55
-1.0	.001	.014	.0052	.03	-1.0	-.002	.011	.0037	.17	-1.0	-.002	.011	.0030	-.20
.1	.029	.015	.0019	1.96	.1	.018	.011	.0020	1.57	0	.015	.011	.0019	1.34
1.2	.056	.016	-.0008	3.54	1.2	.037	.012	-.0003	3.06	1.1	.032	.012	.0008	2.63
2.3	.082	.018	-.0033	4.56	2.3	.056	.014	-.0016	4.04	2.1	.048	.014	-.0007	3.47
3.4	.108	.021	-.0057	5.04	3.3	.076	.017	-.0034	4.58	3.1	.066	.016	-.0019	4.05
4.5	.135	.026	-.0085	5.22	4.4	.096	.020	-.0054	4.85	4.2	.082	.019	-.0034	4.26
5.6	.164	.032	-.0109	5.15	5.5	.121	.025	-.0086	4.88	5.2	.100	.023	-.0040	4.24
6.7	.190	.038	-.0130	4.93	6.6	.142	.030	-.0105	4.71	6.2	.118	.028	-.0053	4.19
7.7	.214	.046	-.0149	4.63	7.7	.161	.036	-.0118	4.47	7.3	.135	.033	-.0072	4.09
8.8	.236	.054	-.0165	4.34	8.8	.181	.043	-.0124	4.21	8.3	.154	.040	-.0087	3.90
9.9	.258	.063	-.0170	4.07	9.9	.199	.050	-.0121	3.96	9.3	.172	.046	-.0105	3.71
11.0	.282	.074	-.0188	3.81						10.4	.192	.054	-.0130	3.53
12.1	.305	.085	-.0209	3.58										
$M_\infty = 0.60$					$M_\infty = 0.80$					$M_\infty = 0.90$				
-4.3	-.195	.0252	.0272	-7.74	-4.6	.224	.0278	.0372	-8.03	-4.7	.259	.0345	.0569	-7.50
-2.1	-.098	.0155	.0280	-6.30	-2.2	-.116	.0157	.0341	-7.36	-2.3	-.140	.0192	.0477	-7.27
0	-.014	.0117	.0267	-1.17	.1	-.020	.0115	.0306	-1.72	.1	-.033	.0132	.0400	-2.47
2.2	.070	.0137	.0302	5.11	2.4	.084	.0140	.0280	6.04	2.4	.070	.0150	.0391	4.66
4.4	.168	.0227	.0328	7.40	4.7	.182	.0246	.0328	7.40	4.9	.196	.0272	.0344	7.20
6.7	.272	.0408	.0344	6.67	7.1	.301	.0459	.0320	6.54	7.3	.320	.0504	.0309	6.34
8.9	.374	.0668	.0402	5.59	9.5	.416	.0773	.0356	5.38	9.7	.398	.0677	.0555	5.87
$M_\infty = 1.00$					$M_\infty = 1.10$					$M_\infty = 1.30$				
-4.6	-.253	.0442	.0728	-5.72	-4.6	.222	.0424	.0653	-5.24	-4.5	..167	.0365	.0417	-4.56
-2.2	-.142	.0295	.0674	-4.80	-2.2	-.111	.0303	.0582	-3.66	-2.1	-.061	.0260	.0321	-2.34
.1	-.041	.0230	.0600	-1.75	.2	-.006	.0259	.0501	-.24	.3	.039	.0240	.0238	1.63
2.6	.083	.0252	.0518	3.28	2.7	.106	.0291	.0380	3.65	2.7	.138	.0292	.0137	4.71
5.1	.214	.0391	.0376	5.47	5.1	.233	.0442	.0245	5.28	5.2	.247	.0443	.0029	5.57
7.5	.344	.0635	.0257	5.41	7.6	.330	.0633	.0298	5.21	7.6	.310	.0606	.0214	5.12
9.8	.382		.0445		9.8	.359			6.46	9.8	.337		.0360	

TABLE II.-LATERAL AERODYNAMIC CHARACTERISTICS FOR THE AIRCRAFT CONFIGURATION
 (a) Body Alone, 9° Nose

$M_{\infty} = 3.0$					$M_{\infty} = 4.0$					$M_{\infty} = 5.0$				
α deg	β deg	C_Y	C_n	C_l	α deg	β deg	C_Y	C_n	C_l	α deg	β deg	C_Y	C_n	C_l
0	-4.0	-0.0126	-0.0010	-0.00031	0.1	-4.0	-0.0121	-0.0005	-0.00027	0	-4.0	-0.0130	-0.0009	-0.00020
0	-3.0	-.0095	-.0008	-.00019	.1	-3.0	-.0090	-.0004	-.00021	0	-3.0	-.0101	-.0005	-.00017
0	-2.0	-.0064	-.0005	-.00012	.1	-2.0	-.0063	-.0002	-.00014	0	-2.0	-.0069	-.0003	-.00015
0	-1.0	-.0033	-.0002	-.00004	.1	-1.0	-.0034	-.0001	-.00006	0	-1.0	-.0040	-.0002	-.00006
0	0	-.0002	0	-.00005	.1	0	-.0006	0	-.00006	0	0	-.0009	-.0001	-.00002
0	1.0	.0029	.0002	.00004	.1	1.0	.0020	.0002	.00001	0	1.0	.0022	-.0001	.00006
0	2.0	.0060	.0005	.00011	.1	2.0	.0050	.0003	.00008	0	2.0	.0051	.0001	.00015
0	3.0	.0092	.0007	.00017	.1	3.0	.0078	.0005	.00014	0	3.0	.0081	.0002	.00019
0	4.0	.0123	.0009	.00024	.1	4.0	.0108	.0006	.00017	0	4.0	.0111	.0005	.00021
7.2	-4.0	-.0160	-.0015	-.00076	7.3	-3.0	-.0109	-.0007	-.00048	7.1	-3.0	-.0102	-.0012	-.00029
7.2	-3.0	-.0124	-.0012	-.00058	7.3	-2.0	-.0076	-.0004	-.00034	7.1	-2.0	-.0070	-.0008	-.00019
7.2	-2.0	-.0081	-.0008	-.00037	7.3	-1.0	-.0043	-.0002	-.00021	7.1	-1.0	-.0036	-.0005	-.00012
7.2	-1.0	-.0044	-.0004	-.00022	7.3	0	-.0008	0	0	7.1	0	-.0001	-.0003	.00003
7.3	0	-.0005	0	-.00007	7.3	1.0	.0027	.0003	.00013	7.1	1.0	.0033	-.0001	.00025
7.3	1.0	.0035	.0004	.00023	7.3	2.0	.0062	.0005	.00028	7.1	2.0	.0071	.0001	.00033
7.3	2.0	.0074	.0008	.00038	7.3	3.0	.0097	.0008	.00041	7.1	3.0	.0107	.0004	.00048
7.3	3.0	.0117	.0011	.00061	7.3									
7.3	4.0	.0156	.0015	.00083										

TABLE II.-LATERAL AERODYNAMIC CHARACTERISTICS FOR THE AIRCRAFT CONFIGURATION - Continued
 (b) Complete Model, 39.5° Nose, $\theta_t = 0^\circ$

$M_\infty = 3.0$						$M_\infty = 4.0$						$M_\infty = 5.0$					
α deg	β deg	c_Y	c_n	c_l	α deg	β deg	c_Y	c_n	c_l	α deg	β deg	c_Y	c_n	c_l			
0.1	-4.0	-0.0209	0.0020	-0.00220	0.1	-4.0	-0.0178	0.0021	-0.00103	0	-4.0	-0.0156	0.0014	-0.00069			
.1	-3.0	-.0166	.0015	-.00181	.1	-3.0	-.0138	.0015	-.00078	0	-3.0	-.0119	.0010	-.00057			
.1	-2.0	-.0109	.0009	-.0015	.1	-2.0	-.0091	.0009	-.00055	0	-2.0	-.0079	.0005	-.00034			
.1	-1.0	-.0057	.0003	-.00062	.1	-1.0	-.0048	.0004	-.00034	0	-1.0	-.0036	0	-.00016			
.1	0	0	-.0003	-.00009	.1	0	-.0004	-.0002	-.00022	0	0	.0006	-.0006	.00001			
.1	1.0	.0049	-.0009	.00039	.1	.5	.0018	-.0005	-.00009	0	.5	.0024	-.0007	.00013			
.1	2.0	.0103	-.0015	.00096	.1	1.0	.0039	-.0007	.00001	0	1.0	.0045	-.0009	.00022			
.1	3.0	.0153	-.0020	.00144	.1	1.5	.0061	-.0010	.00012	0	1.5	.0068	-.0013	.00037			
.1	4.0	.0212	-.0026	.00198	.1	2.0	.0085	-.0014	.00013	0	2.0	.0089	-.0015	.00043			
7.7	-4.0	-.0236	.0014	-.00479	.1	2.5	.0107	-.0016	.00024	0	2.5	.0111	-.0018	.00058			
7.7	-3.0	-.0188	.0012	-.00359	.1	3.0	.0128	-.0019	.00035	0	3.0	.0133	-.0020	.00065			
7.7	-2.0	-.0137	.0010	-.00235	.7.7	-3.5	-.0183	.0017	-.00328	0	3.5	.0151	-.0022	.00077			
7.7	-1.0	-.0087	.0008	-.00110	.7.7	-3.0	-.0165	.0016	-.00295	7.3	-4.0	-.0319	.0053	-.00234			
7.7	0	-.0034	.0006	-.00017	.7.7	-2.5	-.0143	.0014	-.00253	7.3	-3.0	-.0282	.0052	-.00174			
7.7	.5	-.0010	.0005	-.00072	.7.7	-2.0	-.0121	.0012	-.00207	7.3	-2.0	-.0242	.0050	-.00110			
7.7	1.0	.0017	.0002	-.00139	.7.7	-1.5	-.0097	.0010	-.00158	7.3	-1.0	-.0202	.0048	-.00053			
7.7	1.5	.0041	.0002	-.00197	.7.7	-1.0	-.0073	.0009	-.00105	7.3	0	-.0163	.0045	-.00006			
7.7	2.0	.0067	0	-.00258	.7.7	-.5	-.0052	.0007	-.00058	7.3	.3	-.0153	.0045	-.00009			
7.7	2.5	.0093	-.0001	.00320	.7.7	0	-.0030	.0005	-.00009	7.3	.5	-.0141	.0044	.00022			
7.7	3.0	.0117	-.0002	.00379	.7.7	.3	-.0019	.0004	-.00017	7.3	1.0	.0154	-.0046	.00057			
7.7	3.5	.0145	-.0004	.00446	.7.7	.5	-.0007	.0003	-.00042	7.3	1.5	.0174	-.0047	.00084			
					.7.7	1.0	.0013	.0001	-.00085	7.3	2.0	.0194	-.0048	.00112			
					.7.7	1.5	.0036	-.0001	.00134	7.3	2.5	.0215	-.0049	.00144			
					.7.7	2.0	.0060	-.0003	-.00238	7.3	3.0	.0238	-.0050	.00178			
					.7.7	2.5	.0082	-.0005	.00225								
					.7.7	3.0	.0104	-.0006	.00262								

TABLE II.-LATERAL AERODYNAMIC CHARACTERISTICS FOR THE AIRCRAFT CONFIGURATION - Continued
 (c) Complete Model, 9° Nose, $\theta_t = 0^{\circ}$

$M_{\infty} = 3.0$					$M_{\infty} = 4.0$					$M_{\infty} = 5.0$				
α deg	β deg	c_y	c_n	c_l	α deg	β deg	c_y	c_n	c_l	α deg	β deg	c_y	c_n	c_l
0.1	-4.0	-0.0216	0.0016	-0.00214	0.1	-4.0	-0.0196	0.0017	-0.00154	0	-3.0	-0.0133	0.0005	-0.00109
.1	-3.0	-.0165	.0013	-.00163	.1	-3.0	-.0149	.0013	-.00121	0	-2.0	-.0090	.0002	-.00078
.1	-2.0	-.0109	.0008	-.00111	.1	-2.0	-.0101	.0008	-.00086	0	-1.0	-.0043	-.0001	-.00042
.1	-1.0	-.0055	.0003	-.00064	.1	-1.0	-.0054	.0003	-.00053	0	.0003	-.0004	-.00016	
.1	0	-.0002	-.0003	-.00028	.1	0	-.0004	-.0002	-.00027	0	1.0	.0049	-.0007	.00018
.1	1.0	.0054	-.0009	.00023	.1	1.0	.0043	-.0007	.00007	2.0	.0095	-.0011	.00054	
.1	2.0	.0109	-.0014	.00069	.1	2.0	.0093	-.0012	.00041	3.0	.0144	-.0015	.00085	
.1	3.0	.0165	-.0019	.00121	.1	3.0	.0141	-.0017	.00073					
.1	4.0	.0217	-.0023	.00170	.1	4.0	.0190	-.0021	.00111					
7.8	-3.0	-.0238	.0013	-.00351	7.7	-1.0	-.0257	.0015	-.00276					
7.8	-2.0	-.0183	.0013	-.00232	7.7	-3.0	-.0209	.0014	-.00212					
7.8	-1.0	-.0130	.0015	-.00113	7.7	-2.0	-.0161	.0014	-.00147					
7.8	0	-.0070	.0015	-.0001	7.7	-1.0	-.0111	.0013	-.00081					
7.8	1.0	.0043	-.0003	.00141	7.7	0	-.0059	.0012	-.00013					
7.8	2.0	.0104	-.0003	.00262	7.7	1.0	.0036	-.0004	.00055					
7.8	3.0	.0162	-.0002	.00382	7.7	2.0	.0088	-.0005	.00121					
					7.7	3.0	.0142	-.0005	.00189					

TABLE II.-LATERAL AERODYNAMIC CHARACTERISTICS FOR THE AIRCRAFT CONFIGURATION - Continued
 (d) Complete Model, Semi-hemisphere Nose, $\theta_t = 0^\circ$

TABLE II.-LATERAL AERODYNAMIC CHARACTERISTICS FOR THE AIRCRAFT CONFIGURATION - Continued
 (e) Complete Model, 9° Nose, $\theta_t = 45^\circ$

$M_\infty = 3.0$					$M_\infty = 4.0$					$M_\infty = 5.0$				
α deg	β deg	C_Y	C_n	C_l	α deg	β deg	C_Y	C_n	C_l	α deg	β deg	C_Y	C_n	C_l
0.1	-4.0	-0.0272	0.0036	-0.00088	0.1	-3.5	-0.0215	0.0030	-0.00026	0	-4.0	-0.0226	0.0025	-0.00046
.1	-3.0	-.0204	.0027	-.00058	.1	-3.0	-.0186	.0026	-.00024	0	-3.0	-.0175	.0019	-.00038
.1	-2.0	-.0142	.0018	-.00052	.1	-2.0	-.0126	.0018	-.00017	0	-2.0	-.0120	.0014	-.00024
.1	-1.0	-.0075	.0009	-.00029	.1	-1.0	-.0067	.0009	-.00012	0	-1.0	-.0065	.0007	-.00027
.1	0	-.0007	0	-.00005	.1	0	-.0010	0	-.00010	0	0	-.0014	.0001	.00001
.1	1.0	.0053	-.0009	.00016	.1	1.0	.0047	-.0009	-.00004	0	1.0	.0042	-.0007	.00013
.1	2.0	.0122	-.0019	.00037	.1	2.0	.0108	-.0019	.00002	0	2.0	.0097	-.0013	.00025
.1	3.0	.0192	-.0029	.00053	.1	3.0	.0168	-.0026	-.00007	0	3.0	.0151	-.0019	.00037
7.8	-4.0	-.0307	.0015	-.00318	7.7	-4.0	-.0296	.0029	-.00052					
7.8	-3.0	-.0244	.0013	-.00236	7.7	-3.0	-.0231	.0023	-.00036					
7.8	-2.0	-.0182	.0012	-.00154	7.7	-2.0	-.0167	.0018	-.00026					
7.8	-1.0	-.0118	.0010	-.00065	7.7	-1.0	-.0103	.0012	-.00019					
7.8	0	-.0057	.0008	-.00020	7.7	0	-.0036	.0006	-.00002					
7.8	1.0		.00106	7.7	1.0	.0031	-.0001	.0006						
7.8	2.0	.0085	.0004	.00192	7.7	1.5	.0067	-.0004	.00008					
7.8	2.5	.0119	.0003	.00235	7.7	2.0	.0100	-.0007	.00011					

TABLE II.-LATERAL AERODYNAMIC CHARACTERISTICS FOR THE AIRCRAFT CONFIGURATION - Continued
 (f) Complete Model, 9° Nose, $\theta_t = 90^\circ$

TABLE II.-LATERAL AERODYNAMIC CHARACTERISTICS FOR THE AIRCRAFT CONFIGURATION - Concluded
 (g) Complete Model, Except No Vertical Stabilizers, 9° Nose, $\theta_t = 0^{\circ}$

$M_{\infty} = 3.0$					$M_{\infty} = 4.0$					$M_{\infty} = 5.0$				
α deg	β deg	c_Y	c_n	c_l	α deg	β deg	c_Y	c_n	c_l	α deg	β deg	c_Y	c_n	c_l
0.1	-4.0	-0.0126	-0.0009	-0.00116	0.1	-4.0	-0.0126	-0.0006	-0.00079	0.1	-4.0	-0.0122	-0.0013	-0.00086
.1	-3.0	-.0105	-.0007	-.00082	.1	-3.0	-.0094	-.0005	-.00051	0	-3.0	-.0091	-.0011	-.00063
.1	-2.0	-.0073	-.0005	-.00040	.1	-2.0	-.0063	-.0003	-.00025	0	-2.0	-.0059	-.0010	-.00041
.1	-1.0	-.0037	-.0003	-.00004	.1	-1.0	-.0032	-.0002	-.00001	0	-1.0	-.0028	-.0008	-.00005
.1	0	-.0003	0	-.00002	.1	0	-.0005	0	.00024	0	1.0	.0002	-.0006	.00016
.1	1.0	.0032	.0001	-.00004	.1	1.0	.0023	.0002	.00046	0	1.0	.0031	-.0003	.00039
.1	2.0	.0064	.0003	-.00004	.1	2.0	.0053	.0003	.00070	0	2.0	.0061	-.0001	.00060
.1	3.0	.0099	.0005	-.00003	.1	3.0	.0083	.0004	.00094	0	3.0	.0093	.0001	.00082
.1	4.0	.0129	.0008	-.00002	.1	4.0	.0115	.0006	.00118	0	4.0	.0124	.0003	.00107
7.8	-4.0	-.0221	-.0008	-.00390						7.3	-1.0	-.0061	.0001	.00028
7.8	-3.0	-.0176	-.0004	-.00271						7.3	-2.0	-.0103	-.0002	-.00043
7.8	-2.0	-.0126	0	-.00138						7.3	-3.0	-.0147	-.0004	-.00093
7.8	-1.0	-.0080	.0003	-.00031						7.3	0	-.0021	.0002	.00055
7.8	0	-.0032	.0007	.00111						7.3	1.0	.0020	.0005	.00101
7.7	1.0	.0015	.0011	.00232						7.3	2.0	.0062	.0007	.00148
7.7	2.0	.0061	.0014	.00345						7.3	3.0	.0104	.0011	.00198
7.7	3.0	.0108	.0017	.00458										
7.7	4.0	.0153	.0021	.00570										

TABLE III.-LONGITUDINAL AERODYNAMIC CHARACTERISTICS FOR THE ENTRY CONFIGURATION

$M_{\infty} = 3.0$					$M_{\infty} = 4.0$					$M_{\infty} = 5.0$				
α deg	C_L	C_D	C_m	L/D	α deg	C_L	C_D	C_m	L/D	α deg	C_L	C_D	C_m	L/D
-4.1	-0.049	0.039	0.0231	-1.23	-3.3	-0.030	0.031	0.0154	-0.98					
-3.1	-.044	.038	.0224	-1.15	-3.1	-.029	.031	.0151	-.96					
-2.0	-.038	.037	.0215	-1.03	-2.0	-.025	.029	.0143	-.84	-2.0	-0.018	0.028	0.0104	-0.64
-1.0	-.033	.036	.0209	-.92	-1.0	-.021	.028	.0136	-.73	-1.0	-.014	.027	.0097	-.52
0	-.027	.034	.0203	-.79	0	-.015	.027	.0126	-.57	0	-.010	.027	.0092	-.38
1.0	-.022	.034	.0199	-.65	1.0	-.012	.027	.0121	-.43	1.0	-.006	.027	.0089	-.23
2.0	-.017	.034	.0195	-.50	2.0	-.007	.027	.0116	-.28					
3.1	-.010	.033	.0187	-.30	3.6	.001	.027	.0106	.03					
4.1	-.004	.034	.0181	-.13	4.1	.003	.027	.0104	.13	4.5	.008	.027	.0075	.31
5.1	.002	.033	.0173	.05	5.1	.008	.028	.0099	.29	5.5	.012	.028	.0074	.44
6.1	.008	.034	.0167	.24	6.1	.013	.029	.0095	.45	6.1	.014	.028	.0075	.50
7.1	.015	.035	.0162	.43	7.2	.018	.030	.0091	.61	7.1	.018	.029	.0075	.61
8.2	.021	.036	.0158	.59	8.2	.023	.031	.0089	.75	8.1	.022	.030	.0077	.73
9.2	.028	.034	.0152	.76	9.2	.029	.033	.0088	.88	9.1	.027	.032	.0072	.85
10.2	.036	.039	.0145	.91	10.0	.033	.034	.0085	.97					
11.2	.043	.042	.0138	1.03	11.3	.042	.037	.0084	1.13					
12.3	.053	.044	.0138	1.19	12.3	.048	.040	.0083	1.21					
13.3	.061	.049	.0137	1.26	13.3	.053	.042	.0082	1.27					
14.3	.066	.051	.0138	1.29	14.4	.059	.045	.0087	1.30					
15.4	.073	.055	.0136	1.33	15.4	.065	.048	.0085	1.34					
16.4	.080	.058	.0129	1.37	16.4	.071	.052	.0085	1.36					
17.4	.088	.063	.0123	1.40										
18.5	.097	.067	.0106	1.43	18.5	.088	.062	.0059	1.43					
19.5	.104	.072	.0102	1.44	19.5	.093	.066	.0057	1.42					
20.5	.111	.077	.0098	1.44	20.6	.099	.071	.0057	1.41					
21.6	.118	.083	.0085	1.43	21.6	.105	.076	.0057	1.39					
22.2	.107	.086	.0100	1.23	22.1	.108	.078	.0066	1.38	22.1	.091	.074	.0049	1.24
23.2	.113	.091	.0096	1.25						23.1	.096	.078	.0059	1.22
24.3	.120	.096	.0086	1.25						24.1	.101	.083	.0044	1.22
25.3	.126	.102	.0084	1.24						25.1	.106	.088	.0051	1.20
26.3	.132	.108	.0081	1.23						26.1	.110	.095	.0058	1.16
27.3	.139	.114	.0080	1.21						27.1	.114	.100	.0053	1.14
28.3	.144	.120	.0072	1.20						28.1	.118	.106	.0055	1.12
29.3	.149	.127	.0070	1.17						29.2	.126	.115	.0052	1.09
30.4	.154	.134	.0068	1.15	30.4	.129	.120		1.07	30.2	.130	.123	.0051	1.06
31.4	.161	.144		1.12	31.4	.132	.126		1.05	31.2	.134	.126	.0048	1.06
32.4	.166	.151		1.10	32.4	.136	.133		1.03	32.2	.138	.133	.0046	1.04
33.4	.169	.159		1.07	33.5	.140	.139		1.00	33.2	.142	.139	.0037	1.02
34.4	.176	.167	.0044	1.06	34.5	.144	.146		.99	34.2	.144	.148		.98
35.5	.180	.174	.0040	1.03	35.5	.147	.153		.96	35.2	.148	.156		.95
36.5	.183	.186	.0035	.99	36.5	.151	.160		.94	36.2	.155	.161	-.0009	.97
37.5	.187	.194	.0023	.96	37.5	.160	.170	.0069	.94	37.2	.158	.169	-.0009	.94
38.5	.189	.202	.0029	.98	38.6	.163	.178	.0064	.92	38.2	.161	.178	-.0007	.91
39.5	.193	.212	.0021	.91	39.6	.165	.185		.89	39.2	.164	.186	-.0013	.88
40.5	.198	.218	.0018	.91	40.6	.168	.194	.0051	.87	40.3	.166	.193	-.0002	.86
41.6	.201	.228	-.0036	.88	41.6	.169	.202		.84	41.3	.168	.202	-.0003	.83
42.6	.203	.236	-.0034	.86	42.6	.170	.210		.81	42.3	.171	.212	-.0008	.81
43.6	.206	.247	-.0034	.84	43.6	.171	.218		.79	43.3	.172	.220	-.0014	.78
44.6	.209	.256	-.0044	.82	44.7	.172	.234		.74	44.3	.175	.225		.76
				45.7	.178	.252			.71	45.3	.177	.235		
				47.7	.180	.261	.0060		.69	47.3	.181	.256		.71
				48.5	.174	.267			.65	48.3	.182	.266		.68
										49.3	.183	.277		.66

TABLE III LONGITUDINAL AERODYNAMIC CHARACTERISTICS FOR THE ENTRY CONFIGURATION
 PART II - LONGITUDINAL AERODYNAMIC CHARACTERISTICS FOR THE ENTRY CONFIGURATION

TABLE III.-LONGITUDINAL AERODYNAMIC CHARACTERISTICS FOR THE ENTRY CONFIGURATION - Concluded

$M_{\infty} = 0.60$					$M_{\infty} = 0.80$					$M_{\infty} = 0.90$				
α deg	C_L	C_D	C_m	L/D	α deg	C_L	C_D	C_m	L/D	α deg	C_L	C_D	C_m	L/D
-4.1	-0.088	0.0380	0.0274	-2.30	-4.2	-0.095	0.0393	0.0304	-2.41	-4.2	-0.102	0.0428	0.0334	-2.37
-2.1	-0.075	0.035	0.0264	-2.22	-2.1	-0.079	0.0340	0.0288	-2.32	-2.2	-0.085	0.0364	0.0314	-2.34
-1.1	-0.061	0.0298	0.0255	-2.03	-1.1	-0.065	0.0295	0.0276	-2.18	-1.1	-0.069	0.0312	0.0292	-2.21
2.0	-0.049	0.0267	0.0253	-1.81	2.0	-0.050	0.0258	0.0265	-1.94	1.9	-0.053	0.0272	0.0277	-1.95
4.0	-0.034	0.0237	0.0244	-1.45	4.0	-0.036	0.0227	0.0259	-1.57	4.0	-0.038	0.0241	0.0266	-1.56
6.0	-0.020	0.0217	0.0237	-0.92	6.0	-0.021	0.0209	0.0249	-1.01	6.0	-0.021	0.0223	0.0251	-0.93
8.1	-0.008	0.0215	0.0242	-0.37	8.1	-0.008	0.0204	0.0265	-0.39	8.1	-0.007	0.0220	0.0261	-0.32
$M_{\infty} = 1.00$					$M_{\infty} = 1.10$					$M_{\infty} = 1.30$				
-4.3	-0.122	0.0601	0.0496	-2.03	-4.2	-0.124	0.0686	0.0561	-1.81	-4.2	-0.112	0.0689	0.0535	-1.62
-2.2	-0.104	0.0529	0.0461	-1.97	-2.2	-0.108	0.0616	0.0525	-1.74	-2.2	-0.097	0.0623	0.0508	-1.55
-1.1	-0.086	0.0454	0.0417	-1.88	-1.1	-0.093	0.0555	0.0501	-1.67	-1.1	-0.083	0.0570	0.0484	-1.43
1.9	-0.066	0.0389	0.0371	-1.70	1.9	-0.076	0.0503	0.0470	-1.51	2.0	-0.067	0.0528	0.0467	-1.27
4.0	-0.047	0.0337	0.0332	-1.40	4.0	-0.060	0.0459	0.0444	-1.30	4.0	-0.052	0.0492	0.0450	-1.06
6.1	-0.029	0.0313	0.0311	-0.94	6.1	-0.042	0.0429	0.0212	-0.97	6.1	-0.037	0.0468	0.0438	-0.78
8.1	-0.012	0.0301	0.0304	-0.41	8.1	-0.025	0.0413	0.0407	-0.60	8.2	-0.020	0.0459	0.0434	-0.44

TABLE IV.-LATERAL AERODYNAMIC CHARACTERISTICS FOR THE ENTRY CONFIGURATION

TABLE IV.-LATERAL AERODYNAMIC CHARACTERISTICS FOR THE ENTRY CONFIGURATION - Concluded

$M_{\infty} = 3.0$					$M_{\infty} = 4.0$					$M_{\infty} = 5.0$				
α deg	β deg	C_Y	C_n	C_l	α deg.	β deg	C_Y	C_n	C_l	α deg	β deg	C_Y	C_n	C_l
26.3	-4.0	-0.0250	0.0017	-0.00028						26.1	-4.0	-0.0213	0	-0.00041
26.3	-3.0	.0194	.0017	-.00013						26.1	-3.0	-.0162	-.0003	-.00036
26.3	-2.0	-.0136	.0015	-.00004						26.1	-2.0	-.0112	-.0002	-.00018
26.3	-1.0	-.0079	.0014	.00011						26.1	-1.0	-.0059	-.0005	-.00017
26.3	0	-.0022	.0016	.00012						26.1	0	-.0001	-.0006	-.00015
26.3	1.0	.0037	.0016	.00025						26.1	1.0	.0057	-.0010	-.00015
26.3	2.0	.0097	.0016	.00035						26.1	1.5	.0092	-.0016	-.00012
26.3	3.0	.0160	.0014	.00047						26.1	2.0	.0119	-.0018	-.00018
26.3	4.0	.0212	.0015	.00059						26.1	2.5	.0144	-.0018	-.00002
33.4	-4.0	-.0289	.0017	-.00001	33.4	-3.0	-0.0197	0.0017	0.00059	33.2	-4.0	-.0239	.006	-.00031
33.4	-3.0	-.0228	.0016	-.00001	33.4	-2.0	-.0149	.0017	.00066	33.2	-3.0	-.0185	.0003	-.00024
33.4	-2.0	-.0163	.0016	.00013	33.4	-1.0	-.0092	.0015	.00063	33.2	-2.0	-.0129	.0003	-.00006
33.4	-1.0	-.0093	.0013	.00015	33.4	0	-.0032	.0013	.00055	33.2	-1.0	-.0069	-.0001	
33.4	0	-.0014	.0007	.00014	33.4	.5	-.0002	.0009	.00072	33.2	0	-.0010	-.0006	.00008
33.4	1.0	.0042	.0014	.00030	33.4	.8	.0011	.0009	.00074	33.2	.5	.0020	-.0007	.00011
33.4	2.0	.0110	.0012	.00037	33.4	1.0	.0024	.0009	.00076	33.2	1.0	.0053	-.0011	.00010
33.4	3.0	.0175	.0013	.00053	33.4	1.5	.0048	.0008	.00078	33.2	1.5	.0083	-.0012	.00013
33.4	4.0	.0244	.0010	.00056	33.4	2.0	.0075	.0008	.00083	33.2	2.0	.0116	-.0018	.00020
40.6	-4.0	-.0299	.0018	-.00008	40.6	-4.0	-.0252	.0015	.00062	40.3	-4.0	-.0249	0	-.00051
40.5	-3.0	-.0232	.0019	.00002	40.6	-3.0	-.0200	.0014	.00070	40.3	-3.0	-.0191	-.0003	-.00044
40.5	-2.0	-.0168	.0020	.00017	40.6	-2.0	-.0143	.0014	.00076	40.3	-2.0	-.0128	-.0008	-.00054
40.5	-1.0	-.0102	.0020	.00030	40.6	-1.0	-.0090	.0012	.00076	40.3	-1.0	-.0068	-.0010	-.00061
40.5	0	-.0035	.0019	.00048	40.6	0	-.0035	.0011	.00051	40.3	0	.0002	-.0020	-.00026
40.5	1.0	.0036	.0017	.00055	40.6	1.0	.0019	.0005	.00086	40.3	.5	.0035	-.0025	-.00034
40.5	2.0	.0104	.0016	.00069	40.6	1.5	.0047	.0007	.00088	40.3	1.0	.0065	-.0025	-.00024
40.5	3.0	.0171	.0017	.00086	40.6	1.8	.0058	.0005	.00087	40.3	2.0	.0128	-.0030	
40.5	4.0	.0243	.0018	.00099	40.6	2.0	.0072	.0004	.00088					
47.6	-4.0	-.0321	.0027	-.00020	47.7	-2.5	-.0178	.0017	.00068					
47.6	-3.0	-.0256	.0026	-.00005	47.7	-2.0	-.0152	.0017	.00073					
47.6	-2.0	-.0180	.0025	.00013	47.7	-1.5	-.0118	.0011	.00060					
47.6	-1.0	-.0105	.0021	.00015	47.7	-1.0	-.0095	.0016	.00071					
47.6	0	-.0026	.0010	.00037	47.7	-.5	-.0068	.0016	.00074					
47.6	1.0	.0039	.0020	.00058	47.7	0	-.0041	.0014	.00079					
47.6	2.0	.0114	.0017	.00060	47.7	.3	-.0028	.0015	.00079					
47.6	3.0	.0192	.0015	.00070	47.7	.5	-.0015	.0014	.00083					
47.6	4.0	.0262	.0012	.00089	47.7	.8	.0002	.0012	.00084					
					47.7	1.5	.0010	.00081						

TABLE V.-LONGITUDINAL AERODYNAMIC CHARACTERISTICS FOR THE WING UNFOLDING PROCESS
 (a) Complete Model, Semi-hemisphere Nose, $\theta_w = 30^\circ$

$M_\infty = 3.0$					$M_\infty = 4.0$					$M_\infty = 5.0$				
α deg	C_L	C_D	C_m	L/D	α deg	C_L	C_D	C_m	L/D	α deg	C_L	C_D	C_m	L/D
-4.0	-0.013	0.022	0.0037	-0.60	-4.0	-0.005	0.018	0.0034	-0.28	-3.0	0.009	0.018	0.0014	0.51
-3.0	.011	.022	.0002	.51	-2.9	.011	.018	.0012	.62	-2.0	.022	.019	.0001	1.14
-1.9	.032	.023	-.0017	1.41	-1.9	.028	.019	-.0008	1.50	-.9	.035	.020	-.0012	1.73
-.8	.053	.024	-.0040	2.20	-.8	.043	.020	-.0028	2.18	1.1	.047	.022	-.0030	2.19
.2	.073	.027	-.0053	2.74	.2	.058	.022	-.0047	2.70	.1	.059	.024	-.0044	2.50
1.3	.094	.030	-.0075	3.13	1.3	.072	.024	-.0064	3.00	2.1	.072	.027	-.0052	2.71
2.4	.111	.034	-.0085	3.30	2.3	.085	.027	-.0074	3.16	3.2	.083	.030	-.0061	2.82
3.4	.130	.037	-.0105	3.46	3.4	.098	.030	-.0085	3.26	4.2	.095	.032	-.0090	2.95
4.5	.146	.042	-.0115	3.48	3.9	.106	.031	-.0106	3.35	5.2	.107	.036	-.0108	2.93
5.6	.162	.046	-.0145	3.48	4.5	.113	.034	-.0114	3.35	6.2	.117	.041	-.0118	2.87
6.6	.177	.052	-.0157	3.38	5.5	.125	.038	-.0127	3.27	7.2	.127	.046	-.0120	2.79
7.7	.194	.060	-.0182	3.24	6.6	.137	.043	-.0135	3.16	8.3	.138	.051	-.0128	2.71
8.7	.209	.067	-.0189	3.10	7.6	.148	.048	-.0142	3.07	9.3	.148	.057	-.0142	2.62
9.8	.223	.075	-.0195	2.97	8.2	.155	.051	-.0149	3.01	10.3	.158	.063	-.0151	2.53
10.8	.236	.083	-.0209	2.85	8.7	.161	.054	-.0153	2.95					
11.9	.249	.092	-.0207	2.71	9.7	.173	.061	-.0156	2.83					
22.7	.315	.062	0.050	5.04	10.8	.184	.068	-.0154	2.71					
23.7	.327	.070	0.054	4.64										
24.8	.336	.079	0.047	4.27										
25.8	.350	.081	0.034	4.31										
26.8	.361	.083	0.037	4.35										
27.9	.372	.086	0.041	4.31										
28.9	.385	.091	0.049	4.23										
30.0	.406	.091	0.041	4.45										
31.0	.419	.097	0.055	4.32										
32.0	.433	.101	0.056	4.28										
33.1	.444	.105	0.068	4.22										
34.1	.456	.112	0.060	4.07										
35.1	.466	.120	0.032	3.89										
36.1	.481	.125	0.029	3.86										
37.2	.493	.130	0.050	3.79										
38.2	.505	.136	0.035	3.71										
39.2	.502	.137	0.0362	3.67										
40.3	.520	.147	0.0240	3.54										
41.3	.548	.157	0.0165	3.49										
42.3	.569	.168	0.0362	3.38										
43.3	.584	.176	0.0491	3.31										
44.3	.608	.187	0.0772	3.25										
45.4	.627	.198	0.0959	3.16										
46.4	.616	.227	0.0932	2.71										
47.4	.630	.240	0.1074	2.62										
48.4	.658	.256	0.1490	2.56										
49.4	.673	.271	0.1656	2.47										
50.5	.685	.286	0.1791	2.39										
51.5	.760	.313	0.2654	2.43										
52.5	.761	.330	0.2605	2.30										

TABLE V.-LONGITUDINAL AERODYNAMIC CHARACTERISTICS FOR THE WING UNFOLDING PROCESS - Continued
 (a) Complete Model, Semi-hemisphere Nose, $\theta_w = 30^\circ$ - Concluded

$M_\infty = 0.60$					$M_\infty = 0.80$					$M_\infty = 0.90$				
α deg	C_L	C_D	C_m	L/D	α deg	C_L	C_D	C_m	L/D	α deg	C_L	C_D	C_m	L/D
-4.1	-0.056	0.0171	0.0132	-3.27	-4.2	-0.067	0.0165	0.0159	-4.03	-4.2	-0.082	0.0188	0.0228	-4.36
-1.9	.012	.0161	.0149	.74	-1.9	.005	.0150	.0194	.33	-1.9	-.001	.0165	.0239	-.03
.2	.086	.0197	.0174	4.37	.4	.093	.0195	.0191	4.76	.4	.092	.0207	.0204	4.41
2.4	.165	.0289	.0187	5.69	2.6	.176	.0298	.0200	5.90	2.8	.185	.0323	.0205	5.74
4.6	.249	.0452	.0233	5.51	4.9	.266	.0480	.0229	5.55	5.1	.279	.0514	.0222	5.42
6.8	.332	.0672	.0269	4.94	7.2	.355	.0737	.0264	4.81	7.5	.363	.0779	.0271	4.66
9.0	.408	.0945	.0291	4.32	9.5	.428	.1036	.0318	4.13	9.7	.396	.0779	.0271	
$M_\infty = 1.00$					$M_\infty = 1.10$					$M_\infty = 1.30$				
-4.2	-.106	.0316	.0457	-3.35	-4.1	-.083	.0331	.0404	-2.51	-4.1	-.037	.0317	.0169	-1.16
-1.9	-.016	.0284	.0426	.55	-1.8	.010	.0312	.0341	.32	-1.7	.049	.0317	.0101	1.55
.5	.082	.0315	.0384	2.61	.6	.104	.0360	.0261	2.87	.6	.131	.0378	.0034	3.47
2.9	.190	.0441	.0293	4.30	3.0	.209	.0495	.0154	4.22	3.0	.215	.0510	-.0031	4.21
5.3	.301	.0658	.0158	4.57	5.4	.305	.0715	.0083	4.27	5.3	.292	.0711	-.0066	4.10
7.6	.357		.0339	4.23	7.7	.341		.0367	4.29	7.6	.335		.0250	3.76
9.8	.377		.0460	4.90	9.8	.359		.0389	4.55	9.8	.333		.0346	4.22

TABLE V.-LONGITUDINAL AERODYNAMIC CHARACTERISTICS FOR THE WING UNFOLDING PROCESS - Continued
 (b) Complete Model, Semi-hemisphere Nose, $\theta_w = 60^\circ$

$M_\infty = 3.0$					$M_\infty = 4.0$					$M_\infty = 5.0$				
α deg	C_L	C_D	C_m	L/D	α deg	C_L	C_D	C_m	L/D	α deg	C_L	C_D	C_m	L/D
-3.9	0.023	0.028	-0.0028	0.83	-3.9	0.023	0.021	-0.0029	1.09	-4.0	0.020	0.021	-0.0031	0.93
-2.9	.036	.028	-.0034	1.25	-2.9	.032	.022	-.0035	1.44	-3.0	.028	.022	-.0038	1.24
-1.8	.048	.030	-.0043	1.62	-1.8	.041	.023	-.0041	1.76	-1.9	.036	.023	-.0042	1.53
-.8	.061		-.0047		-.8	.049	.025	-.0046	1.97	-.9	.043	.025	-.0047	1.72
.2	.058	.031	-.0051	2.18	.2	.056	.026	-.0049	2.14	.1	.050	.026	-.0048	1.88
1.3	.079	.034	-.0055	2.32	1.3	.064	.029	-.0054	2.23	1.1	.056	.028	-.0061	1.97
2.3	.089	.037	-.0058	2.41	2.3	.071	.031	-.0058	2.29	2.1	.062	.031	-.0051	2.01
3.3	.097	.040	-.0055	2.42	3.3	.077	.033	-.0056	2.32	3.1	.067	.033	-.0050	2.03
4.4	.105	.043	-.0055	2.43	4.3	.048	.034	-.0138	1.39	3.6	.070	.034	-.0052	2.03
5.4	.069	.045	.0196	1.54	5.3	.051	.036	.0155	1.40	4.1	.075	.037	-.0050	2.05
6.4	.074	.048	.0215	1.55	6.4	.054	.039	.0170	1.40	5.2	.080	.040	-.0045	2.02
7.4	.077	.050	.0252	1.52	7.4	.057	.041	.0185	1.40	6.2	.086	.043	-.0045	2.00
8.4	.080	.054	.0270	1.48	8.4	.060	.043	.0204	1.38	7.2	.090	.045	-.0038	1.98
9.5	.085	.058	.0291	1.46	9.4	.063	.046	.0220	1.37	8.2	.095	.049	-.0036	1.94
10.5	.087	.060	.0306	1.45	10.5	.066	.048	.0238	1.35	9.2	.101	.053	-.0036	1.91
11.5	.094	.066	.0334	1.41						9.7	.104	.055	-.0039	1.89
22.4	.215	.164	-.0038	1.31						10.2	.107	.057	-.0038	1.87
23.4	.222	.172	-.0050	1.28						22.2	.165	.126	-.0069	1.31
24.5	.227	.182	-.0043	1.25						23.2	.170	.133	-.0057	1.27
25.5	.233	.191	-.0052	1.22						24.2	.175	.142	-.0049	1.23
26.5	.238	.200	-.0049	1.18						25.2	.181	.151	-.0056	1.19
27.0	.242	.206	-.0060	1.17						26.2	.187	.160	-.0066	1.17
27.5	.244	.211	-.0055	1.15						26.7	.191	.166	-.0068	1.15
28.0	.247	.216	-.0051	1.14						27.2	.193	.171	-.0065	1.13
28.5	.251	.222	-.0067	1.12						27.7	.197	.177	-.0081	1.11
29.0	.253	.227	-.0071	1.11						28.2	.200	.182	-.0076	1.09
29.6	.263	.245	-.0064	1.07						28.7	.203	.188	-.0089	1.08
30.6	.269	.257	-.0076	1.04						29.2	.205	.193	-.0070	1.06
31.6	.271	.266	-.0071	1.01						30.3	.213	.204	-.0132	1.04
32.6	.275	.279	-.0063	.98						31.3	.217	.215	-.0118	1.00
33.7	.278	.290	-.0074	.95						32.3	.222	.227	-.0122	.97
34.7	.282	.303	-.0077	.93						33.3	.226	.239	-.0130	.94
35.7	.286	.309	-.0071	.92						34.3	.231	.252	-.0134	.91
36.7	.291	.312	-.0106	.93						35.3	.236	.266	-.0164	.88
37.7	.289	.314	.0015	.92						35.8	.237	.271	-.0157	.87
38.7	.292	.320	-.0093	.91						36.3	.236	.260	-.0195	.90
39.8	.295	.324	-.0086	.91						37.3	.238	.272	-.0200	.87
40.8	.295	.331	-.0077	.89						38.3	.241	.286	-.0196	.84
41.8	.298	.340	-.0093	.87						39.3	.243	.299	-.0202	.81
42.8	.299	.345	-.0071	.86						40.4	.245	.311	-.0208	.78
43.8	.302	.344	-.0041	.87						40.9	.247	.320	-.0220	.77
44.9	.304	.347	-.0023	.87						41.4	.247	.326	-.0216	.75
45.9	.316	.359	-.0068	.88						41.9	.249	.333	-.0230	.74
46.9	.317	.364	-.0048	.87						42.1	.249	.336	-.0224	.74
47.9	.319	.368	-.0053	.86										
48.9	.322	.374	-.0048	.86										
50.0	.322	.380	-.0052	.84										
51.0	.324	.386	-.0033	.83										
52.0	.325	.389	-.0028	.83										

TABLE V.-LONGITUDINAL AERODYNAMIC CHARACTERISTICS FOR THE WING UNFOLDING PROCESS - Continued
 (b) Complete Model, Semi-hemisphere Nose, $\theta_w = 60^\circ$ - Concluded

$M_\infty = 0.60$					$M_\infty = 0.80$					$M_\infty = 0.90$				
α deg	C_L	C_D	C_m	L/D	α deg	C_L	C_D	C_m	L/D	α deg	C_L	C_D	C_m	L/D
-3.9	0.022	0.0199	0.0057	1.09	-3.9	0.022	0.0201	0.0069	1.09	-3.9	0.019	0.0218	0.0085	0.85
-1.8	.076	.0241	.0076	3.16	-1.7	.080	.0252	.0078	3.17	-1.7	.077	.0266	.0091	2.89
.3	.128	.0319	.0101	4.00	.5	.135	.0340	.0101	3.97	.5	.139	.0360	.0091	3.84
2.4	.180	.0436	.0136	4.12	2.7	.190	.0463	.0131	4.10	2.8	.194	.0490	.0121	3.96
4.5	.232	.0589	.0163	3.93	4.8	.242	.0628	.0157	3.85	5.0	.251	.0667	.0142	3.77
6.7	.277	.0768	.0209	3.61	7.0	.293	.0833	.0196	3.52	7.2	.300	.0878	.0187	3.41
8.8	.322	.0977	.0265	3.29	9.2	.331	.1041	.0249	3.18	9.3	.326	.1075	.0266	3.03
$M_\infty = 1.00$					$M_\infty = 1.10$					$M_\infty = 1.30$				
-3.9	-.009	.0340	.0296	-0.27	-3.8	.011	.0367	.0239	.29	-3.8	.042	.0374	.0024	1.11
-1.6	.059	.0374	.0270	1.58	-1.6	.077	.0418	.0183	1.84	-1.6	.094	.0430	.0002	2.17
.6	.130	.0471	.0202	2.75	.7	.140	.0516	.0124	2.71	.7	.147	.0527	-.0035	2.78
2.9	.199	.0610	.0127	3.26	2.9	.209	.0666	.0023	3.14	2.9	.198	.0661	-.0072	2.99
5.1	.255	.0782	.0126	3.25	5.2	.268	.0860	-.0029	3.11	5.1	.247	.0832	-.0116	2.96
7.3	.298	.0978	.0143	3.04	7.4	.311	.1058	-.0006	2.93	7.3	.286	.1030	-.0110	2.77
9.5	.326	.1166	.0202	2.79	9.5	.322		.0181	2.69	9.5	.296		.0067	2.53

TABLE V.-LONGITUDINAL AERODYNAMIC CHARACTERISTICS FOR THE WING UNFOLDING PROCESS - Continued
 (c) Complete Model, Semi-hemisphere Nose, $\theta_w = 90^\circ$

$M_\infty = 3.0$					$M_\infty = 5.0$				
α deg	C_L	C_D	C_m	L/D	α deg	C_L	C_D	C_m	L/D
22.3	0.141	0.120	0.0157	1.16	22.1	0.116	0.094	0.0062	1.22
23.3	.146	.127	.0177	1.15	23.1	.121	.099	.0057	1.21
24.3	.153	.133	.0168	1.14	24.1	.126	.105	.0051	1.20
25.4	.160	.141	.0161	1.13	25.2	.131	.110	.0048	1.19
26.4	.167	.148	.0149	1.13	26.2	.137	.117	.0057	1.17
27.4	.173	.155	.0149	1.11	27.2	.144	.125	.0011	1.15
28.4	.176	.160	.0154	1.09	28.2	.151	.132	-.0027	1.14
29.4	.180	.165	.0161	1.09	29.2	.157	.143	-.0044	1.09
30.4	.185	.171	.0177	1.08	30.2	.133	.100	.0296	1.32
31.4	.140	.162	.0560	.86	31.2	.135	.111	.0309	1.21
32.4	.135	.180	.0610	.75	32.2	.138	.124	.0318	1.11
33.4	.133	.194	.0651	.68	33.2	.145	.155	.0247	.93
34.4	.132	.204	.0671	.64	34.2	.148	.168	.0245	.88
35.5	.134	.212	.0696	.63	35.2	.153	.183	.0215	.83
36.5	.135	.218	.0715	.61	35.7	.156	.191	.0184	.81
37.5	.138	.220	.0729	.62	36.3	.169	.169	.0212	1.00
38.5	.175	.225	.0547	.78	37.3	.166	.182	.0241	.91
39.6	.173	.227	.0591	.76	38.3	.168	.194	.0238	.86
40.6	.172	.227	.0625	.75	39.3	.172	.205	.0225	.83
41.6	.171	.230	.0653	.74	40.3	.179	.215	.0181	.83
42.6	.172	.233	.0669	.73	40.8	.180	.223	.0167	.80
43.6	.175	.238	.0653	.73	41.3	.181	.228	.0164	.79
44.6	.177	.243	.0660	.73	41.8	.183	.237	.0143	.77
45.6	.190	.239	.0606	.79					
46.7	.188	.239	.0679	.78					
47.7	.185	.237	.0904	.77					
48.7	.187	.240	.0918	.77					
49.7	.188	.245	.0912	.76					
50.7	.182	.249	.0957	.72					
51.7	.175	.248	.1034	.70					

TABLE V.-LONGITUDINAL AERODYNAMIC CHARACTERISTICS FOR THE WING UNFOLDING PROCESS - Concluded
 (d) Complete Model, Semi-hemisphere Nose, $\theta_w = 120^\circ$

$M_\infty = 3.0$					$M_\infty = 5.0$				
α deg	C_L	C_D	C_m	L/D	α deg	C_L	C_D	C_m	L/D
22.3	0.133	0.104	0.0163	1.28	22.1	0.109	0.084	0.0101	1.29
23.3	.140	.109	.0153	1.27	23.1	.113	.089	.0111	1.27
24.3	.147	.116	.0150	1.26	24.1	.120	.095	.0090	1.26
25.4	.154	.124	.0145	1.24	25.2	.124	.101	.0109	1.22
26.4	.160	.131	.0144	1.22	26.2	.129	.107	.0108	1.20
27.4	.168	.137	.0123	1.22	27.2	.134	.114	.0111	1.17
28.4	.173	.145	.0131	1.19	27.7	.137	.117	.0106	1.16
29.4	.179	.154	.0131	1.16	28.2	.139	.121	.0112	1.14
30.4	.184	.162	.0140	1.13	29.2	.144	.129	.0116	1.11
31.5	.189	.165	.0137	1.14	30.2	.152	.138	.0087	1.10
32.5	.195	.174	.0126	1.11	31.2	.157	.146	.0073	1.07
33.5	.200	.185	.0113	1.08	32.2	.161	.154	.0077	1.04
34.5	.204	.194	.0109	1.05	33.2	.165	.157	.0088	1.04
35.5	.208	.203	.0107	1.02	33.7	.167	.162	.0085	1.03
36.5	.211	.212	.0134	.99	34.2	.169	.167	.0078	1.01
37.5	.216	.222	.0124	.97	34.7	.171	.172	.0077	.99
38.6	.217	.231	.0160	.94	35.2	.173	.177	.0079	.97
39.6	.222	.241	.0144	.91	36.3	.178	.183	.0067	.97
40.6	.226	.253	.0088	.89	37.3	.181	.191	.0070	.94
41.6	.227	.264	.0117	.86	38.3	.184	.200	.0066	.92
42.6	.228	.273	.0114	.83	39.3	.188	.210	.0055	.89
43.7	.230	.284	.0105	.81	40.3	.191	.218	.0050	.87
44.7	.230	.294	.0115	.78	41.3	.193	.228	.0060	.84
45.7	.232	.319	.0142	.72	41.8	.194	.234	.0056	.82
46.7	.232	.328	.0125	.70	42.3	.195	.240	.0044	.81
47.7	.239	.335	-.0001	.71	42.8	.195	.245	.0044	.79
48.8	.238	.346	-.0022	.68					
49.8	.236	.356	-.0048	.66					
50.8	.234	.366	-.0060	.63					
51.8	.230	.377	-.0042	.61					

TABLE VI.-LATERAL AERODYNAMIC CHARACTERISTICS FOR THE WING UNFOLDING PROCESS
 (a) Complete Model, Semi-hemisphere Nose, $\theta_w = 30^\circ$

TABLE VI.-LATERAL AERODYNAMIC CHARACTERISTICS FOR THE WING UNFOLDING PROCESS - Continued
 (b) Complete Model, Semi-hemisphere Nose, $\theta_w = 60^\circ$

$M_\infty = 3.0$					$M_\infty = 4.0$					$M_\infty = 5.0$				
α deg	β deg	C_Y	C_n	C_l	α deg	β deg	C_Y	C_n	C_l	α deg	β deg	C_Y	C_n	C_l
0.2	-4.0	-0.0528	0.0034	-0.00953	0.2	-4.0	-0.0465	0.0040	-0.00798	0.1	-2.5	-0.0222	-0.0008	-0.00406
.2	-3.0	-0.0397	.0021	-.00715	.2	-3.0	-.0353	.0027	-.00607	.1	-2.0	-.0169	-.0014	-.00317
.2	-2.0	-.0259	.0006	-.00470	.2	-2.0	-.0234	.0012	-.00407	.1	-1.0	-.0061	-.0028	-.00139
.2	-1.0	-.0121	-.0008	-.00222	.2	-1.0	-.0114	-.0002	-.00201	.1	0	.0040	-.0039	.00059
.3	0	.0021	-.0022	.00047	.2	0	.0012	-.0018	.00021	.1	1.0	.0151	-.0053	-.00062
.3	1.0	.0153	-.0029	.00285	.2	1.0	.0127	-.0026	.00225	.1	2.0	.0244	-.0053	.00111
.2	2.0	.0295	-.0043	.00538	.2	2.0	.0247	-.0040	.00427	.1	3.0	.0356	-.0066	.00298
.3	3.0	.0426	-.0056	.00778	.3	3.0	.0369	-.0053	.00640	.1	4.0	.0464	-.0078	.00482
7.4	-4.0	-.0561	.0056	-.00806	.3	3.5	.0422	-.0058	.00734	7.2	-4.0	-.0473	.0055	-.00822
7.4	-3.0	-.0417	.0041	-.00582	7.4	-4.0	-.0503	.0057	-.00741	7.2	-3.0	-.0360	.0041	-.00631
7.4	-2.0	-.0323	.0068	-.00375	7.4	-3.0	-.0381	.0043	-.00547	7.2	-2.0	-.0241	.0026	-.00452
7.4	-1.0	-.0151	.0013	-.00154	7.4	-2.0	-.0257	.0028	-.00352	7.2	-1.0	-.0119	.0011	-.00229
7.4	0	-.0003	-.0003	.00077	7.4	-1.0	-.0138	.0015	-.00155	7.2	0	.0004	-.0005	.00004
7.4	1.0	.0201	-.0087	.00293	7.4	0	-.0006	-.0001	.00050	7.2	.5	.0061	-.0009	.00092
7.4	1.9	.0425	-.0190	.00506	7.4	1.0	.0112	-.0016	.00233	7.2	1.0	.0123	-.0017	.00181
7.4	2.9	.0641	-.0289	.00718	7.4	2.0	.0238	-.0030	.00427	7.2	1.5	.0182	-.0024	.00292
26.5	-3.9	-.1038			7.4	3.0	.0357	-.0044	.00616	7.2	2.0	.0241	-.0031	.00390
26.5	-3.0	-.0547	.0079	-.00066						7.2	3.0	.0363	-.0045	.00584
26.5	-2.0	-.0369	.0050	-.00008						26.2	-3.0	-.0477	.0034	-.00262
26.5	-1.0	-.0198	.0023	.00014						26.2	-2.0	-.0324	.0001	-.00231
26.5	0	-.0008	-.0008	.00056						26.2	1.0	-.0156	-.0029	-.00185
26.5	.5	.0078	-.0022	.00057						26.2	0	.0013	-.0060	-.00103
26.5	1.0	.0168	-.0037	.00091						26.2	.5	.0099	-.0080	-.00084
26.5	1.5	.0268	-.0053	.00108						26.2	1.0	.0168	-.0082	-.00052
26.5	2.0	.0358	-.0069	.00133						26.2	1.5	.0258	-.0100	-.00029
26.5	2.5	.0434	-.0080	.00144						26.2	2.0	.0338	-.0114	-.00015
26.5	3.0	.0525	-.0095	.00175						26.2	2.5	.0416	-.0129	.00025
26.5	3.5	.0610	-.0108	.00203						33.3	-3.0	-.0549	.0067	-.00259
26.5	4.0	.0694	-.0120	.00237						33.3	-2.0	-.0362	.0033	-.00210
33.6	-4.0	-.0763	.0115	-.00108						33.3	-1.0	-.0179	-.0002	-.00153
33.6	-3.0	-.0581	.0087	-.00070						33.3	0	0	-.0036	-.00082
33.6	-2.0	-.0390	.0057	-.00023						33.3	.5	.0105	-.0053	-.00069
33.6	-1.0	-.0201	.0028	-.00012						33.3	1.0	.0188	-.0068	-.00054
33.7	0	-.0009	0	.00036						33.3	1.5	.0283	-.0085	-.00039
33.7	1.0	.0196	-.0033	.00086						33.3	2.0	.0368	-.0101	-.00020
33.7	2.0	.0402	-.0063	.00113						33.3	2.5	.0458	-.0118	.00001
33.7	3.0	.0587	-.0094	.00142						40.3	-3.8	-.0729	.0110	-.00159
33.7	4.0	.0774	-.0118	.00181						40.3	-3.0	-.0586	.0083	-.00129
40.8	-4.0	-.0831	.0141	-.00031						40.3	-2.0	-.0396	.0046	-.00085
40.8	-3.0	-.0638	.0112	.00001						40.3	-1.0	-.0192	.0006	-.00037
40.8	-2.0	-.0438	.0078	.00028						40.3	0	0	-.0030	.00032
40.8	-1.0	-.0228	.0045	.00066						40.3	.5	.0095	-.0049	.00059
40.8	0	-.0011	.0008	.00086						40.3	1.0	.0195	-.0073	.00080
40.8	1.0	.0197	-.0030	.00114						40.3	1.5	.0296	-.0090	.00100
40.8	2.0	.0406	-.0064	.00154						40.3	2.0	.0400	-.0111	.00123
40.8	3.0	.0610	-.0097	.00182						40.3	2.5	.0506	-.0132	.00151
40.8	4.0	.0809	-.0127	.00215										
47.9	-4.0	-.0901	.0140	-.00046										
47.9	-3.0	-.0717	.0128	-.00005										
47.9	-2.0	-.0487	.0085	.00045										
47.9	-1.0	-.0255	.0046	.00070										
47.9	0	-.0024	.0008	.00102										
47.9	1.0	.0201	-.0025	.00047										
47.9	2.0	.0431	-.0064	.00072										
47.9	3.0	.0665	-.0105	.00117										
47.9	4.0	.0871	-.0125	.00206										

TABLE VI.-LATERAL AERODYNAMIC CHARACTERISTICS FOR THE WING UNFOLDING PROCESS - Continued
(c) Complete Model, Semi-hemisphere Nose, $\theta_w = 90^\circ$

$M_\infty = 3.0$					$M_\infty = 5.0$				
α deg	β deg	C_Y	C_n	C_l	α deg	β deg	C_Y	C_n	C_l
26.4	-4.0	-0.0617	0.0075	0.00145	26.2	-2.0	-0.0293	0.0014	0.00066
26.4	-3.0	-.0491	.0062	.00126	26.2	-1.0	-.0183	.0003	.00061
26.4	-2.0	-.0353	.0046	.00108	26.2	0	-.0065	-.0011	.00057
26.4	-1.0	-.0206	.0025	.00080	26.2	.5	-.0013	-.0016	.00069
26.4	0	-.0047		.00051	26.2	1.0	.0040	-.0020	.00070
26.4	1.0	.0099	-.0025	.00020					
26.4	2.0	.0247	-.0045	-.00010					
26.4	3.0	.0390	-.0062	-.00026					
26.4	4.0	.0523	-.0078	-.00038					
33.4	-3.8	-.0034	-.0144	-.00357					
33.4	-3.0	-.0042	-.0129	-.00313					
33.4	-2.0	-.0031	-.0096	-.00213					
33.4	-1.0	-.0006	-.0064	-.00113					
33.4	0	.0030	-.0039	-.00003					
33.4	1.0	.0088	-.0023	.00037					
33.4	2.0	.0129	.0002	.00114					
33.4	3.0	.0154	.0034	.00214					
33.4	4.0	.0148	.0081	.00408					
40.6	-3.0	-.0035	-.0128	-.00484	40.3	-3.0	-.0173	-.0037	-.00136
40.6	-2.0	.0003	-.0102	-.00406	40.3	-2.0	-.0140	-.0012	-.00059
40.6	-1.0	.0025	-.0064	-.00193	40.3	-1.0	-.0122	.0055	.00062
40.6	0	.0043	-.0027	-.00093	40.3	0	-.0045	.0031	.00094
40.6	1.0	.0078	.0001	-.00006	40.3	.5	-.0048	.0056	.00189
40.6	2.0	.0135	.0019	.00038	40.3	1.0	-.0040	.0072	.00214
40.6	3.0	.0194	.0034	.00072	40.3	1.5	-.0022	.0083	.00264
40.6	4.0	.0251	.0075	.00341	40.3	2.0	-.0005	.0098	.00316
47.7	-4.0	-.0304	-.0056	-.00239					
47.7	-3.0	-.0247	-.0034	-.00119					
47.7	-2.0	-.0197	-.0006	.00016					
47.7	-1.0	-.0130	.0014	.00037					
47.7	0	-.0075	.0031	.00113					
47.7	1.0	-.0002	.0041	.00143					
47.7	2.0	.0033	.0080	.00231					
47.7	3.0	.0155	.0065	.00152					
47.7	4.0	.0263	.0059	.00131					

TABLE VI.-LATERAL AERODYNAMIC CHARACTERISTICS FOR THE WING UNFOLDING PROCESS - Concluded
 (d) Complete Model, Semi-hemisphere Nose, $\theta_w = 120^\circ$

$M_\infty = 3.0$					$M_\infty = 5.0$				
α deg	β deg	C_Y	C_n	C_l	α deg	β deg	C_Y	C_n	C_l
26.4	-4.0	-0.0319	0.0018	-0.00104	26.2	-4.0	-0.0303	0.0019	-0.00077
26.4	-3.0	.0260	.0021	-.00061	26.2	-3.0	-.0234	.0014	-.00074
26.4	-2.0	-.0187	.0019	-.00039	26.2	-2.0	-.0162	.0008	-.00069
26.4	-1.0	-.0114	.0016	-.00051	26.2	-1.0	-.0096	.0003	-.00044
26.4	0	-.0034	.0010	-.00092	26.2	0	-.0015	-.0015	-.00024
26.4	1.0	-.0079			26.2	.5	.0024	-.0027	-.00026
26.4	2.0	.0107	.0009	.00066	26.2	1.0	.0058	-.0029	-.00016
26.4	3.0	.0187	.0004	.00087	26.2	1.5	.0096	-.0034	-.00009
26.4	4.0	.0266	.0001	.00110	33.2	-4.0	-.0349	.0019	.00019
33.5	-4.0	-.0379	.0032	-.00053	33.2	-3.0	-.0279	.0015	-.00001
33.5	-3.0	-.0296	.0028	-.00047	33.2	-2.0	-.0201	.0011	.00030
33.5	-2.0	-.0217	.0027	-.00024	33.2	-1.0	-.0123	.0005	.00056
33.5	-1.0	-.0136	.0023	.00004	33.2	0	.0048	-.0063	-.00028
33.5	0	-.0055	.0019	.00026	33.2	.5	-.0004	-.0009	-.00011
33.5	1.0	.0025	.0015	.00048	33.2	1.0	.0037	-.0012	
33.5	2.0	.0107	.0014	.00075	33.2	1.5	.0077	-.0016	
33.5	3.0	.0194	.0009	.00089	33.2	1.8	.0099	-.0020	
33.5	4.0	.0285	.0005	.00099	40.3	-4.0	-.0393	.0033	-.00062
40.6	-4.0	-.0365	.0014	-.00132	40.3	-3.0	-.0309	.0025	-.00065
40.6	-3.0	-.0277	.0008	-.00100	40.3	-2.0	-.0227	.0021	-.00032
40.6	-2.0	-.0201	.0009	-.00056	40.3	-1.0	-.0142	.0016	-.00016
40.6	-1.0	-.0124	.0014	-.00017	40.3	0	-.0043	.0002	-.00004
40.6	0	-.0061	.0022	.00031	40.3	.5	-.0003	-.0001	.00004
40.6	1.0	.0024	.0022	.00052	40.3	1.0	.0043	-.0008	.00015
40.6	2.0	.0127	.0014	.00072	40.3	1.5	.0092	-.0014	.00022
40.6	3.0	.0221	.0009	.00096	40.3	2.0	.0136	-.0019	.00034
40.6	4.0	.0313	.0008	.00114					
47.7	-4.0	-.0311	-.0024	-.00284					
47.7	-3.0	-.0261	-.0010	-.00199					
47.7	-2.0	-.0177	-.0010	-.00148					
47.7	-1.0	-.0121	.0003	-.00065					
47.7	0	-.0060	.0017	.00014					
47.7	1.0	.0041	.0016	.00056					
47.7	2.0	.0143	.0010	.00068					
47.7	3.0	.0245	.0005	.00089					
47.7	4.0	.0344	.0002	.00114					

[REDACTED]

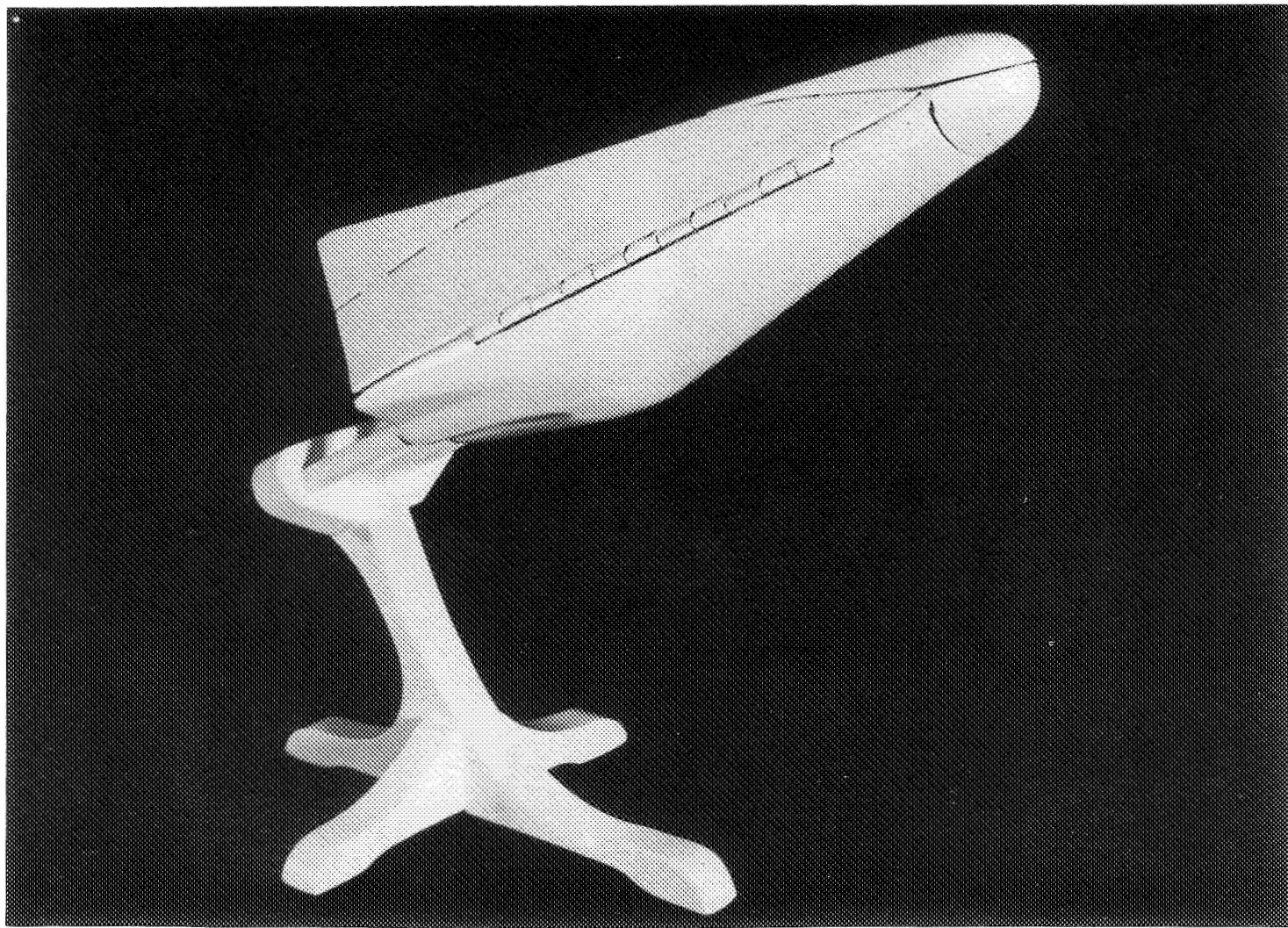
*

*

*

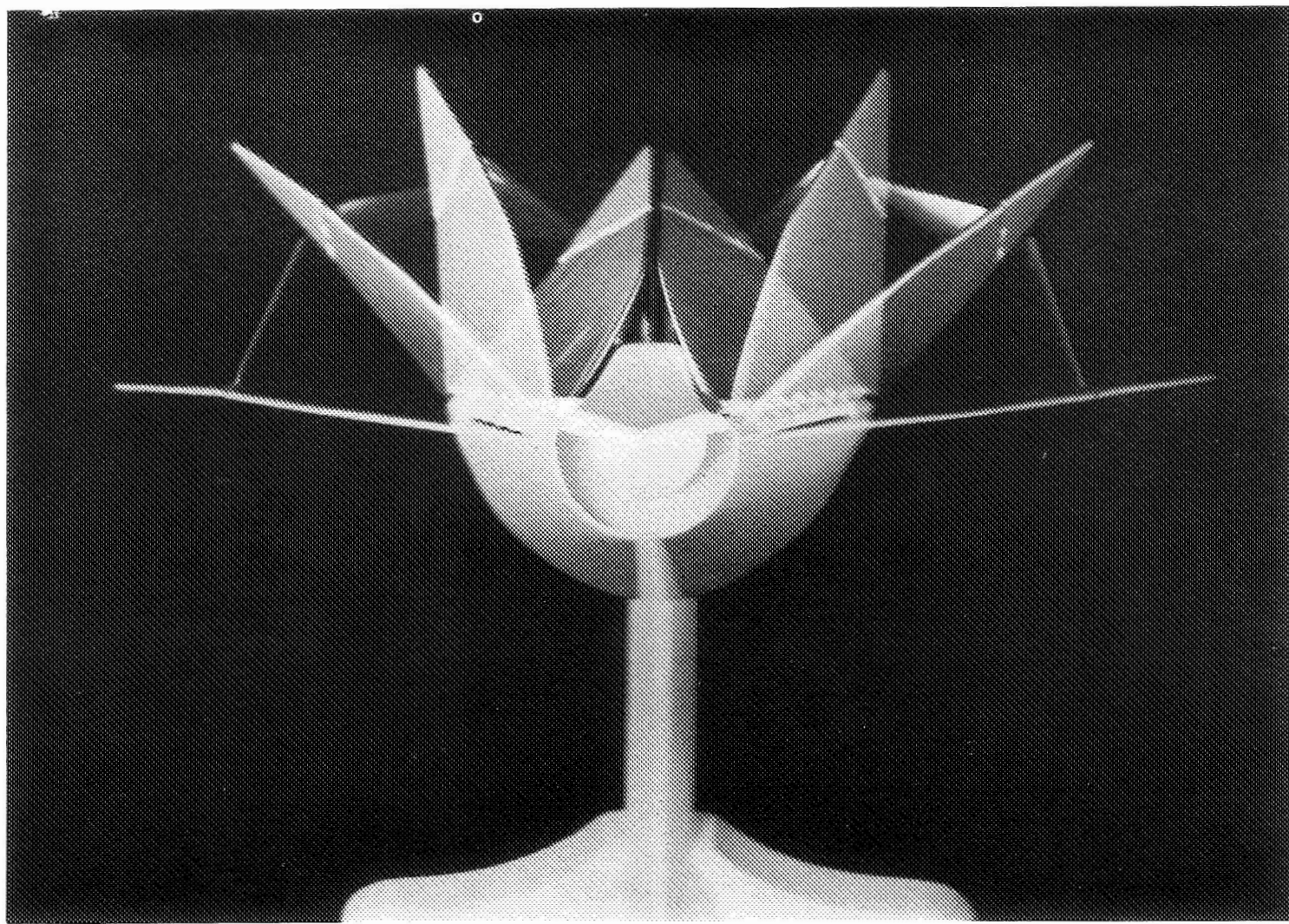
[REDACTED]

*



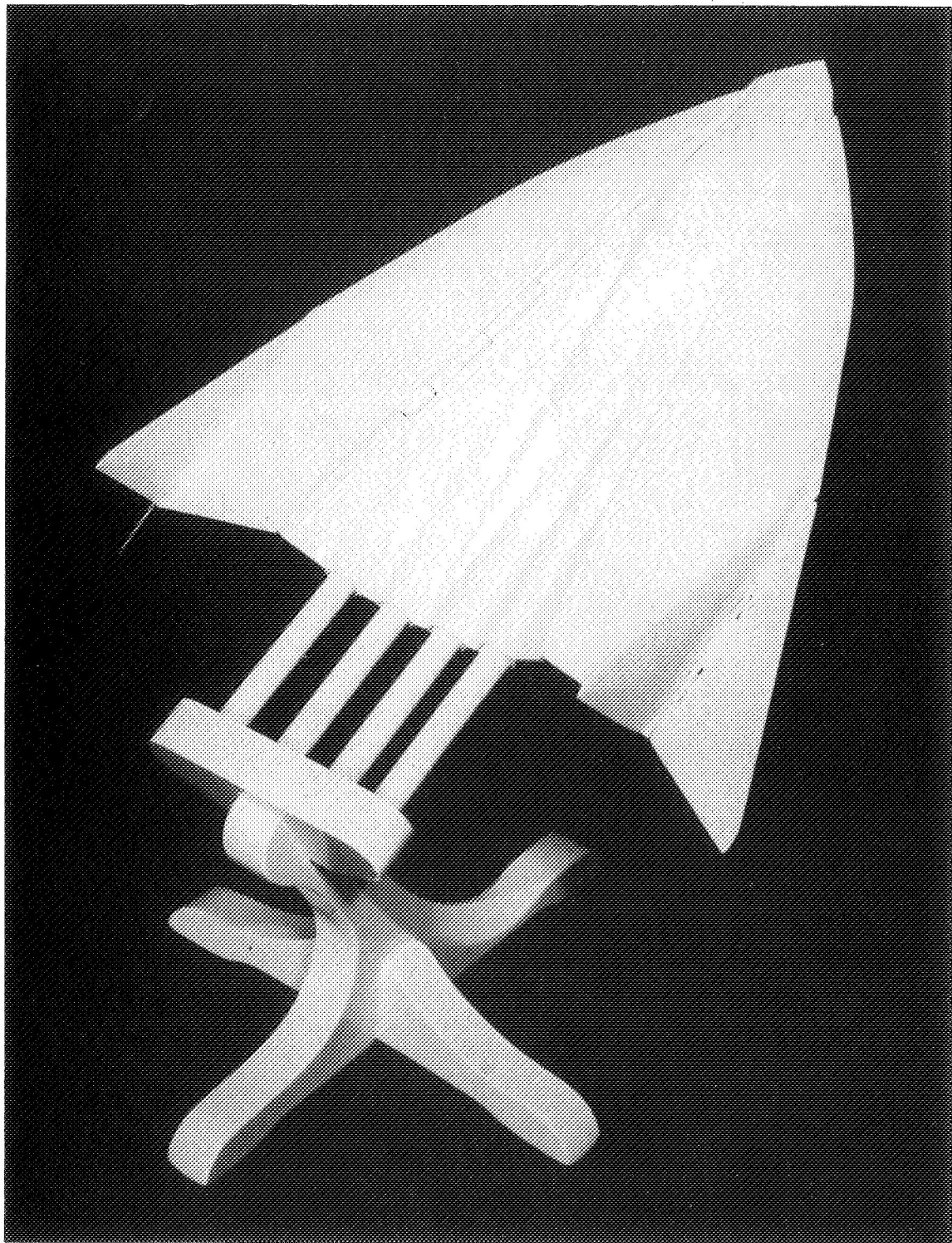
A-27939

Figure 1.- Entry configuration with wings folded and fairings covering the nose.



A-28086.1

Figure 2.- Multiple exposure of unfolding wings with wing tips undeflected.



A-27943

Figure 3.- Aircraft configuration with wing tips rotated downward 45° .

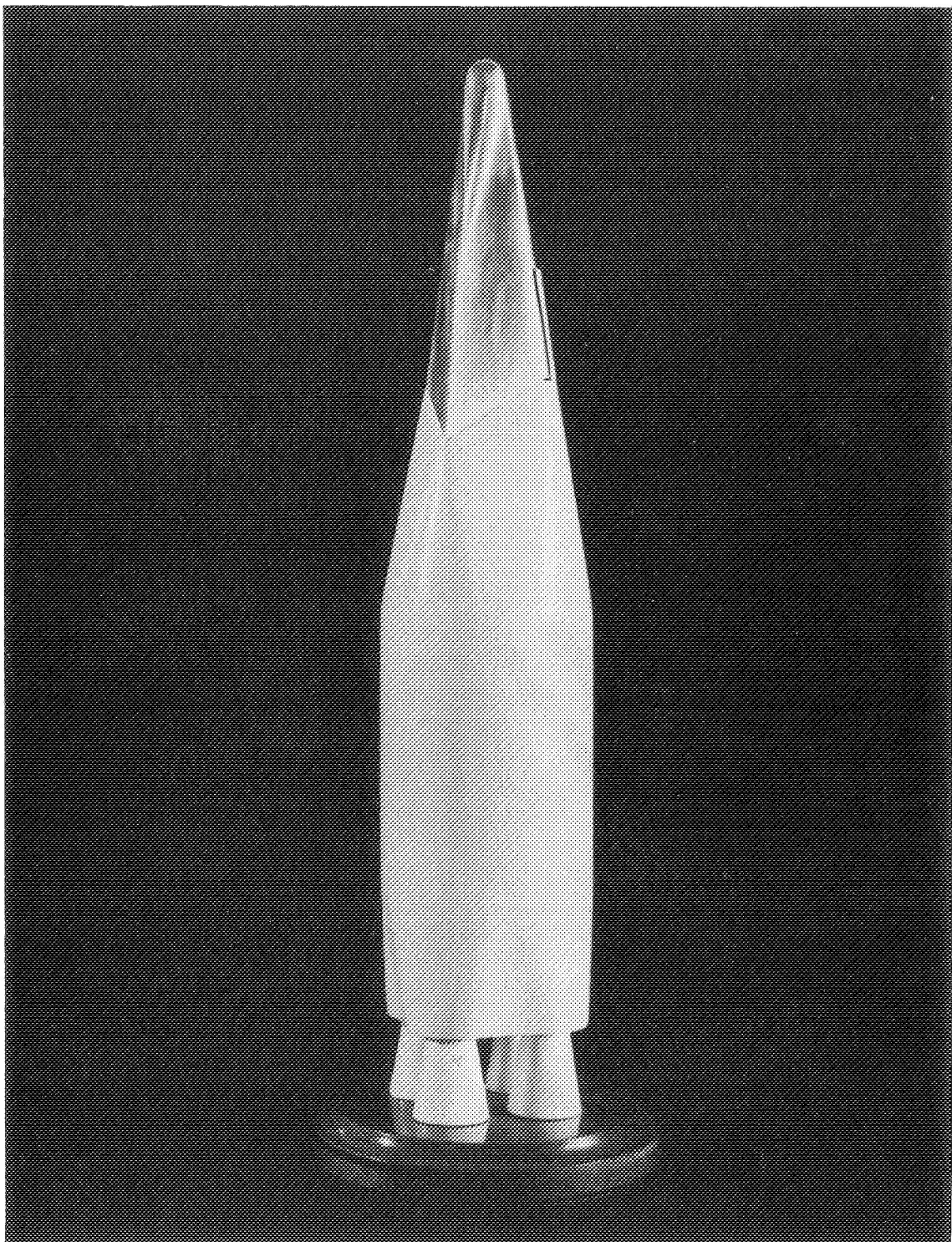
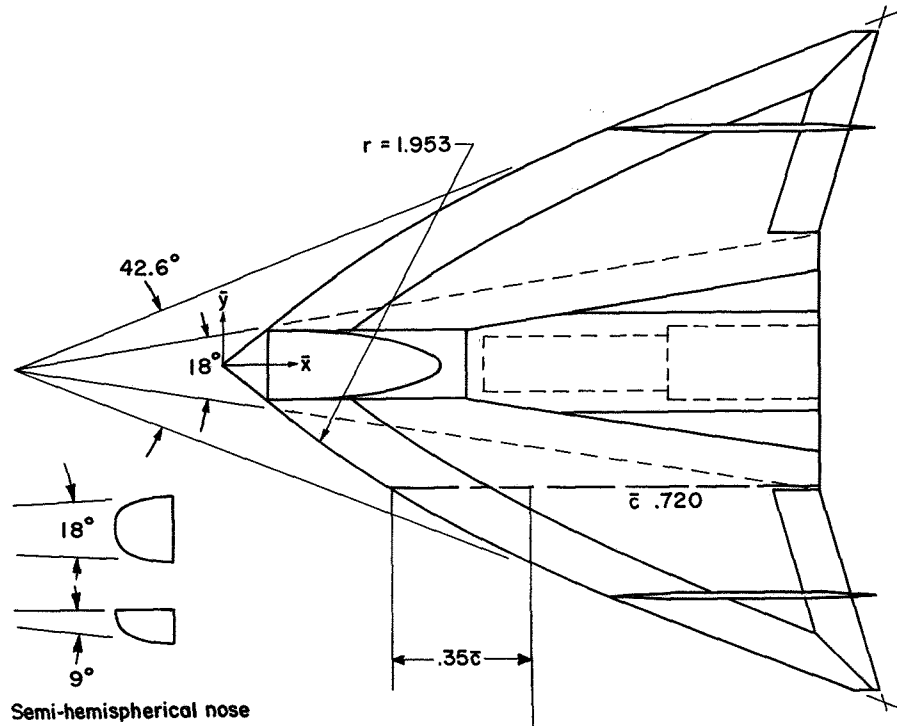
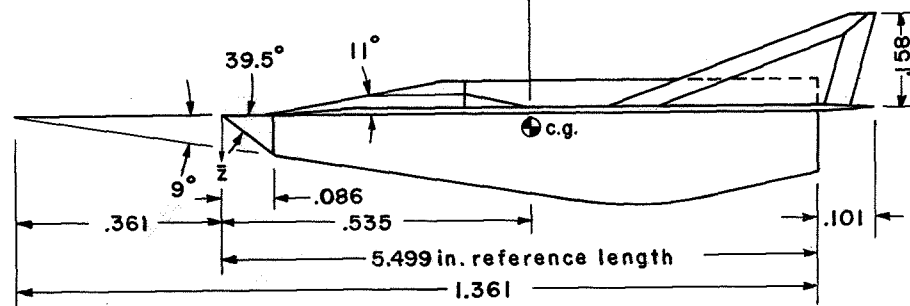


Figure 4.- Launch configuration.

A-28087



Semi-hemispherical nose



5.499 in. reference length

\bar{y}	$\bar{z} = .666$	$\bar{z} = .784$	$\bar{z} = .892$	$\bar{z} = 1.0$
0	0.1547	0.1411	0.1208	0.1005
.0179	.1538	.1403	.1202	.1001
.0359	.1508	.1382	.1188	.0991
.0558	.1457	.1344	.1161	.0973
.0718	.1382	.1290	.1123	.0946
.0897	.1280	.1219	.1073	.0912
.1077	.1143	.1123	.1009	.0867
.1256	.0955	.1000	.0926	.0811
.1436	.0678	.0836	.0820	.0741
.1525	.0459	.0729	.0756	.0700
.1597	0	-	-	-
.1615		.0596	.0680	.0653
.1705		.0411	.0590	.0601
.1782		0	-	-
.1795			.0477	.0538
.1884			.0319	.0467
.1954			0	-
.1974				.0373
.2064				.0242
.2127				0

Dimensions in fractions of reference length
Reference area, S , 19.58 sq in.

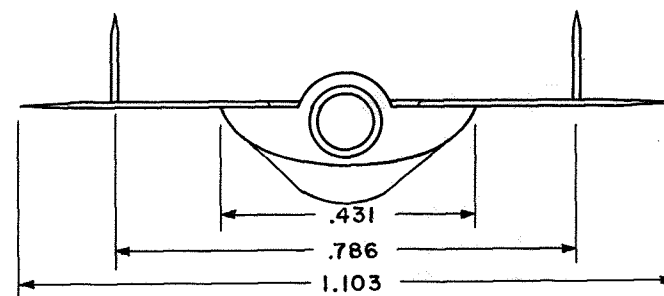
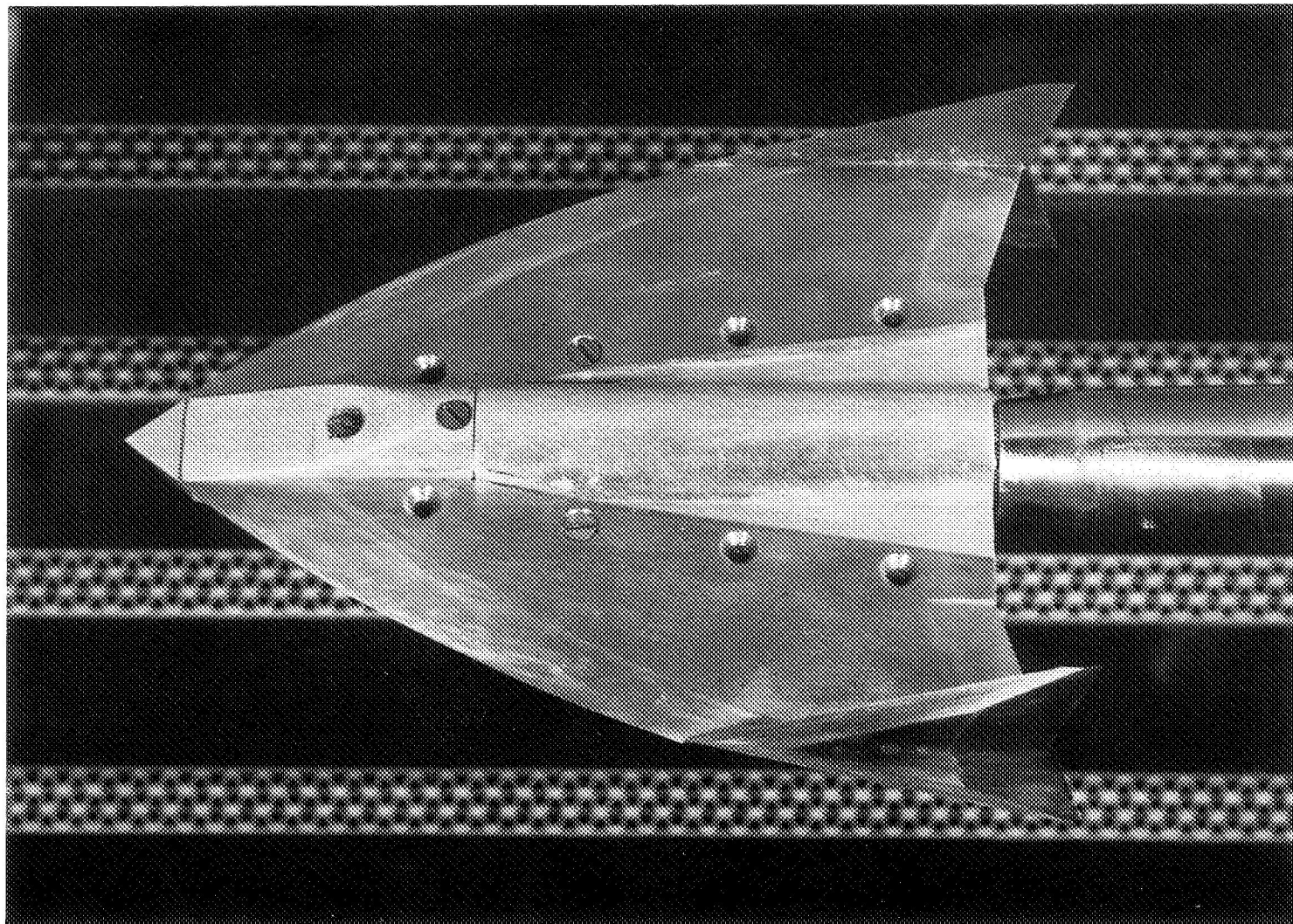
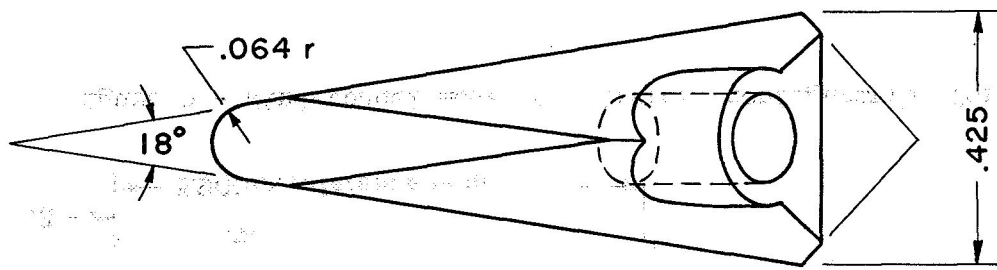


Figure 5.- Model dimensions.



A-27675

Figure 6.- Model with wing tips deflected 90° mounted in transonic wind tunnel.



Dimensions in fractions of reference length

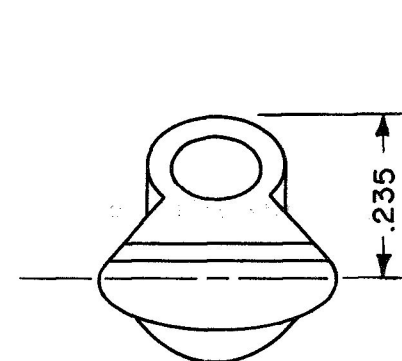
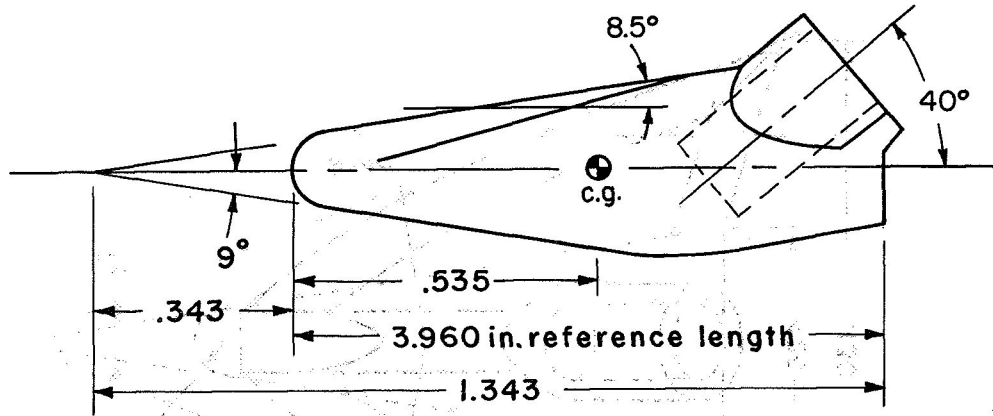


Figure 7.-- Wind-tunnel model of entry configuration for high angles of attack.

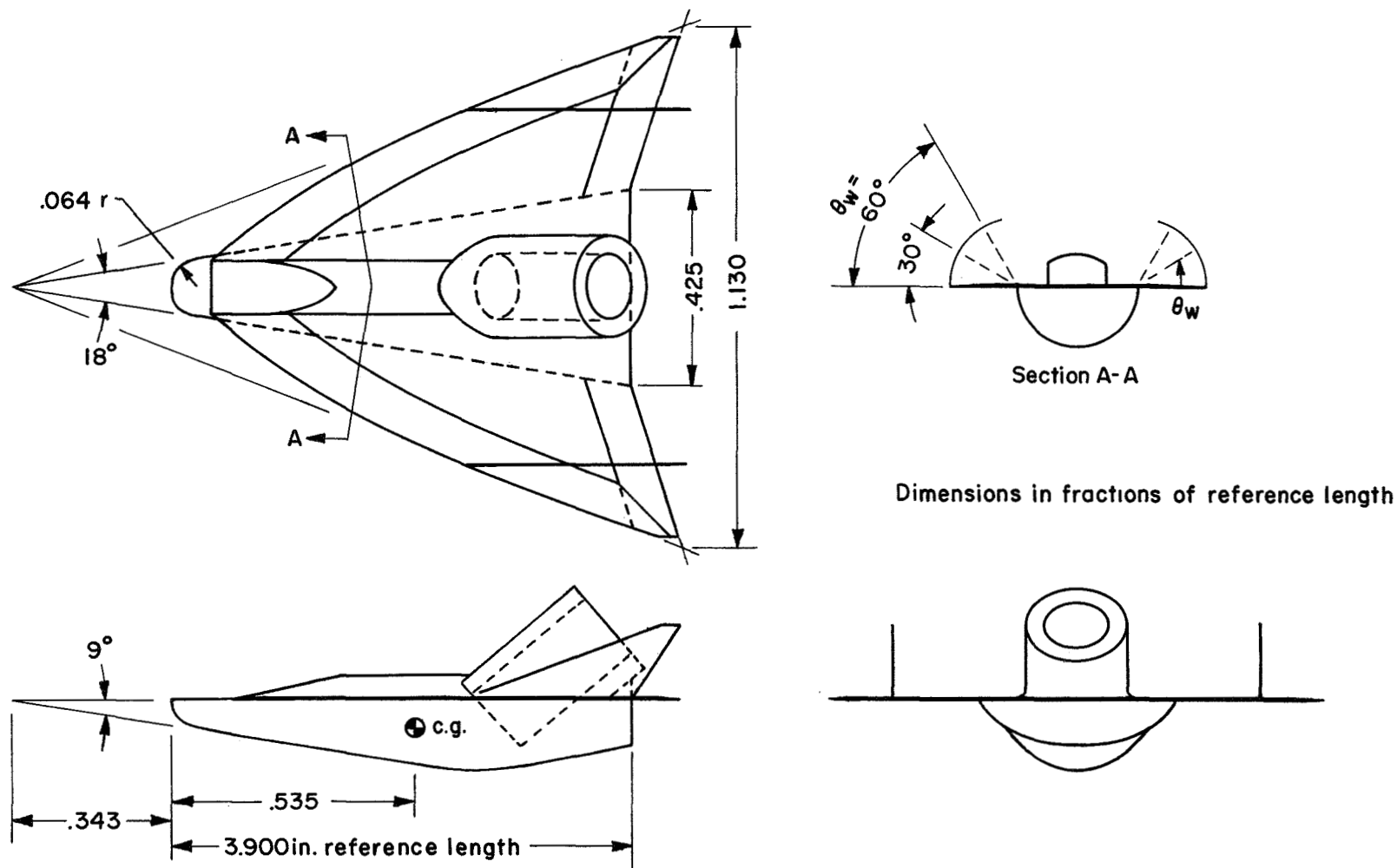
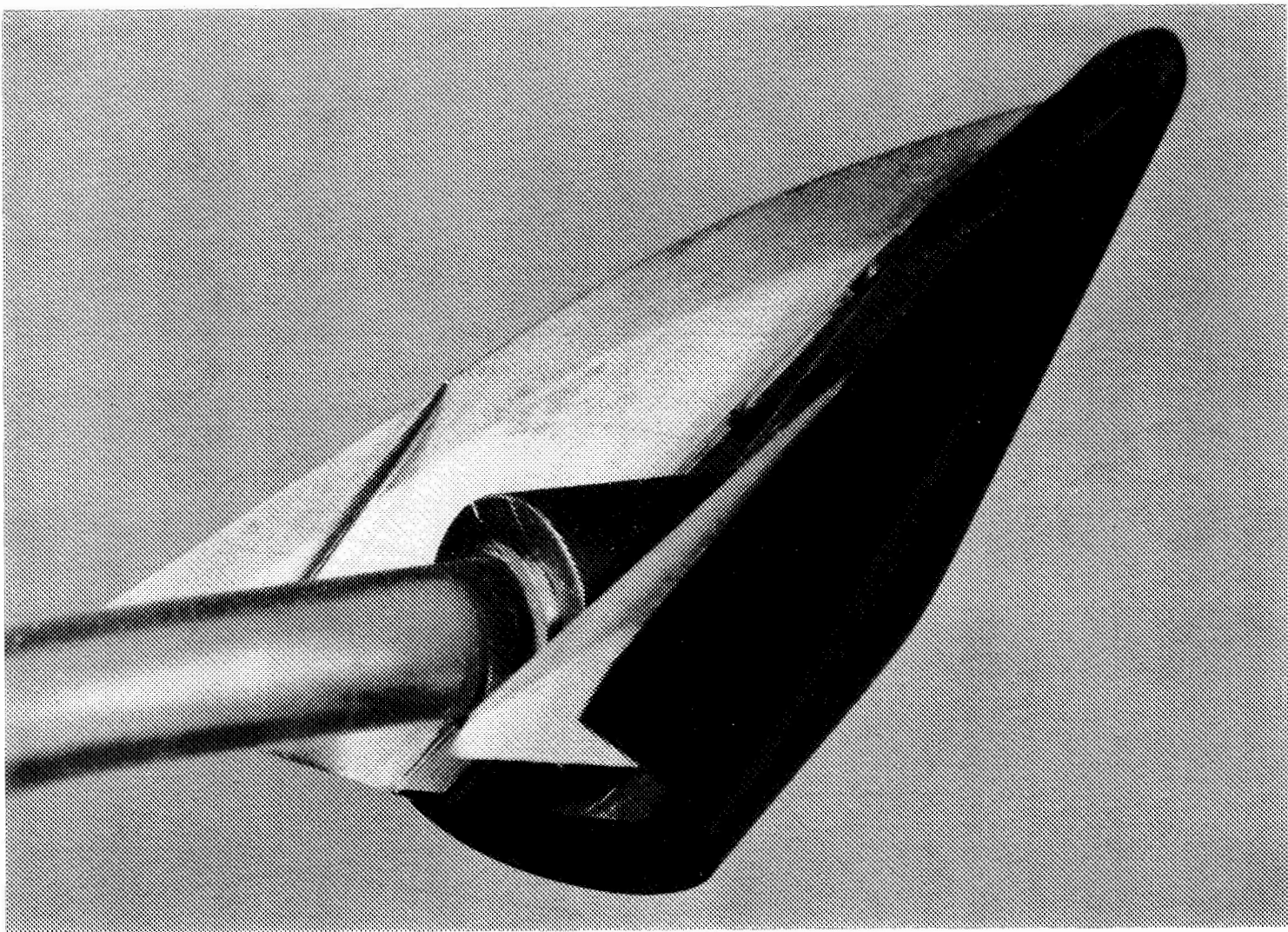


Figure 8.- Wind-tunnel model of aircraft configuration for high angles of attack.



A-28696

Figure 9.- View of model with wings partially unfolded; $\theta_w = 60^\circ$.

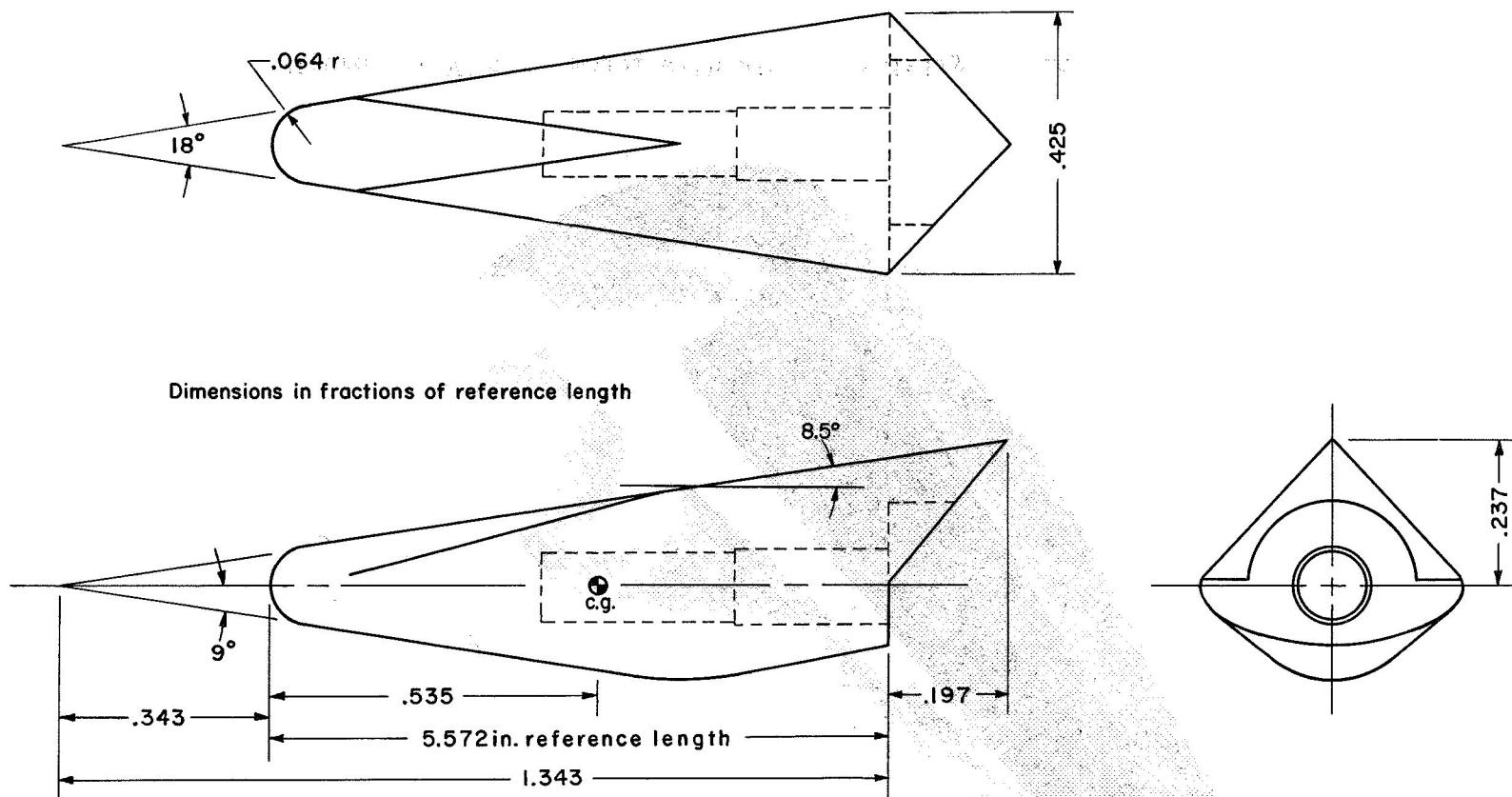
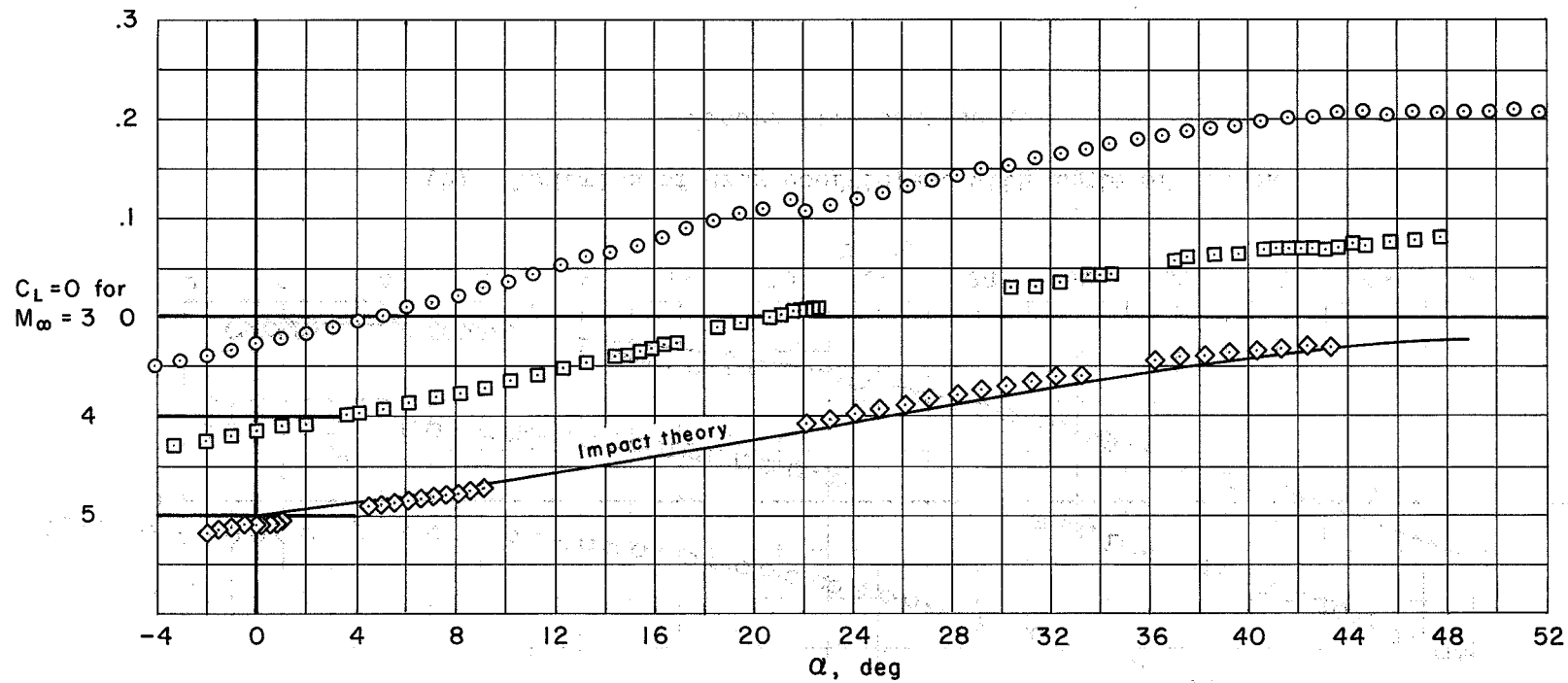
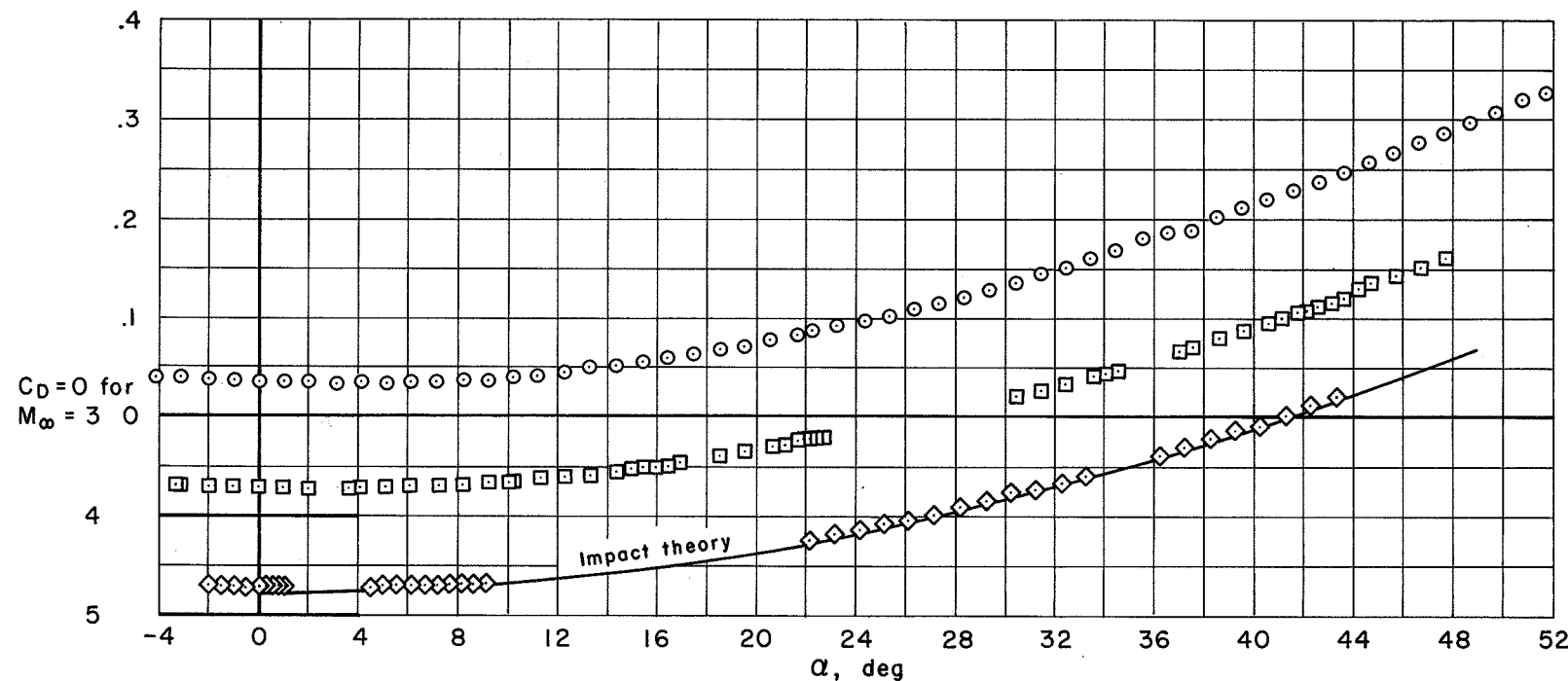


Figure 10.- Wind-tunnel model of entry configuration.



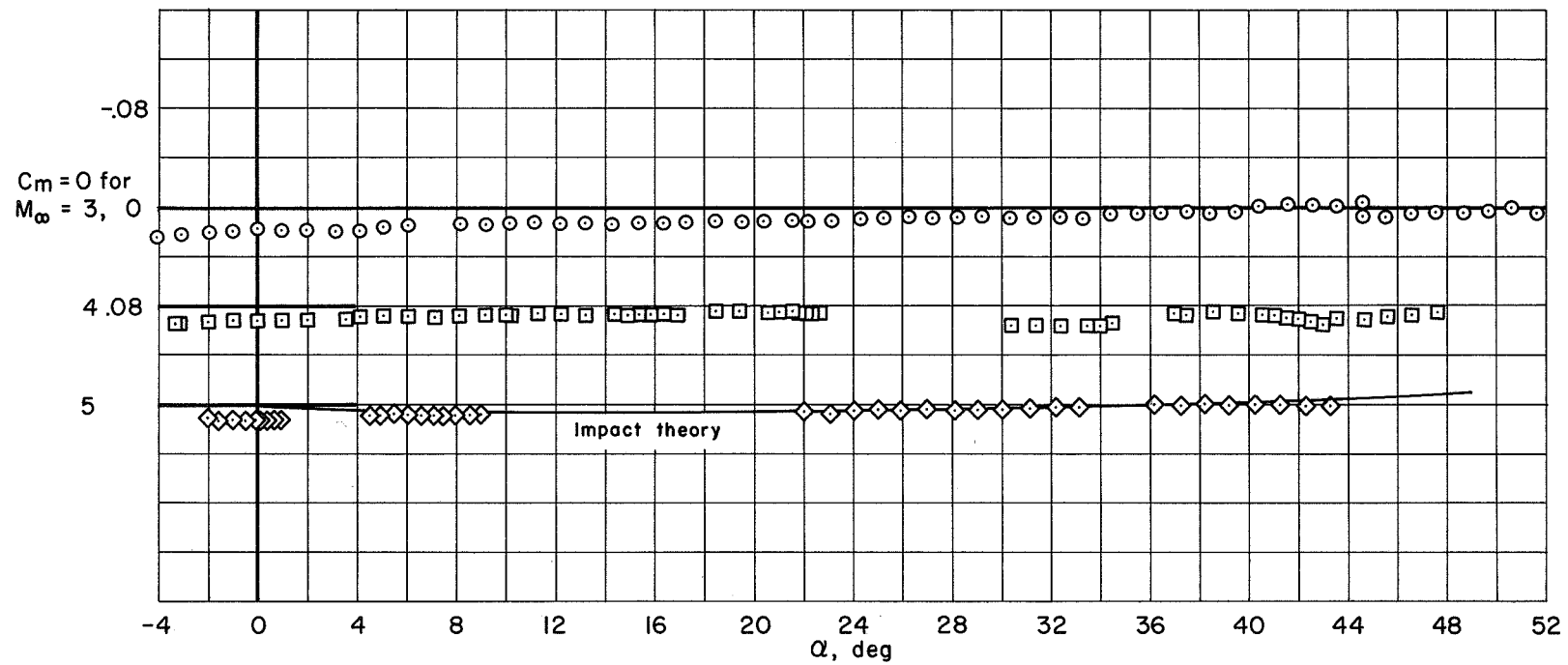
(a) Variation of lift coefficient with angle of attack.

Figure 11.- Longitudinal aerodynamic characteristics for entry configuration.



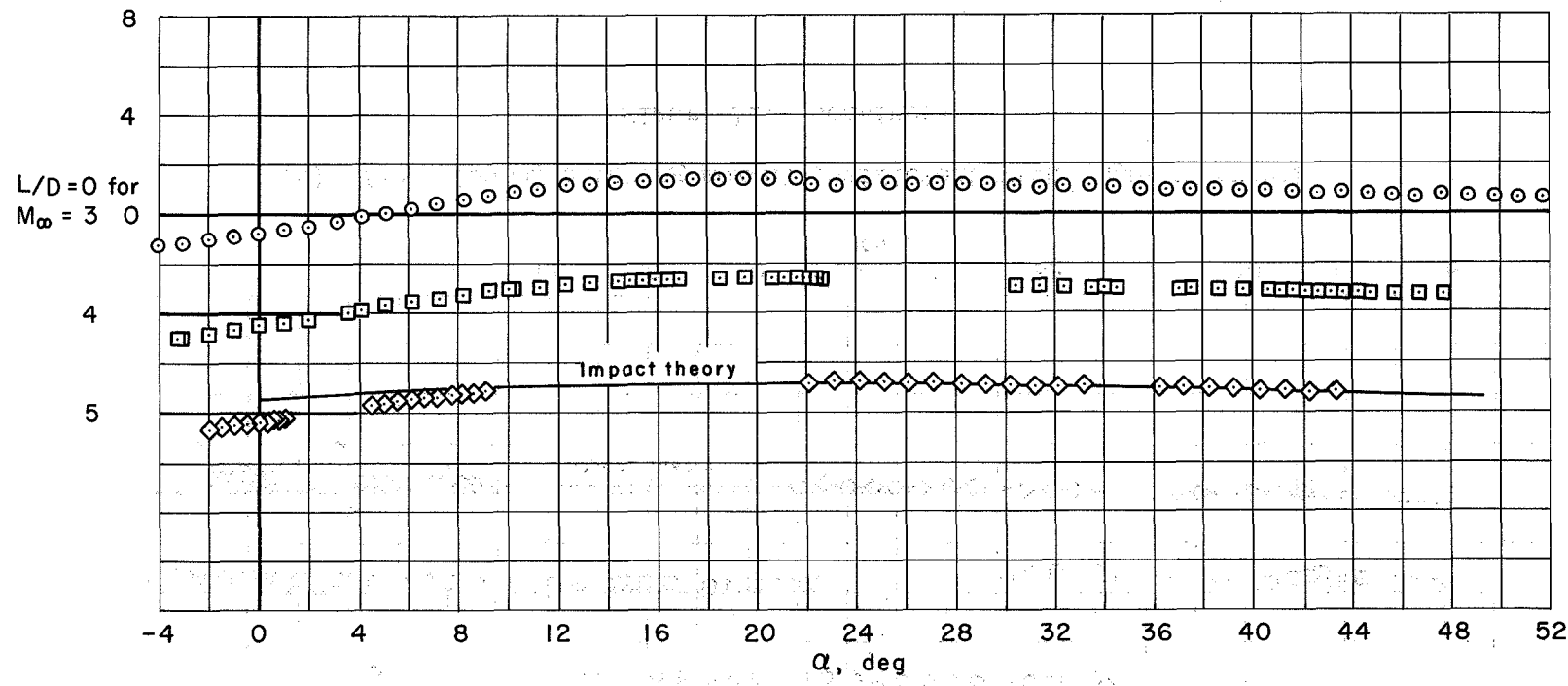
(b) Variation of drag coefficient with angle of attack.

Figure 11.- Continued.



(c) Variation of pitching-moment coefficient with angle of attack.

Figure 11.- Continued.



(d) Variation of lift-drag ratio with angle of attack.

Figure 11.- Concluded.

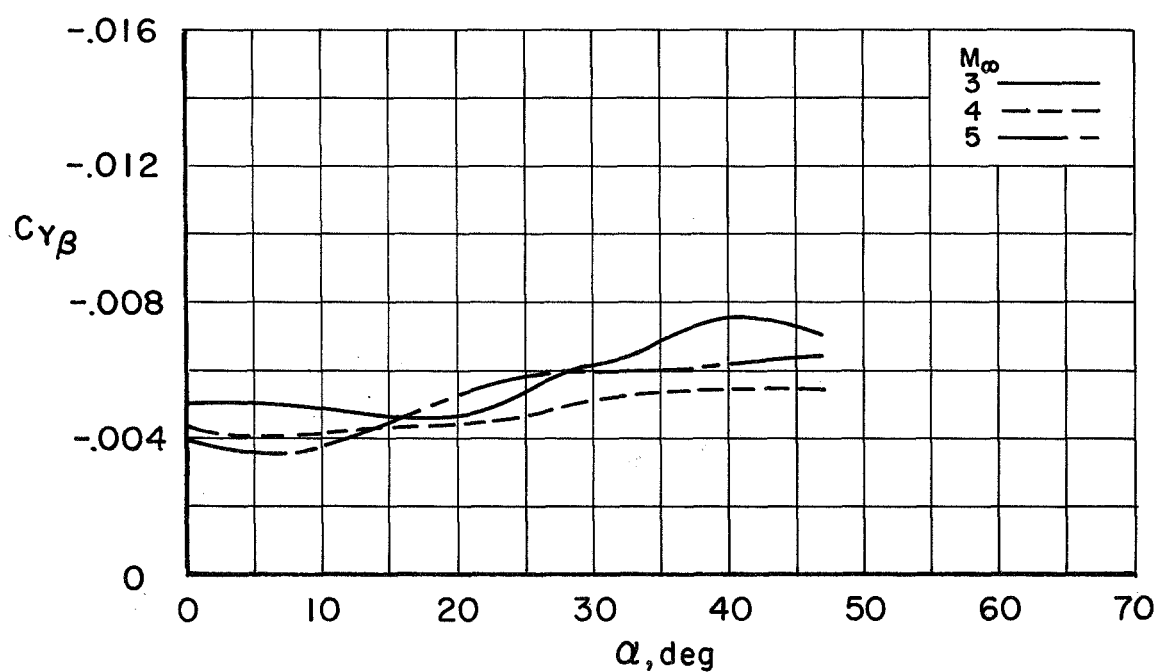
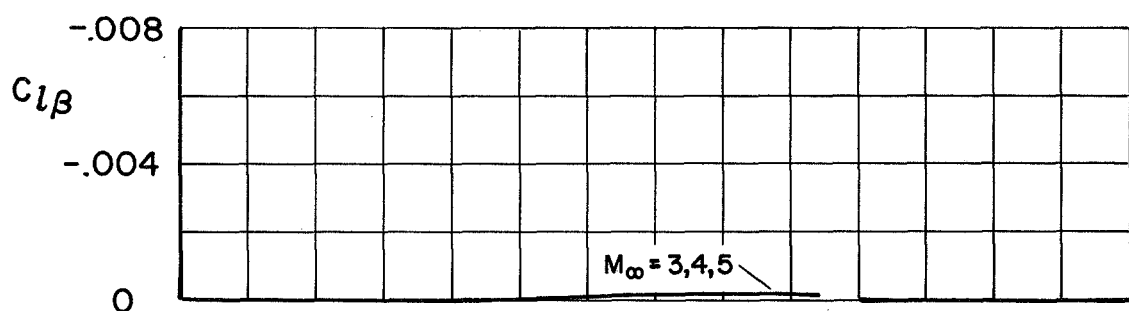
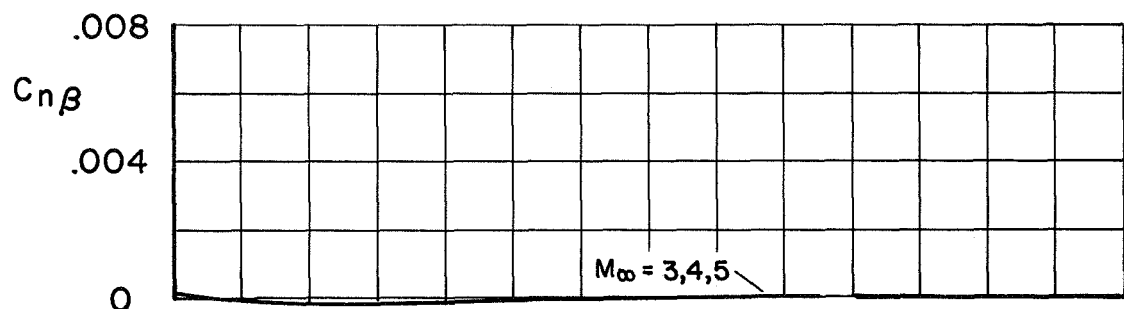
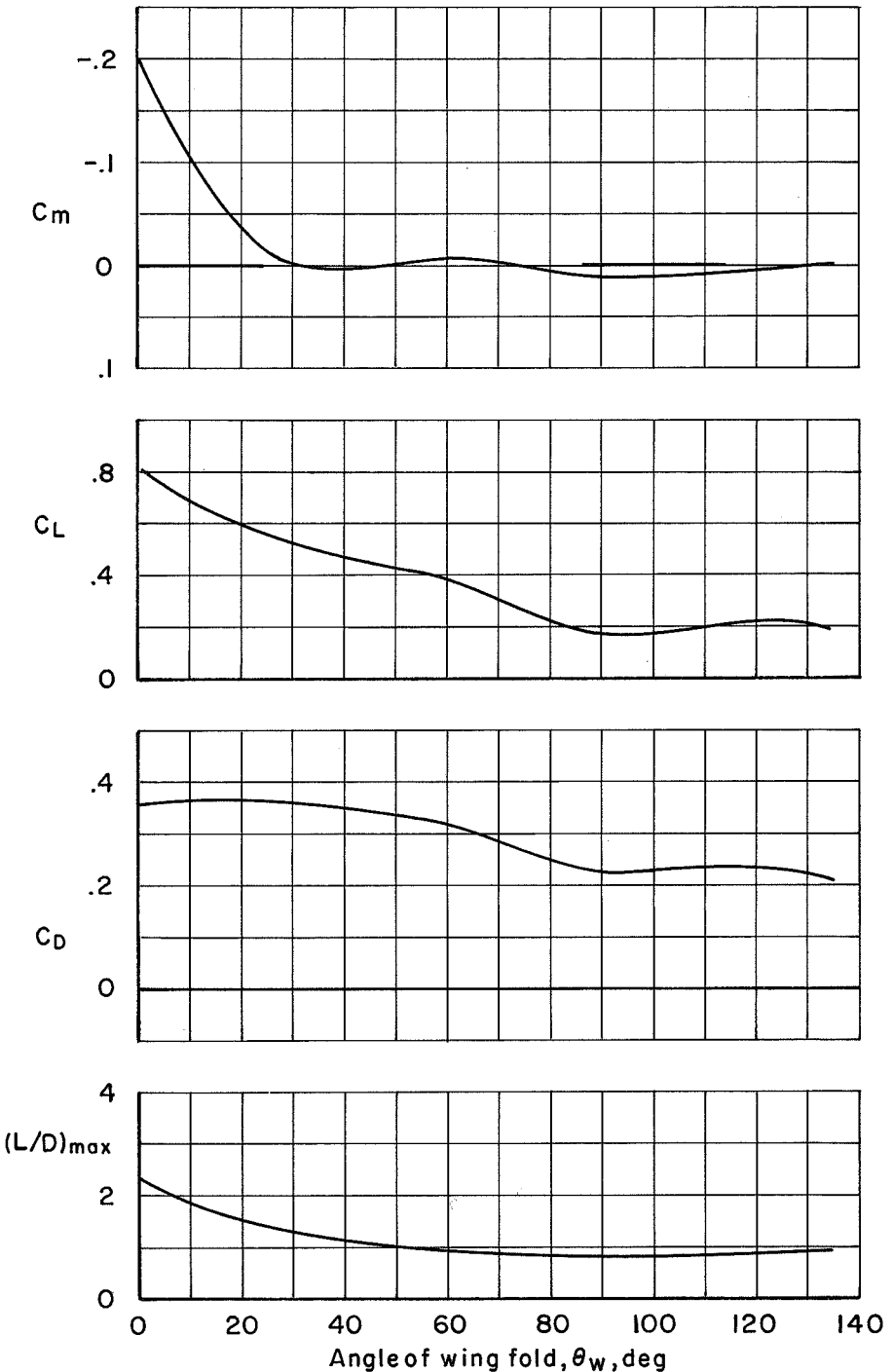
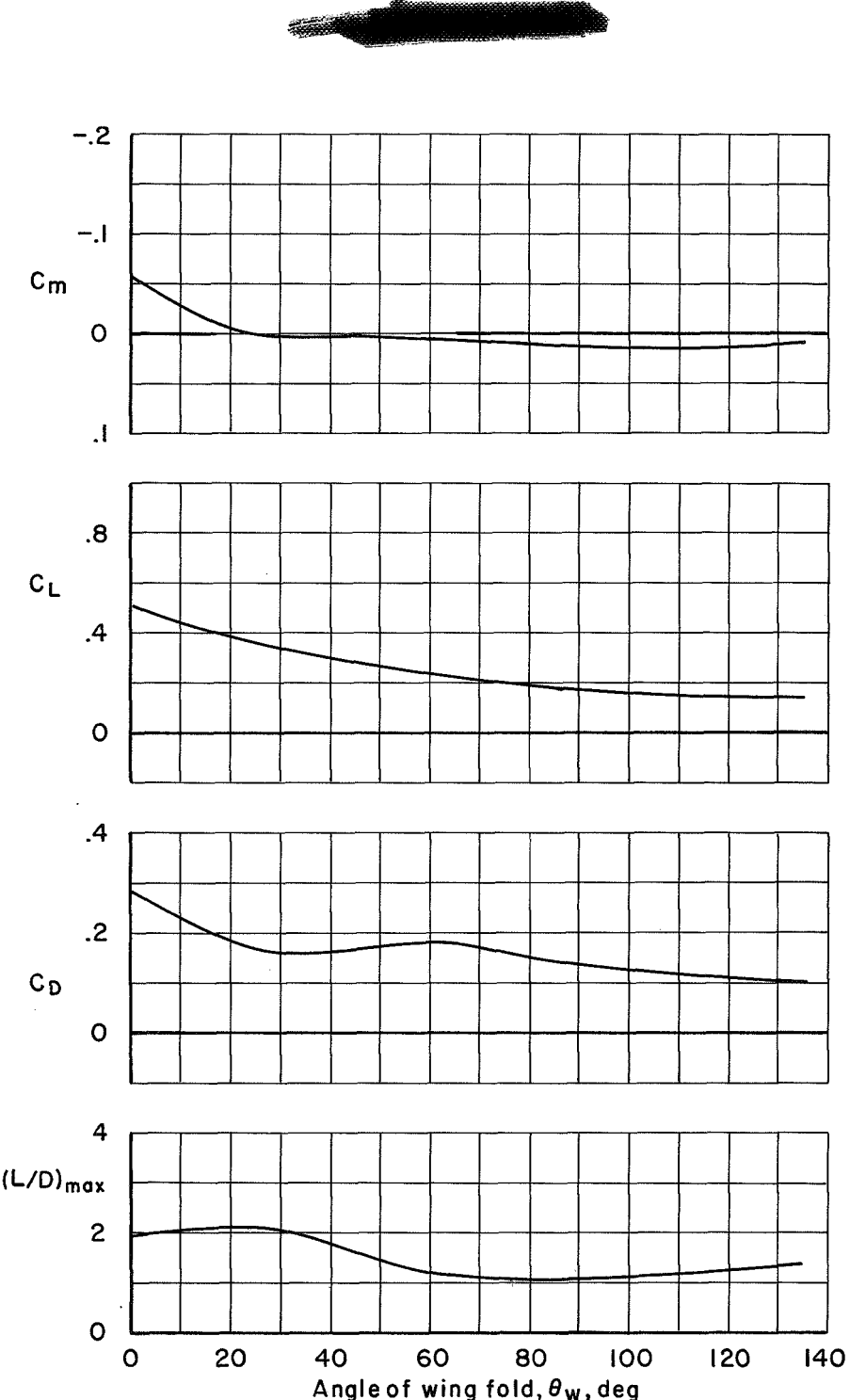


Figure 12.- Lateral stability derivatives for entry configuration.



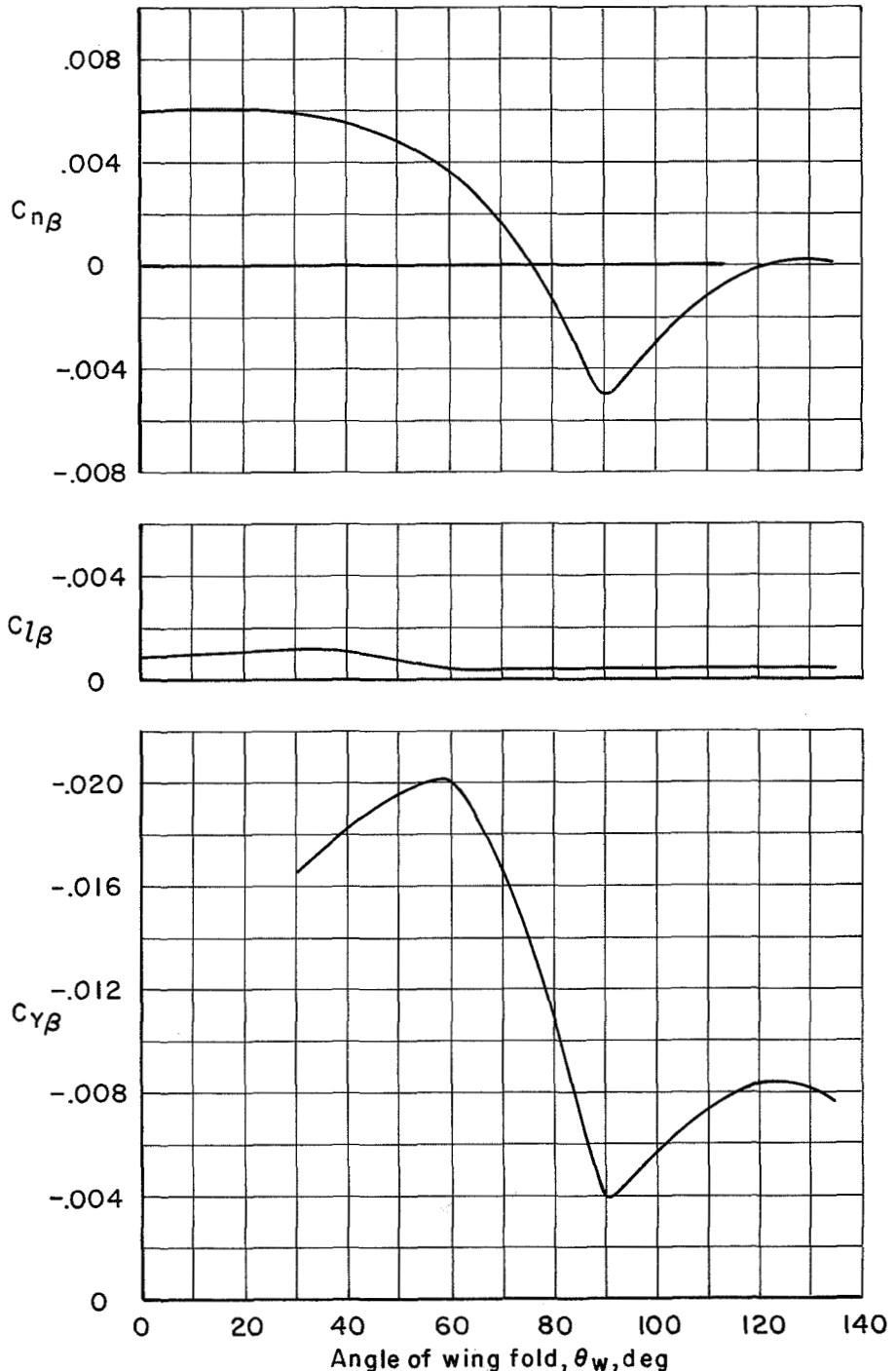
(a) $\alpha = 40^\circ$

Figure 13.- Effect of wing-fold angle on longitudinal aerodynamic characteristics; $M = 3$.



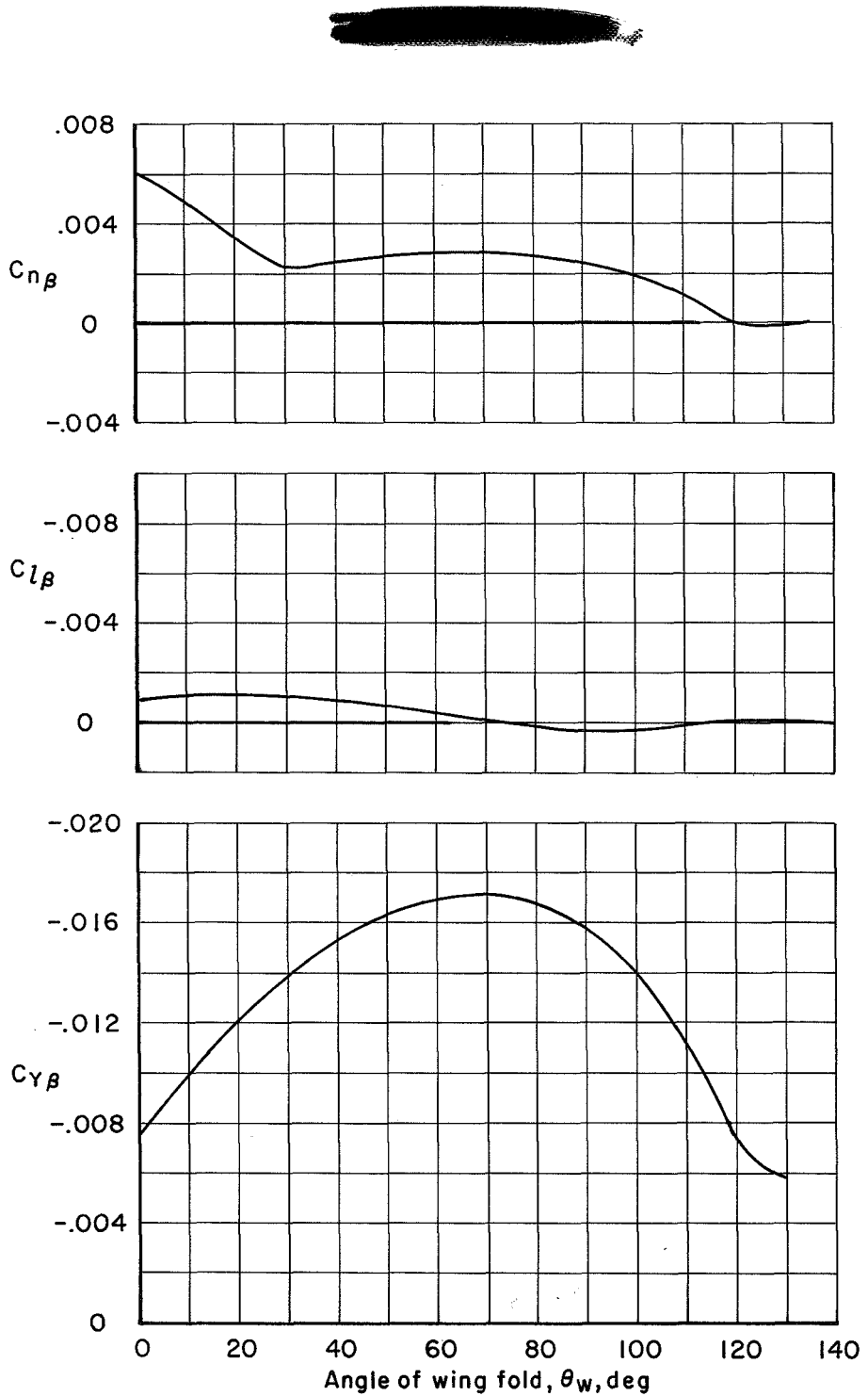
(b) $\alpha = 25^\circ$

Figure 13.- Concluded.



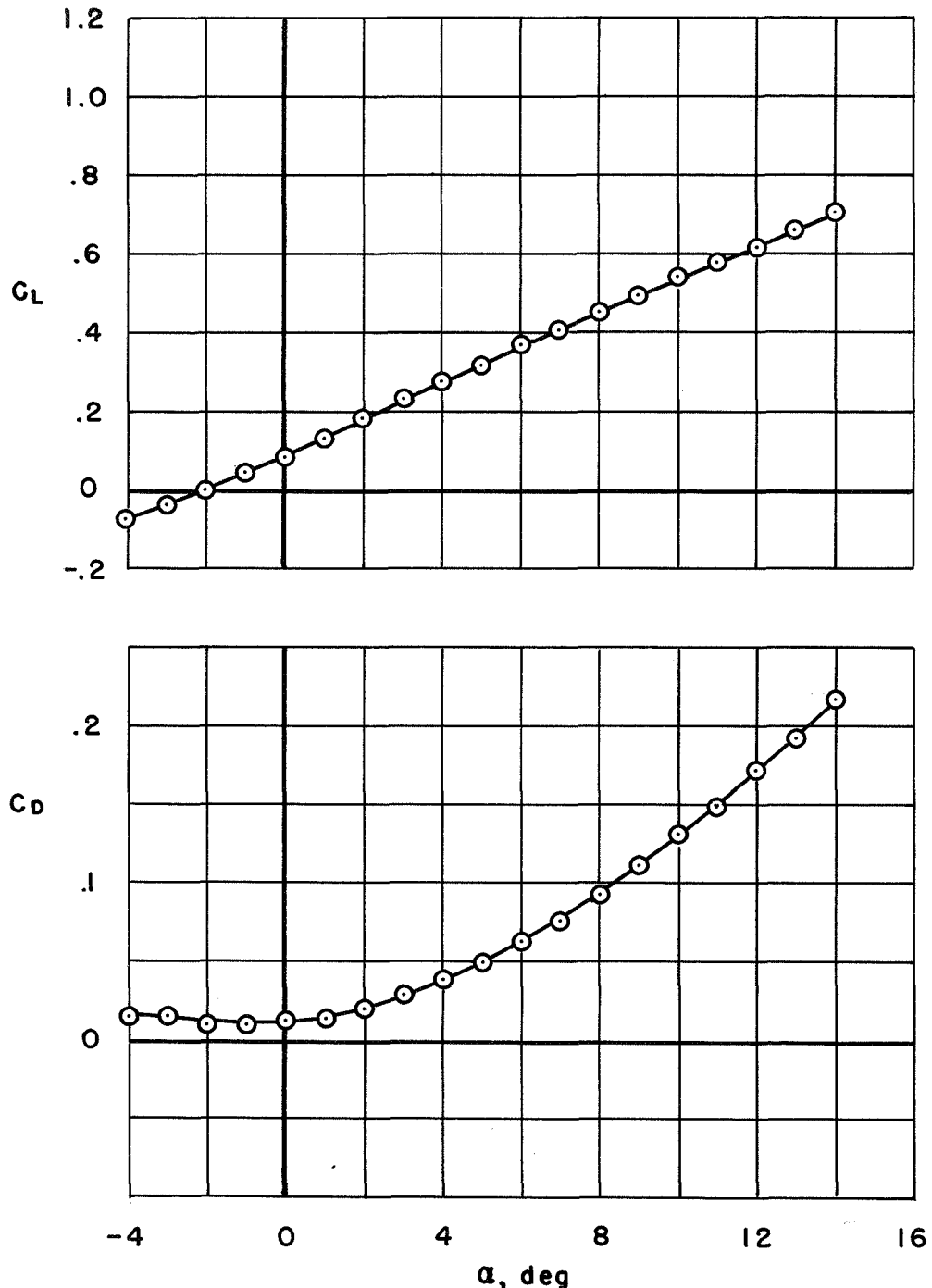
(a) $\alpha = 40^\circ$

Figure 14.- Effect of wing-fold angle on lateral aerodynamic characteristics; $M_\infty = 3$, $\theta_t = 0^\circ$.



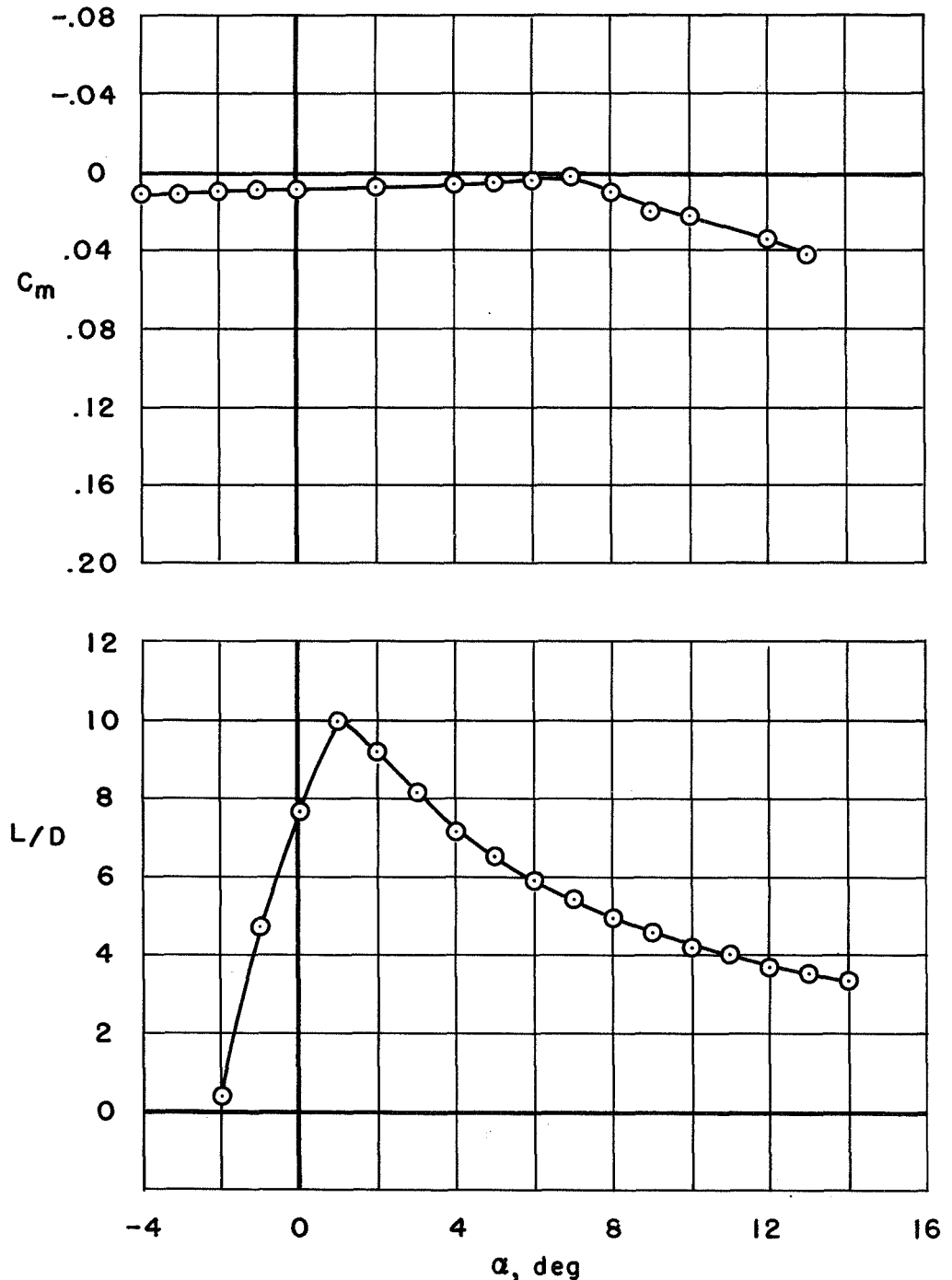
(b) $\alpha = 25^\circ$

Figure 14.- Concluded.



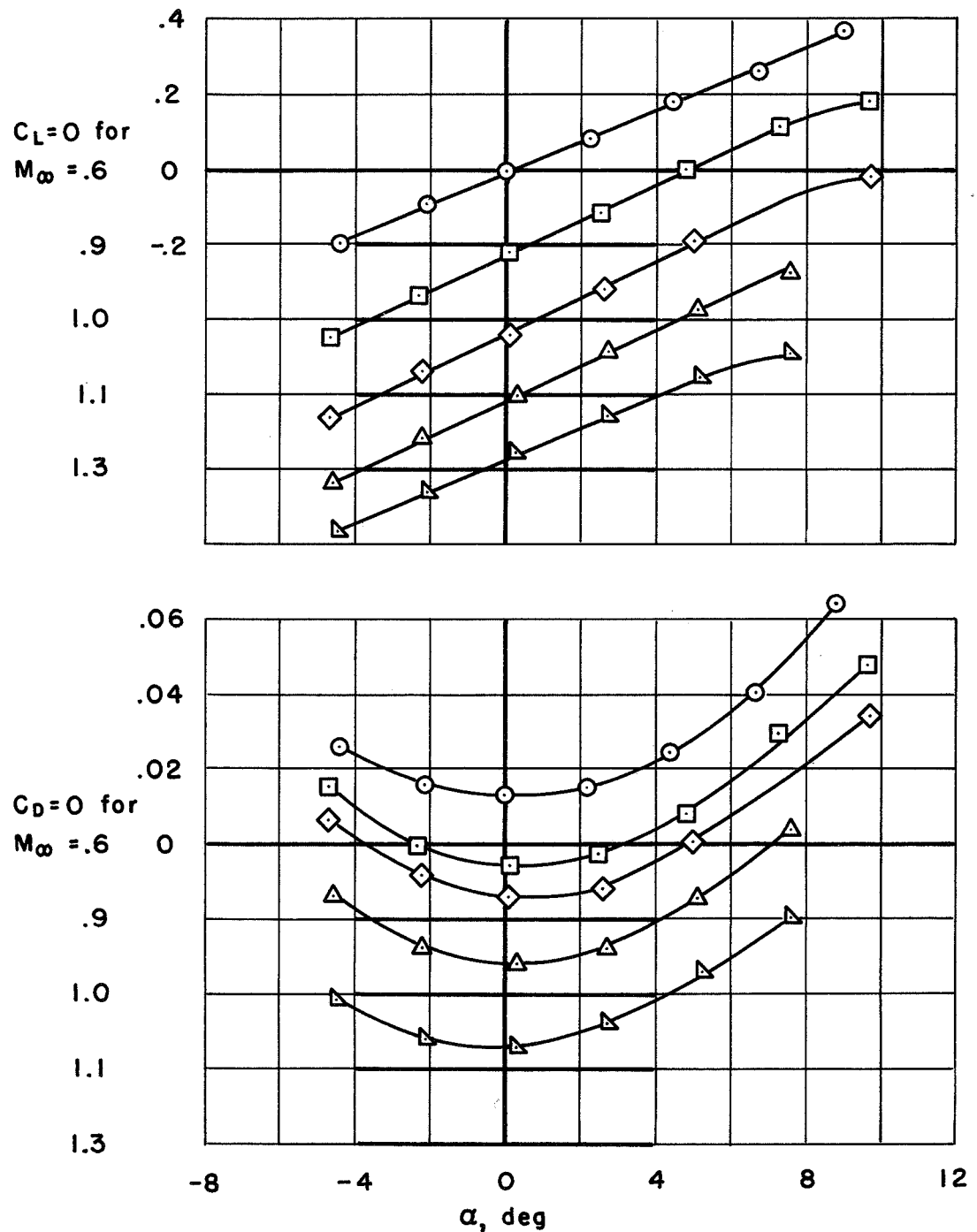
(a) Variation of lift coefficient and drag coefficient with angle of attack.

Figure 15.- Low-speed characteristics of aircraft configuration;
 $q = 50$, $\theta_t = \theta_w = 0^\circ$.



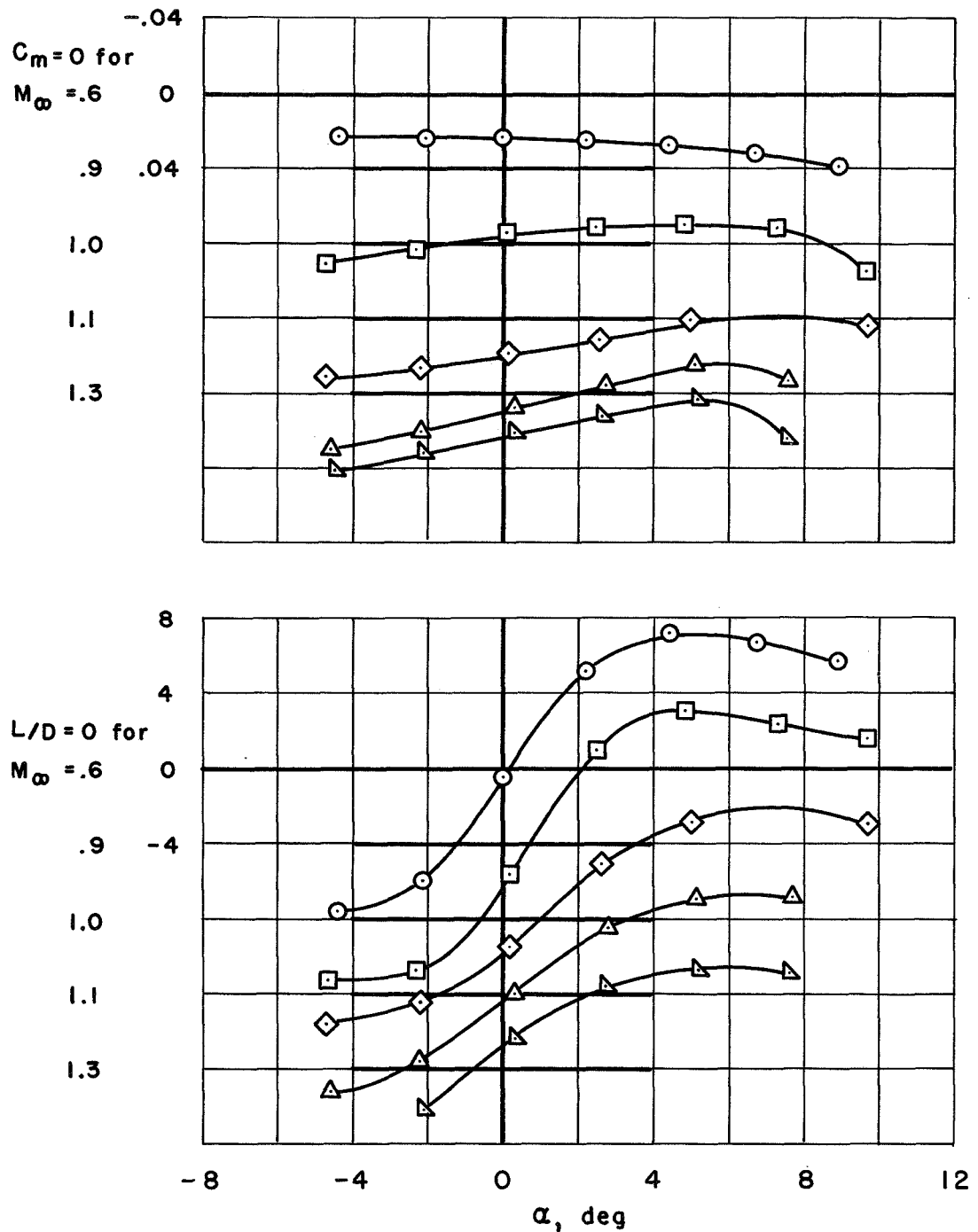
(b) Variation of pitching-moment coefficient and lift-drag ratio with angle of attack.

Figure 15.- Concluded.



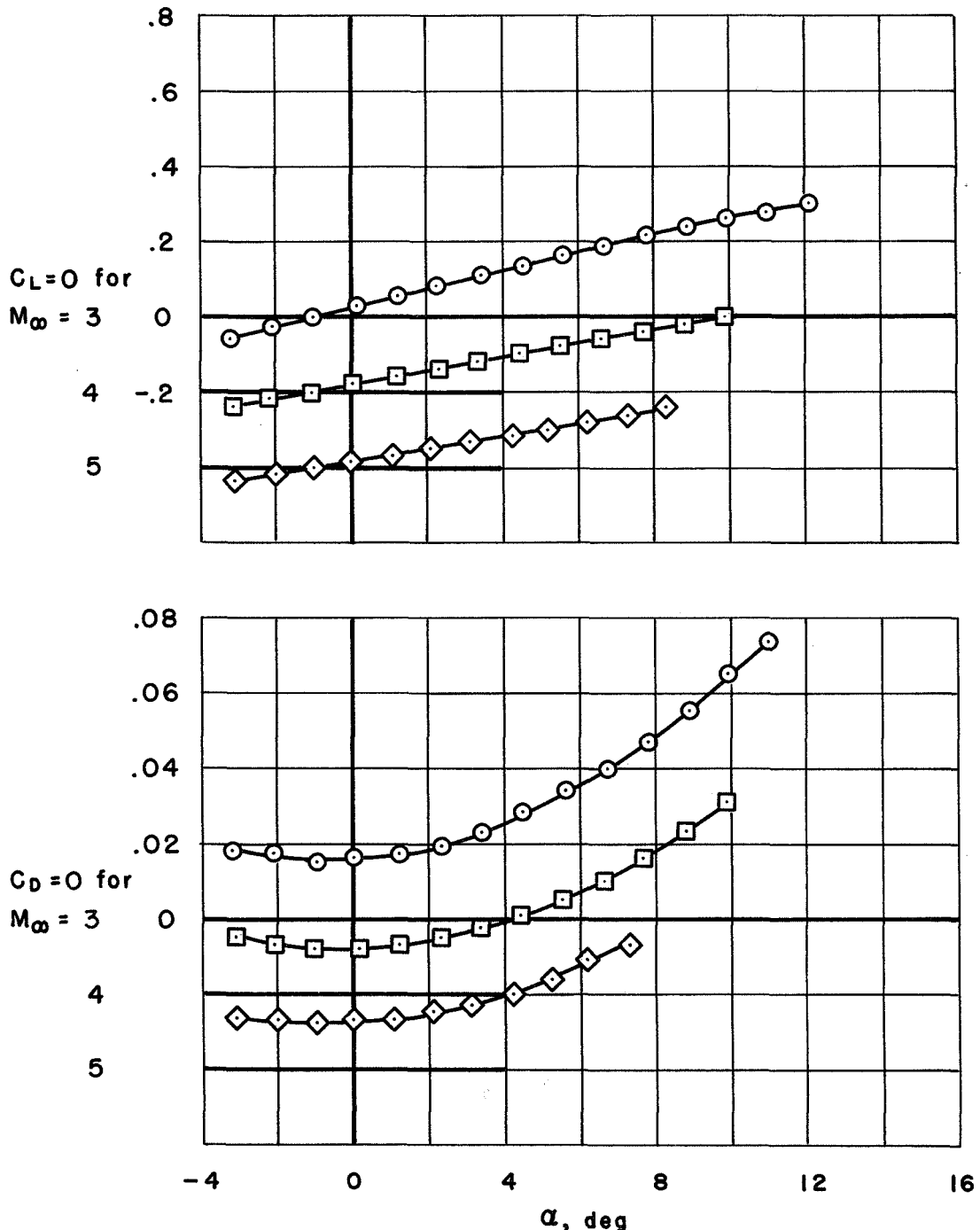
(a) Variation of lift coefficient and drag coefficient with angle of attack.

Figure 16.- Transonic characteristics for the aircraft configuration.



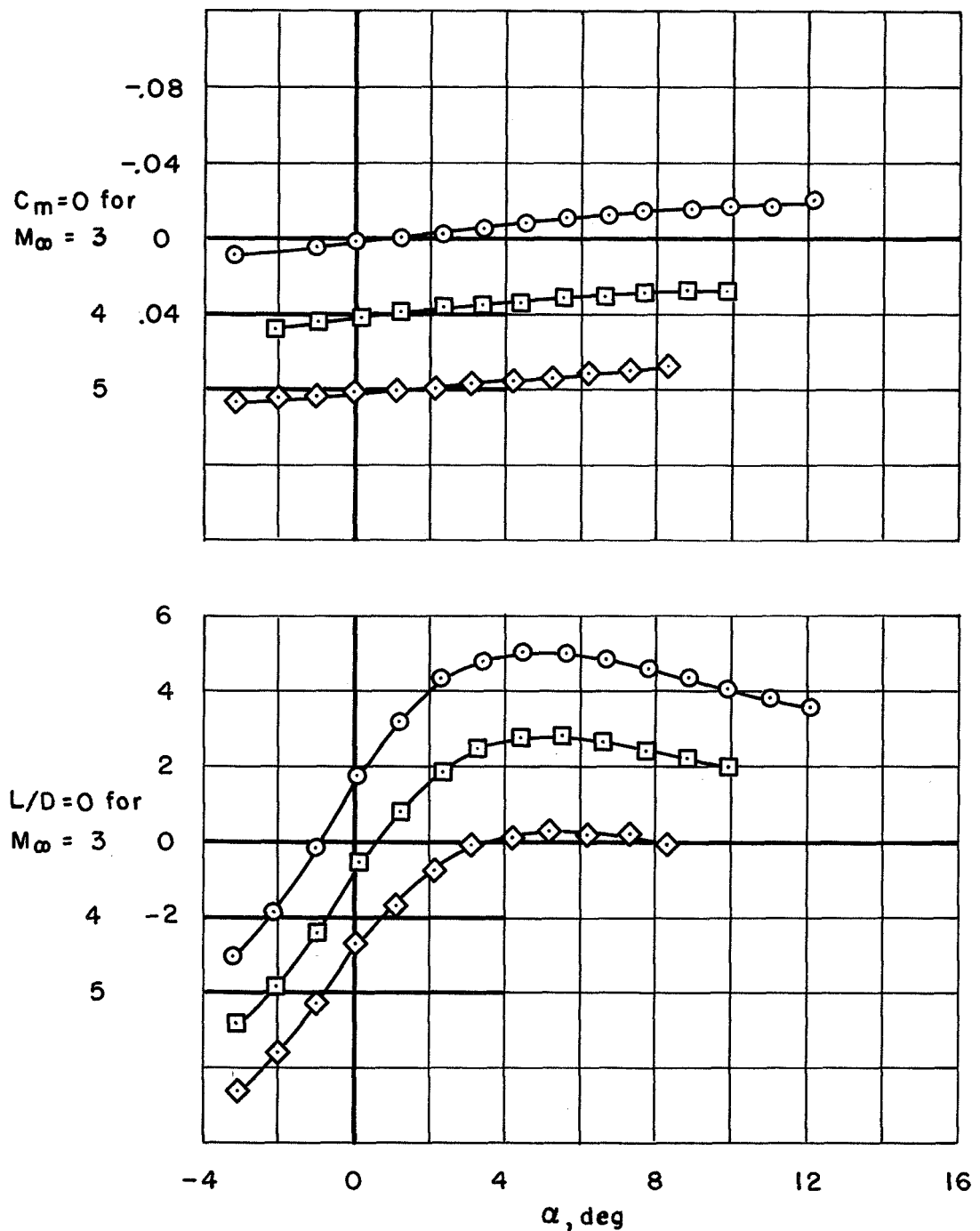
(b) Variation of pitching-moment coefficient and lift-drag ratio with angle of attack.

Figure 16.- Concluded.



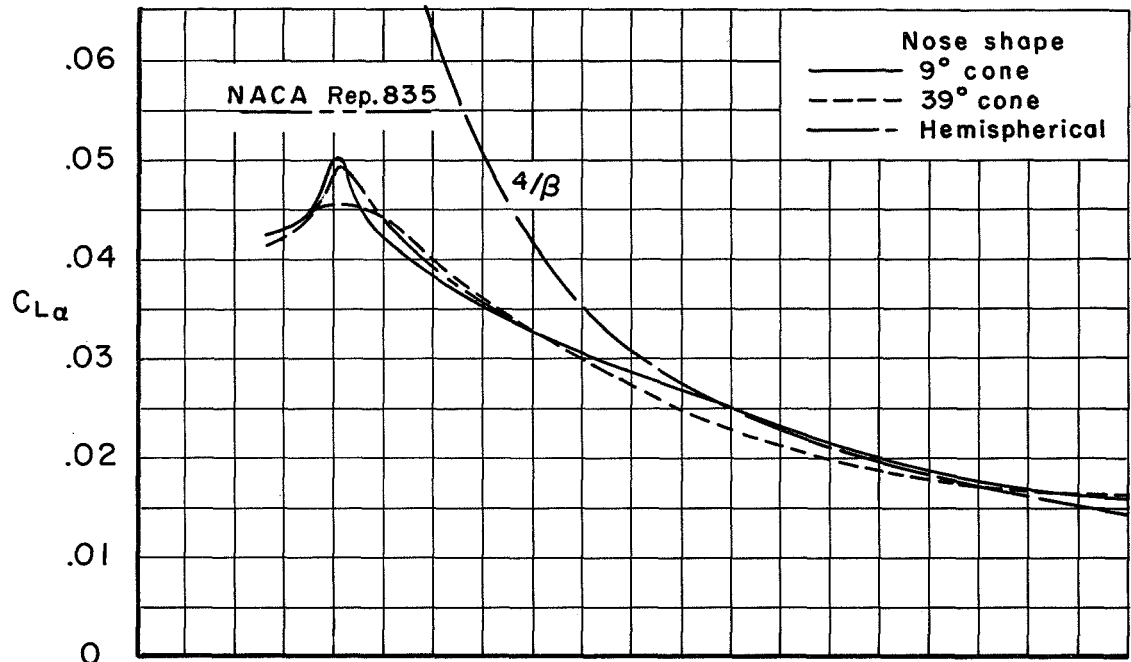
(a) Variation of lift coefficient and drag coefficient with angle of attack.

Figure 17.- Supersonic characteristics for aircraft configuration.

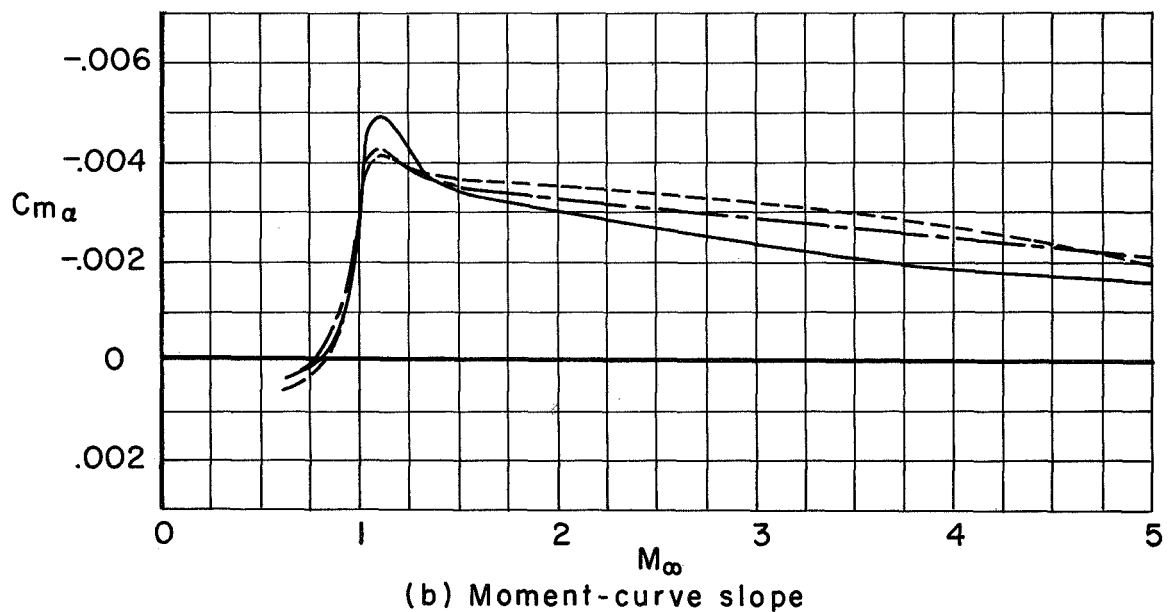


(b) Variation of pitching-moment coefficient and lift-drag ratio with angle of attack.

Figure 17.- Concluded.

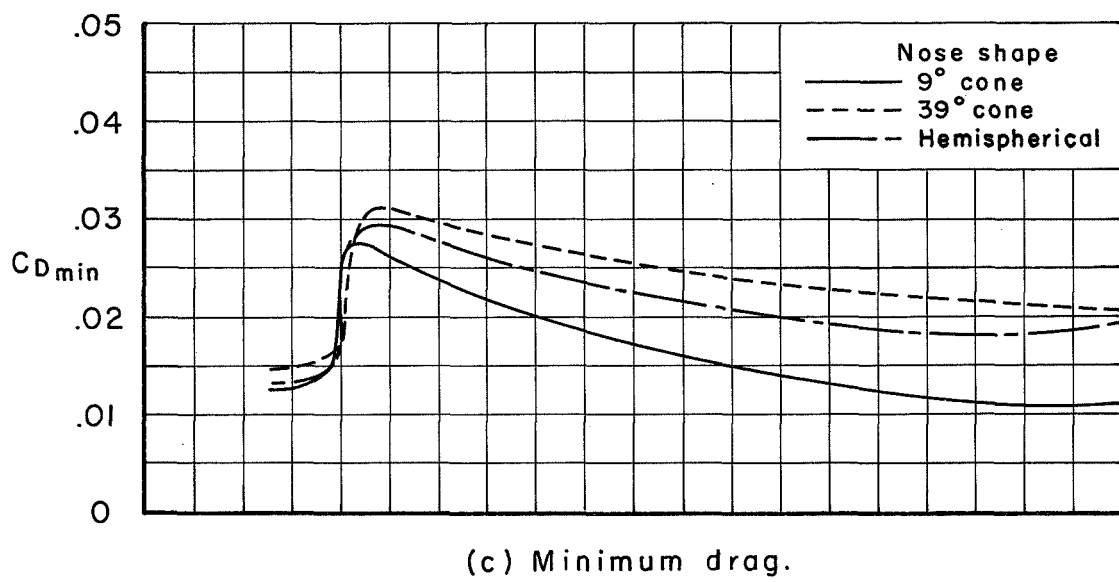


(a) Lift-curve slope

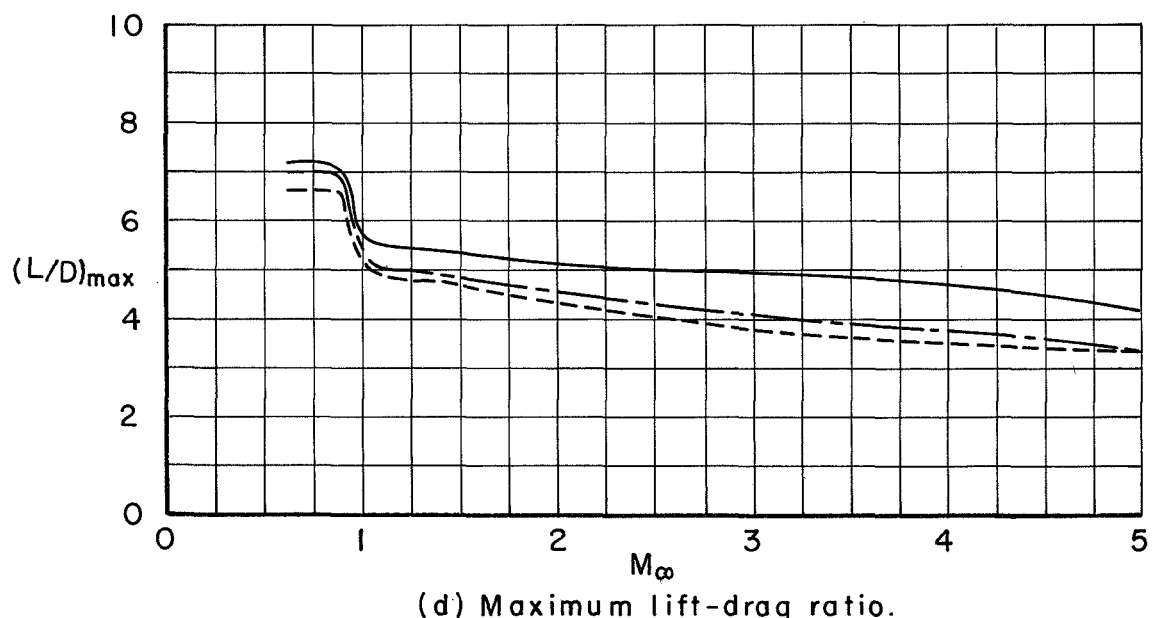


(b) Moment-curve slope

Figure 18.- Longitudinal aerodynamic characteristics for the aircraft configuration showing the effect of nose shape; $\theta_t = \theta_w = 0^\circ$.

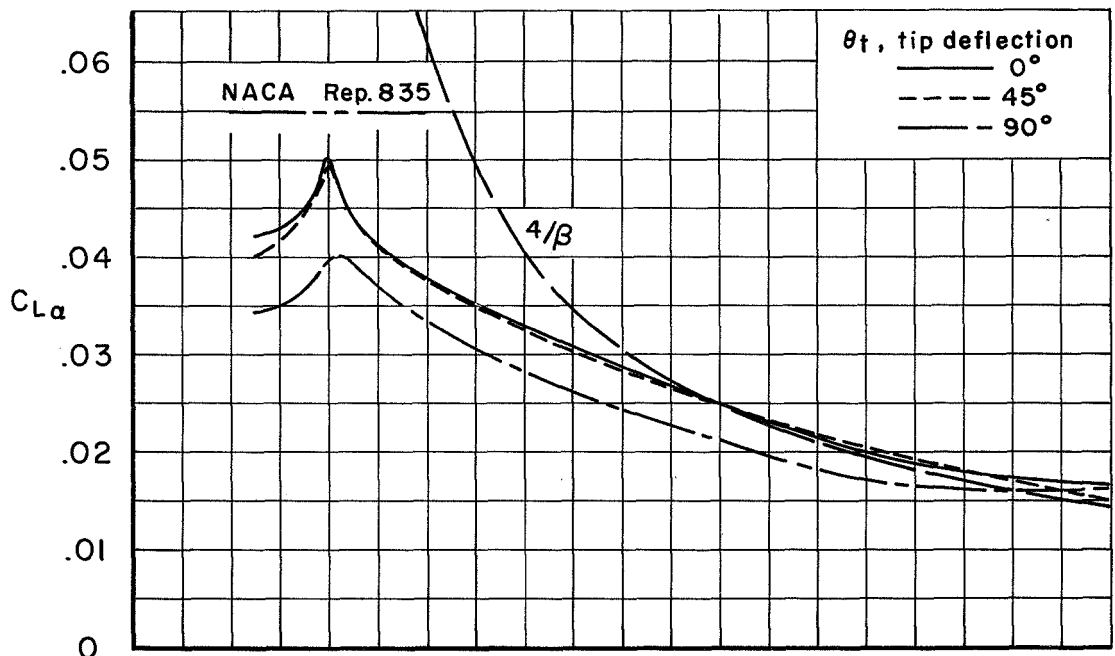


(c) Minimum drag.

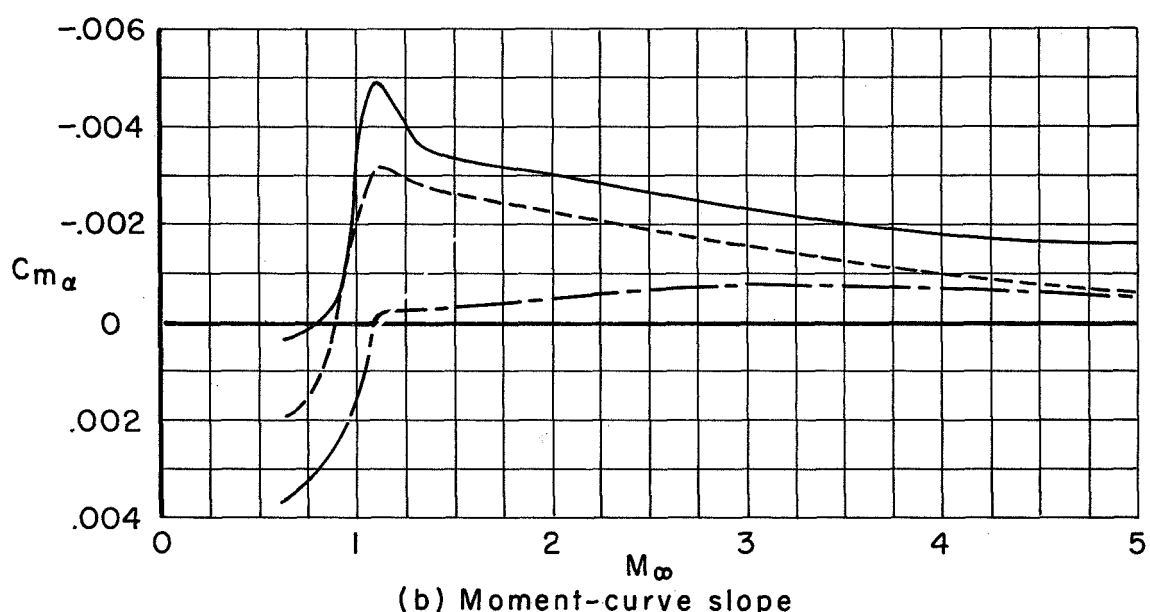


(d) Maximum lift-drag ratio.

Figure 18.- Concluded.

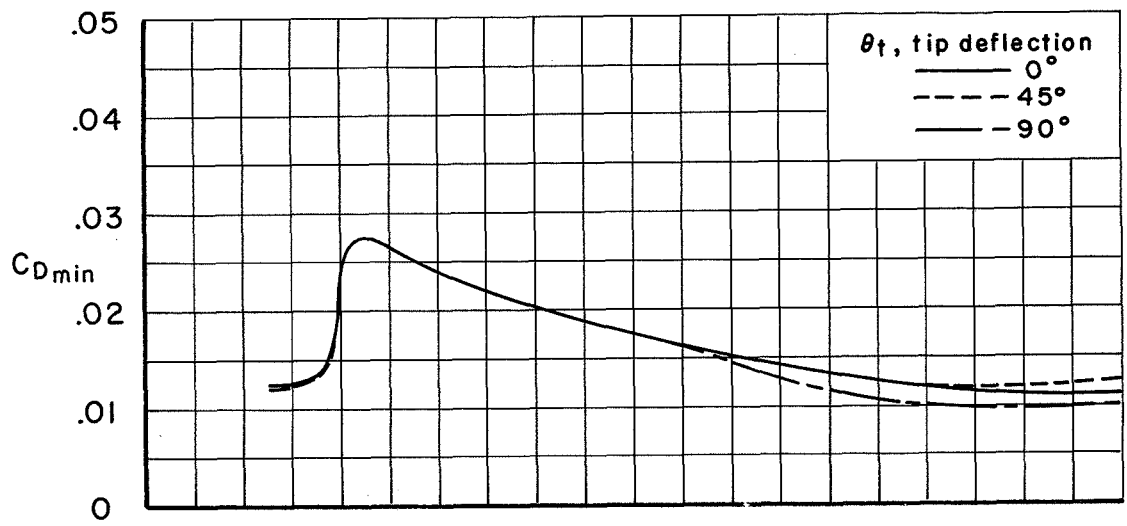


(a) Lift-curve slope

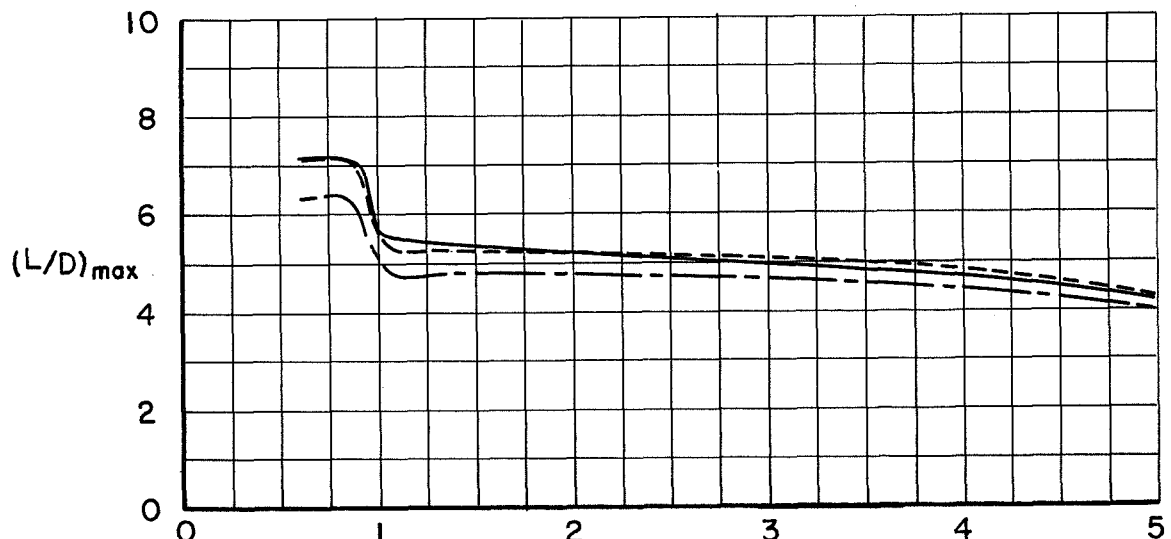


(b) Moment-curve slope

Figure 19.- The effect of wing-tip deflection on the longitudinal aerodynamic characteristics of the aircraft configuration;
 $\theta_w = 0^\circ$.



(c) Minimum drag.



(d) Maximum lift-drag ratio.

Figure 19.- Concluded.

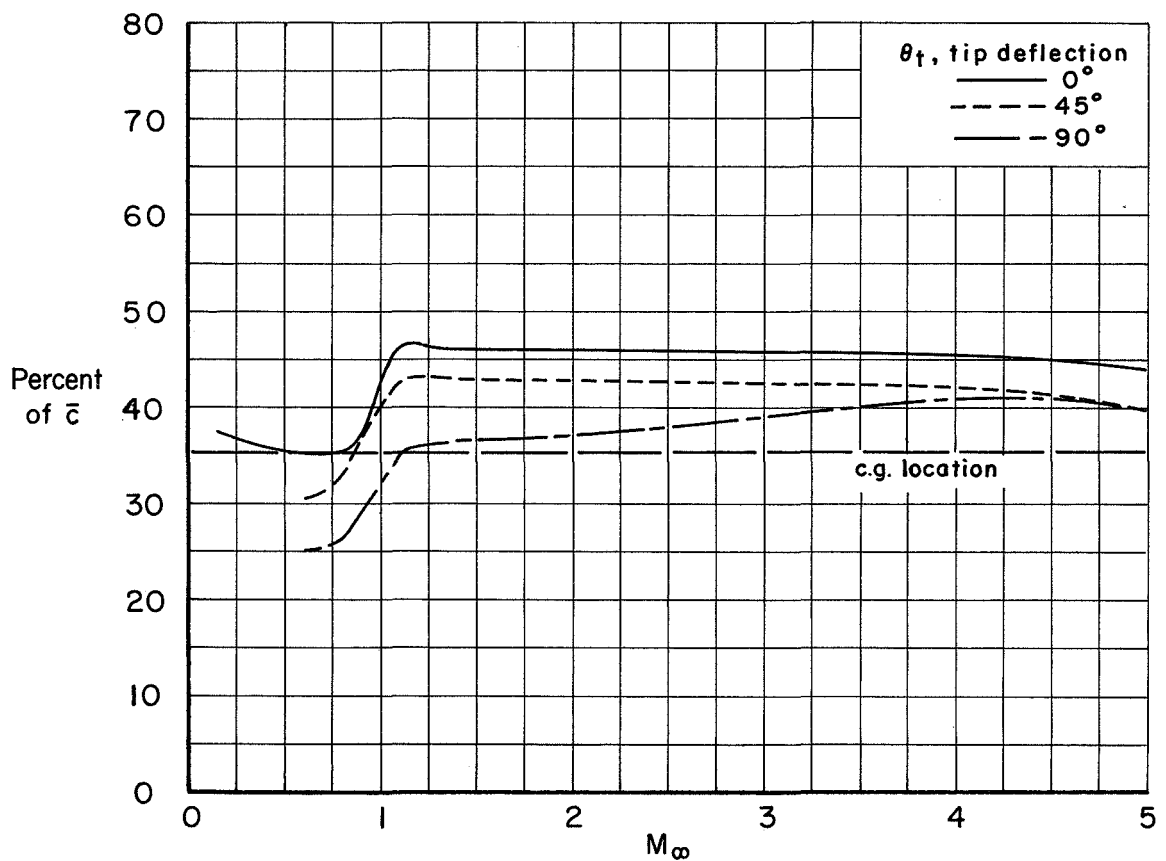


Figure 20.- Location of aerodynamic center for various wing-tip deflections; $\theta_w = 0^\circ$.

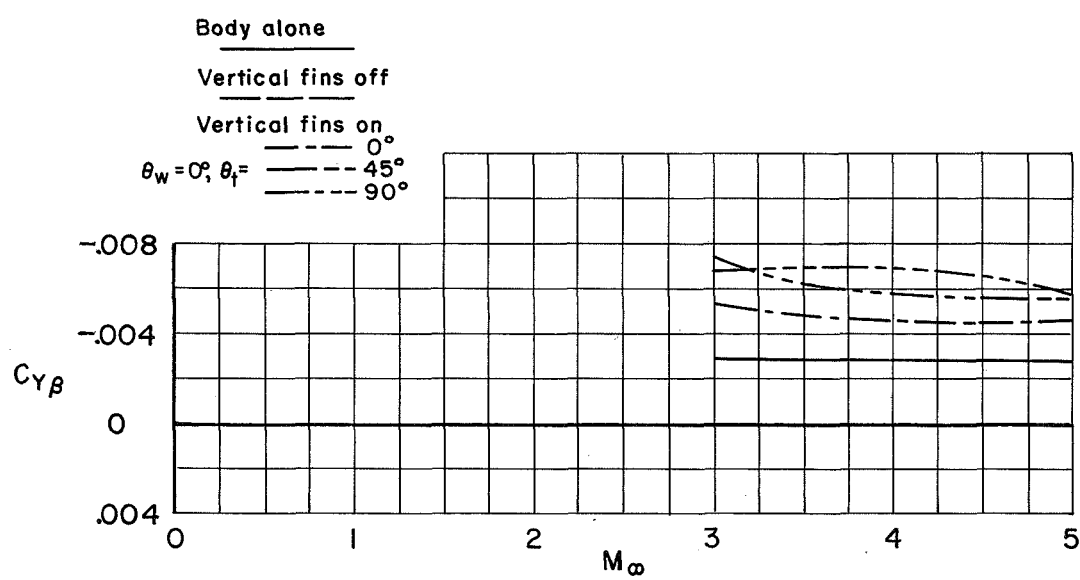
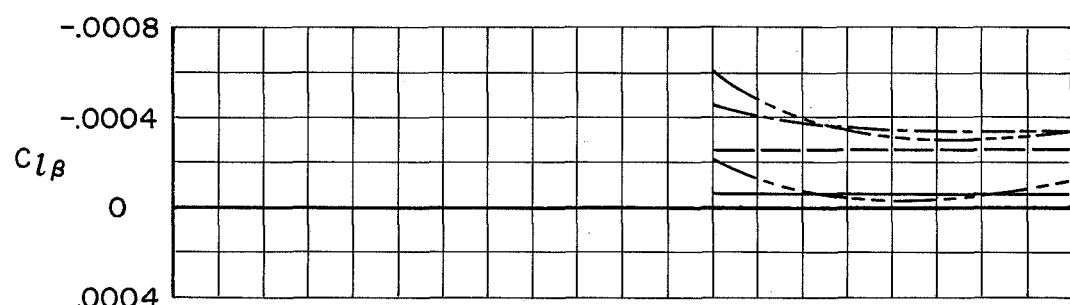
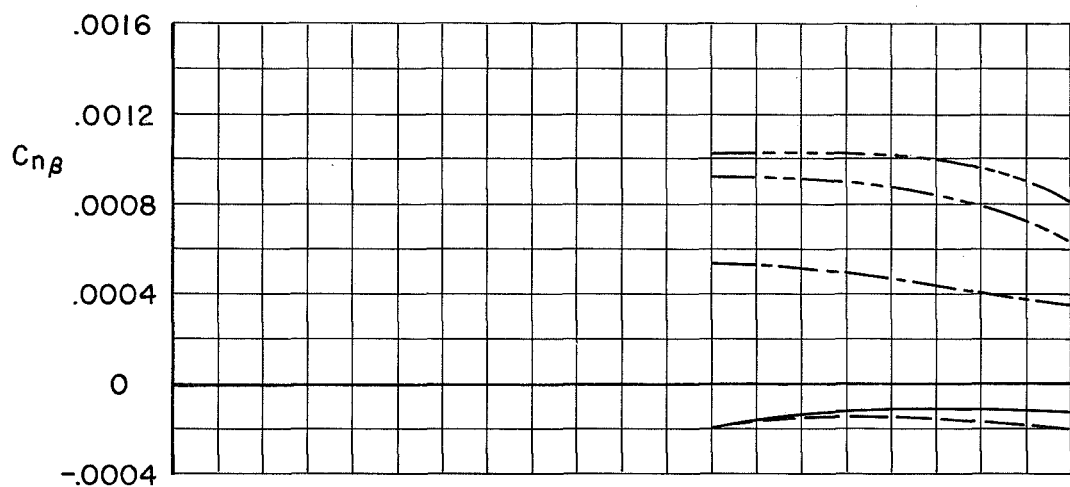


Figure 21.- Lateral stability derivatives for aircraft configuration;
 $\alpha = 0^\circ$.

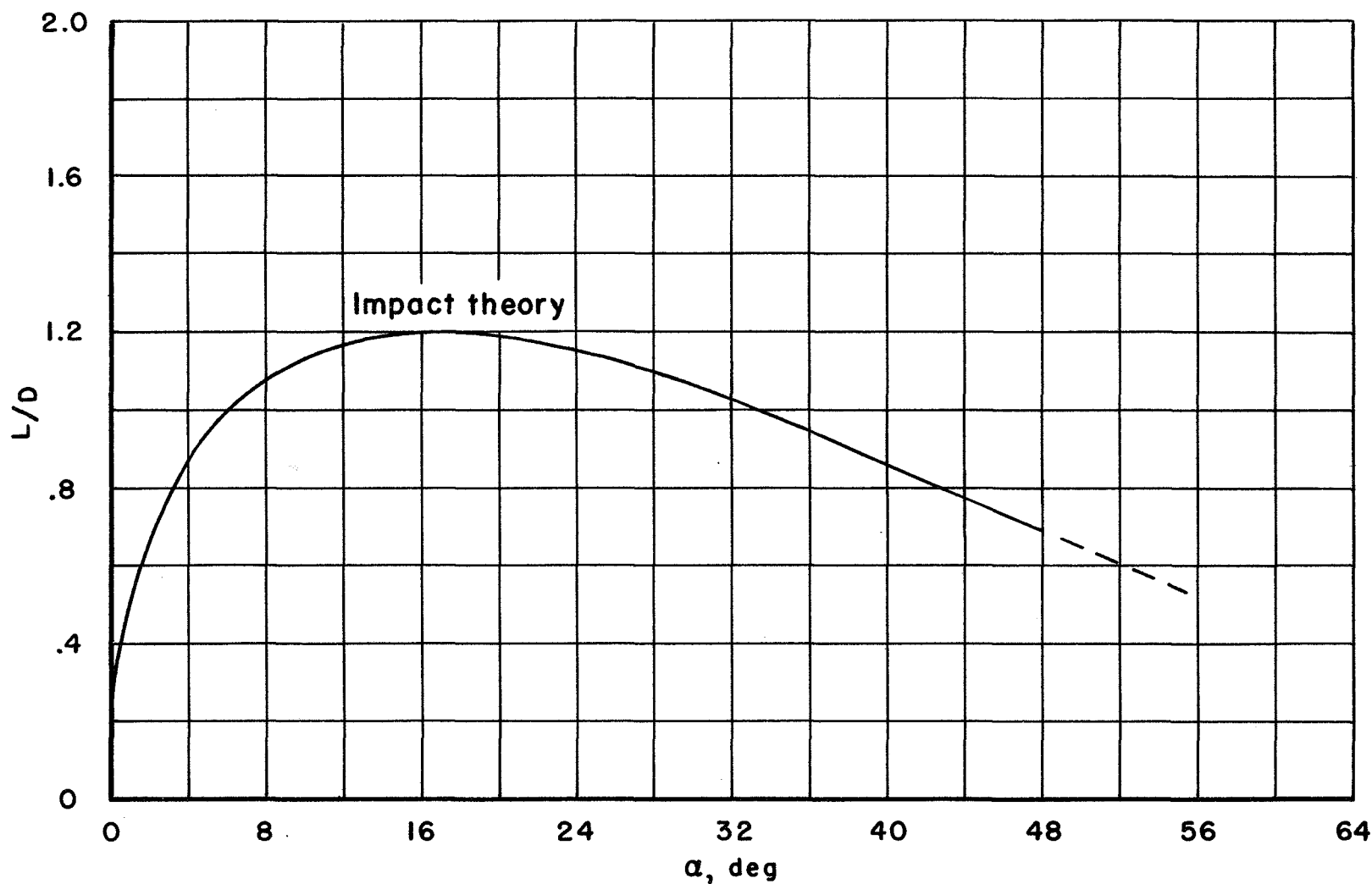


Figure 22.- Estimated lift-drag ratio at hypersonic Mach numbers for entry configuration; wings folded and fairings in place.

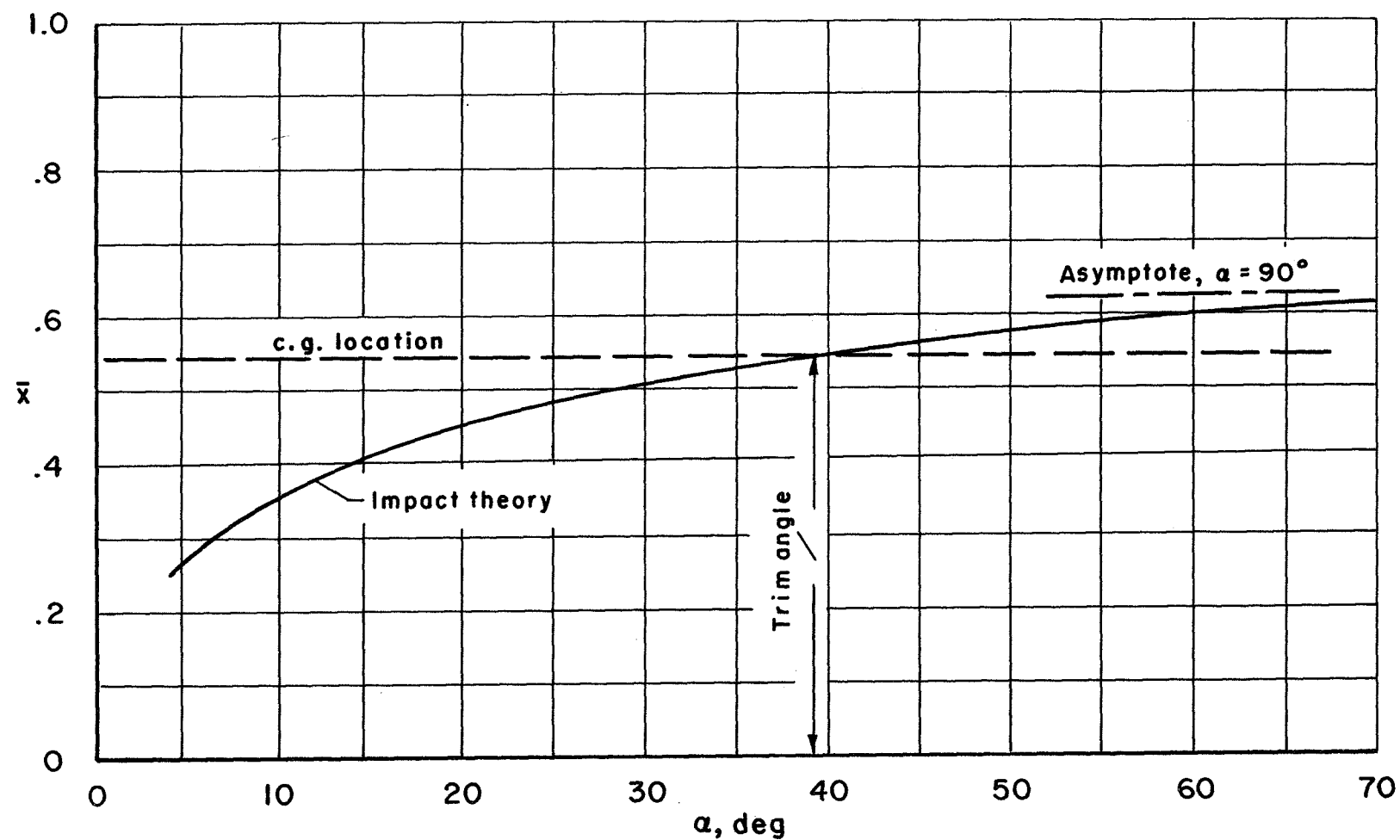


Figure 23.- Estimated center-of-pressure location at hypersonic Mach numbers for entry configuration.

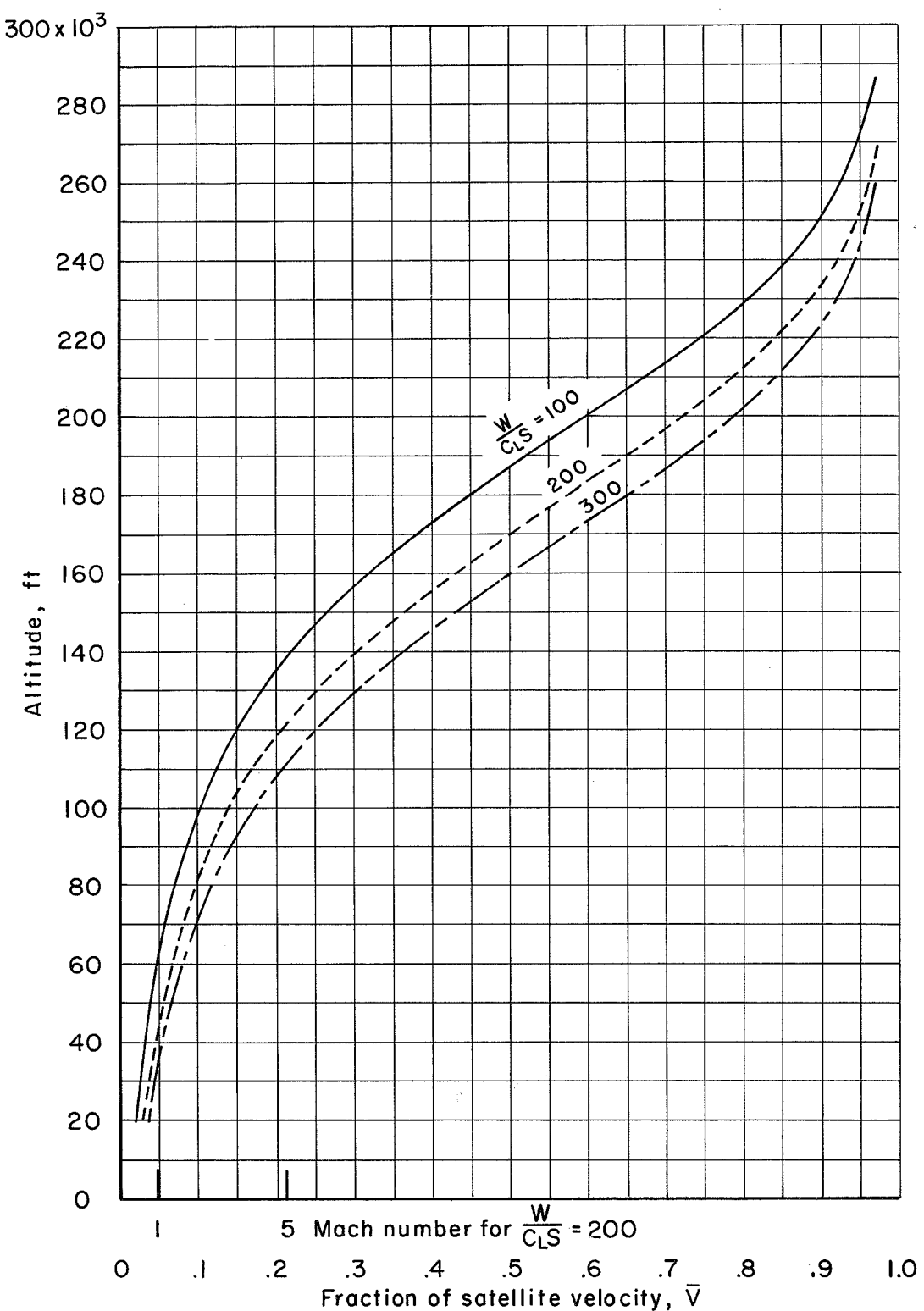


Figure 24.- Equilibrium glide trajectories.

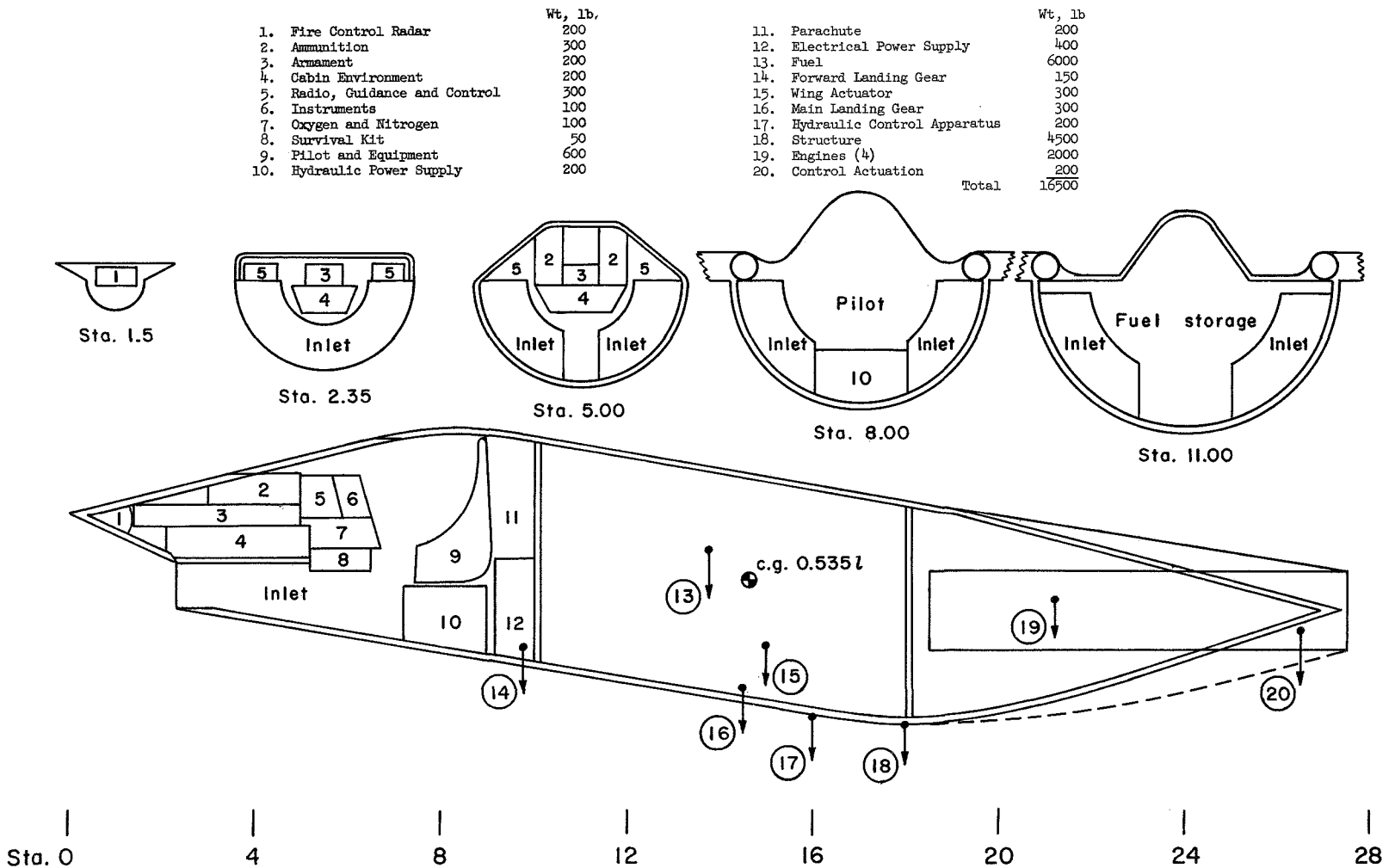


Figure 25.- Fuselage internal arrangement for four-engine vehicle.

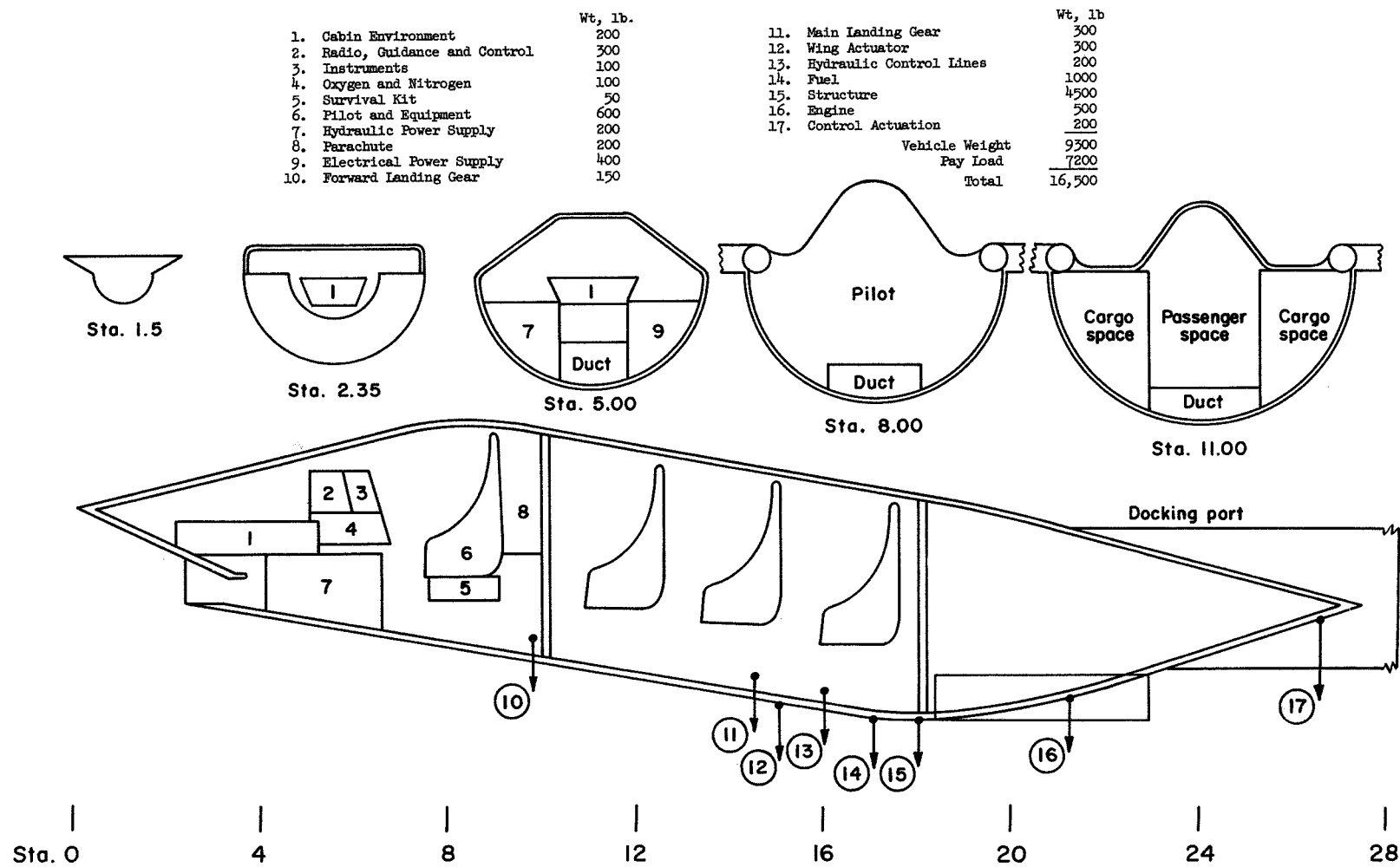


Figure 26.- Fuselage internal arrangement for single-engine vehicle.

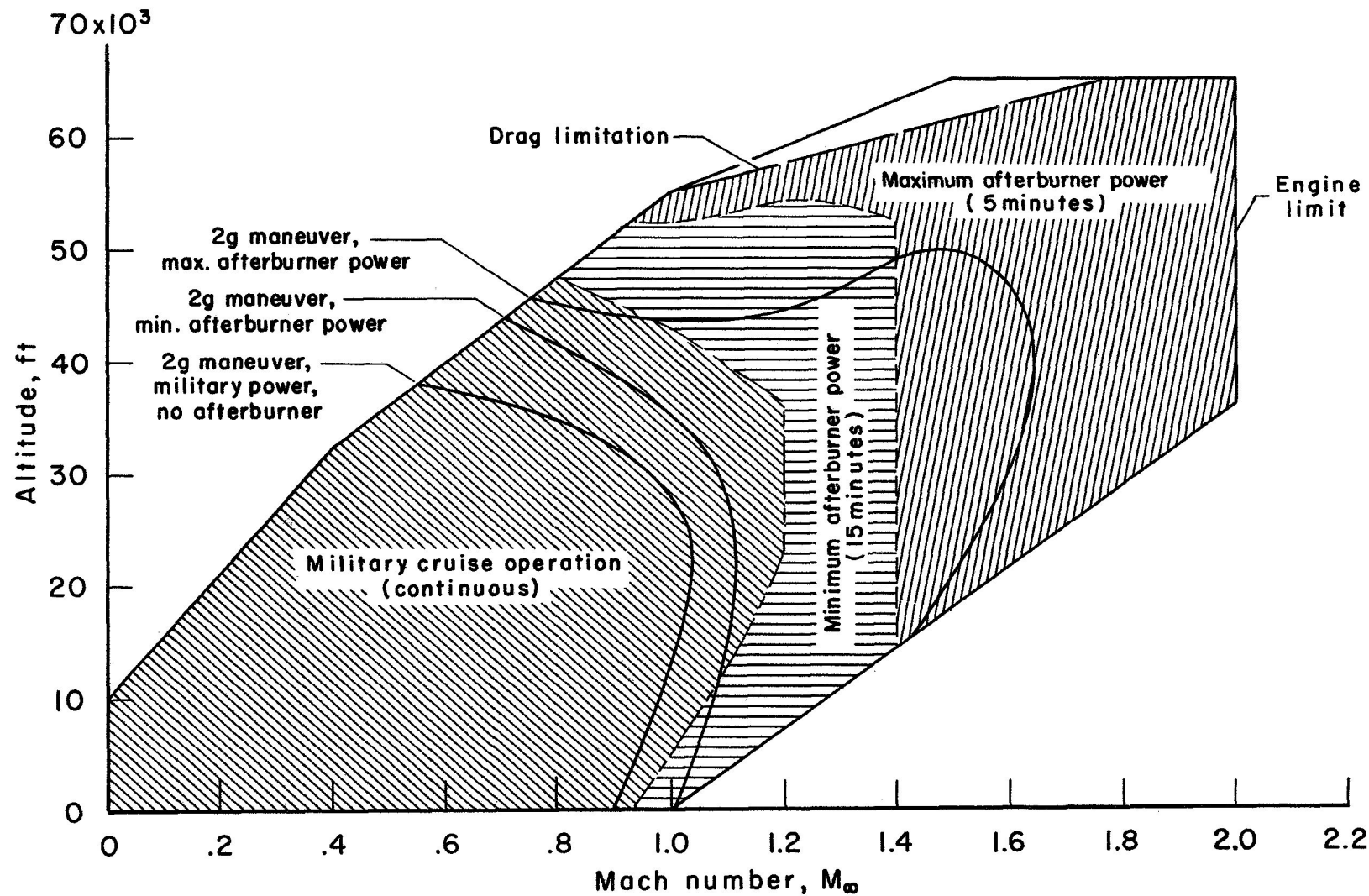


Figure 27.- Flight operation envelope for four-engine vehicle.

[REDACTED]

b
d

r
s

b

c

a

b

b

c

[REDACTED]

